AD-A043 608 WESTINGHOUSE DEFENSE AND ELECTRONIC SYSTEMS CENTER B--ETC F/G 9/5
CCD ADAPTIVE DISCRETE ANALOG SIGNAL PROCESSING.(U)
JUL 77 M H WHITE, I A MACK, L L LEWIS N00173-76-C-0147

UNCLASSIFIED NL

1 OF 2
AD A043608

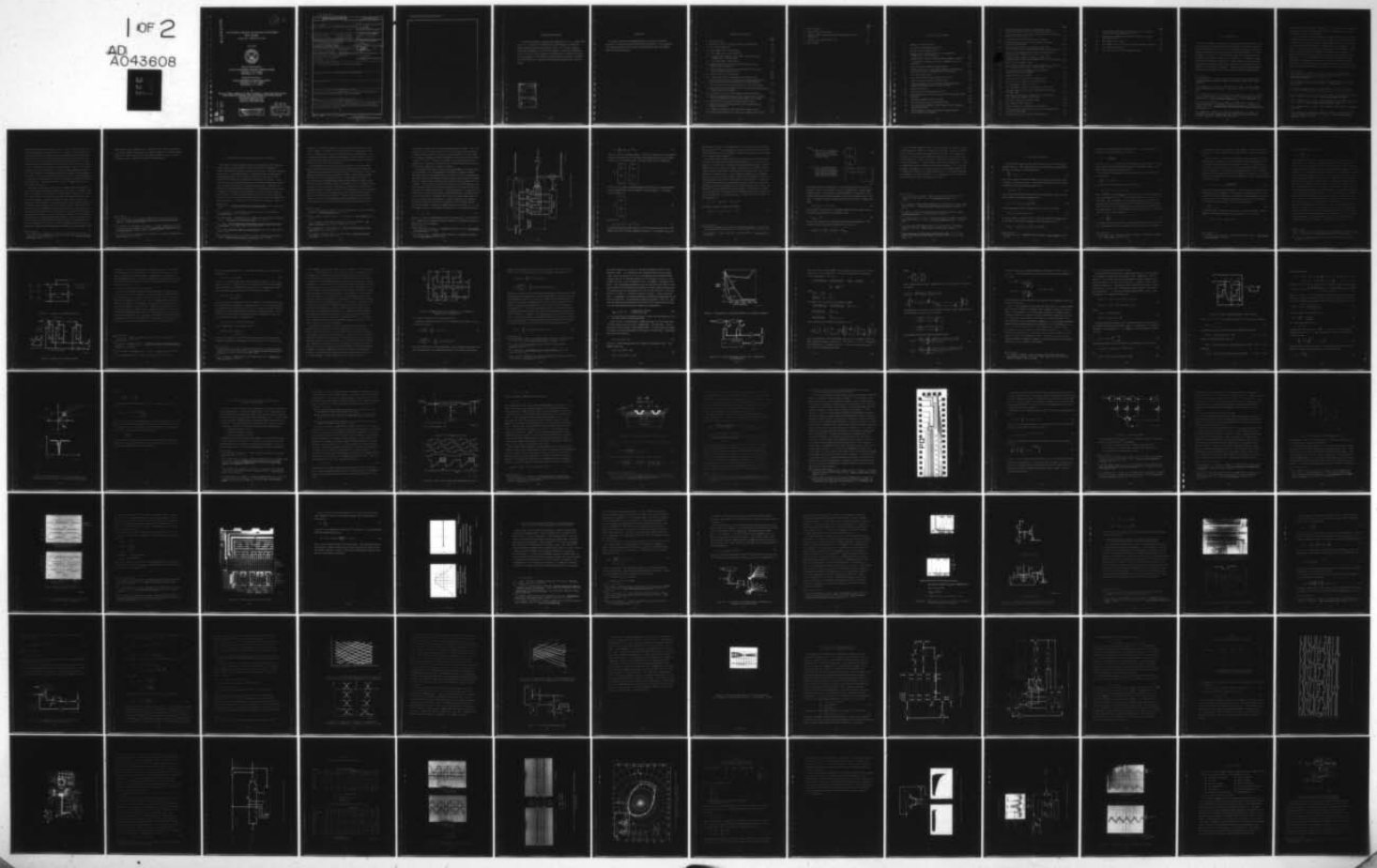

(12) 4

CCD ADAPTIVE DISCRETE ANALOG SIGNAL PROCESSING

FINAL REPORT

Contract No. N00173-76-C-0147

July 1977

Research Sponsored by:

NAVAL ELECTRONIC SYSTEMS COMMAND N00039
Code 304, L.W. Sumney
Washington, D.C. 20360

Research Directed by:

NAVAL RESEARCH LABORATORY N00173
Code 5262, Dr. W.D. Baker
Washington, D.C. 20375

By

Marvin H. White, Ingham A.G. Mack, Leonard L. Lewis, Gerald M. Borsuk
WESTINGHOUSE DEFENSE AND ELECTRONIC SYSTEMS CENTER
Systems Development Division
Advanced Technology Labs.
Baltimore, Maryland 21203

UNCLASSIFIED

SECURITY CLASSIFICATION OF THIS PAGE (When Data Entered)

REPORT DOCUMENTATION PAGE	READ INSTRUCTIONS BEFORE COMPLETING FORM
1. REPORT NUMBER	2. GOVT ACCESSION NO. / 3. RECIPIENT'S CATALOG NUMBER
4. TITLE (and Subtitle): CCD Adaptive Discrete Analog Signal Processing	5. TYPE OF REPORT & PERIOD COVERED: Final Report
	6. PERFORMING ORG. REPORT NUMBER
7. AUTHOR(s): Marvin H. White, Leonard L. Lewis, Ingham A.G. Mack, Gerald M. Borsuk	8. CONTRACT OR GRANT NUMBER(s): N00173-76-C-0147
9. PERFORMING ORGANIZATION NAME AND ADDRESS: Westinghouse Defense and Electronic Systems Ctr, Systems Development Division, Advanced Technology Labs., Baltimore, Maryland 21203	10. PROGRAM ELEMENT, PROJECT, TASK AREA & WORK UNIT NUMBERS: 62762N, XF54582002, F54582
11. CONTROLLING OFFICE NAME AND ADDRESS: Naval Electronic Systems Command N00039, Code 304, L. W. Sumney, Washington, D.C. 20360	12. REPORT DATE: July 1977
	13. NUMBER OF PAGES: 110
14. MONITORING AGENCY NAME & ADDRESS (if different from Controlling Office): Naval Research Laboratory N00173, Code 5262, Dr. W.D. Baker, Washington, D.C. 20375	15. SECURITY CLASS. (of this report): Unclassified
	15a. DECLASSIFICATION DOWNGRADING SCHEDULE

16. DISTRIBUTION STATEMENT (of this Report)

A. Approved for public release, distribution unlimited

17. DISTRIBUTION STATEMENT (of the abstract entered in Block 20, if different from Report)

18. SUPPLEMENTARY NOTES

19. KEY WORDS (Continue on reverse side if necessary and identify by block number)

Adaptive Processing, CCD Signal Processing, Charge-Coupled Devices
MNOS Devices, LMS Algorithm, Noise Cancellation

20. ABSTRACT (Continue on reverse side if necessary and identify by block number)

This report describes the implementation of a recursive stochastic algorithm, the least mean square (LMS) error algorithm, in a 2-tap weight CCD adaptive filter with electrically-reprogrammable MNOS nonvolatile, analog conductance weights.

DD FORM 1 JAN 73 1473 EDITION OF 1 NOV 65 IS OBSOLETE S/N 0102-014-6601

UNCLASSIFIED

SECURITY CLASSIFICATION OF THIS PAGE (When Data Entered)

408 138

ACKNOWLEDGEMENTS

The authors would like to express their appreciation to Dr. J. Dzimianski and Dr. P.C. Smith for the MNOS memory transistors, R. Stehlik for analog processor design contributions, and Dr. W.S. Corak, manager, Solid-State Technology; Dr. G. Strull, manager, Science and Technology; and Dr. P.M. Pan, chief scientist, R&D Operations, for their encouragement and support of CCD/DASP for adaptive signal processing. We would also like to thank D.G. Peterson for the technical preparation of the final report.

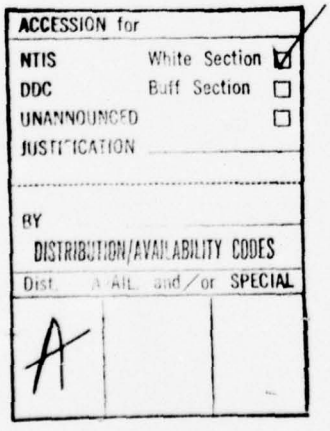

ABSTRACT

This report describes the implementation of a recursive stochastic algorithm, the least mean square (LMS) error algorithm, in a 2-tap weight CCD adaptive filter with electrically-reprogrammable MNOS nonvolatile, analog conductance weights.

TABLE OF CONTENTS

LIST OF ILLUSTRATIONS

1. INTRODUCTION

The recommendation of an early study program[1] was to examine the possibility of electrically reprogrammable analog weights at tap positions along a CCD analog delay line in order to form a basic linear combiner for adaptive filtering. A step was taken in this direction with the development of a serial in/parallel out (SI/PO) CCD[2] with a floating clock electrode circuit for the attachment of conductance weights.[3] The latter circuit combined the advantages of MOS and bipolar technologies[4] to sense nondestructively the signal charge under a floating gate electrode in the form of a displacement charge stored on a MOS transistor amplifier.[5] The idea of electrically reprogrammable analog conductances with MNOS memory transistors biased in their

---

[1] M. H. White and W. R. Webb, "Study of the Use of Charge-Coupled Devices in Analog Signal Processing Systems," Final Report, N00014-74-C-0069, May 1974.

[2] M. H. White, I. A. Mack, F. J. Kub, and D. R. Lampe, "Charge-Coupled Device Analog Signal Processing," Final Report N00014-75-C-0283, Feb. 1976.

[3] M. H. White, I. A. Mack, F. J. Kub, D. R. Lampe and J. L. Fagan, "An Analog CCD Transversal Filter with Floating Clock Electrode Sensor and Variable Top Gains," ISSCC Technical Digest (1976), pg. 194, Philadelphia, Pa.

[4] F. J. Kub, M. H. White, D. R. Lampe, J. L. Fagan and I. A. Mack, "CCD/Bipolar Monolithic IC Technology," Abstract #107, pg 207. Extended Abstracts, Vol. 76-1. Spring Meeting, Electrochemical Society, May 2-7, 1976, (Washington, D. C.).

[5] I. A. Mack, M. H. White, F. J. Kub, D. R. Lampe, and J. L. Fagan, "A Versatile CCD Analog Transversal Filter with Floating Clock Electrode Sensors" NAECON 76 (Dayton, Ohio, May 1976).

triode regions was discussed in the literature[6, 7] with the intention of adaptive filter based on the least mean square (LMS) error algorithm[8] to optimize MNOS analog conductance tap weights.

Early in this program a decision had to be made with regards to the type of analog weighting, since the option existed between conventional MOS triode multipliers[9] with capacitor storage and electrically reprogrammable MNOS triode multipliers which used direct tunneling through thin oxide (20 to 30Å) layers.[10] In order to implement the LMS algorithm, the multiplier or weight had to be adjustable and some technique of integration or storage was required. Since storage times of several minutes were anticipated for some applications,[11] this meant either large "off-chip" capacitors for the MOS multipliers or the inherent "memory" of the MNOS multipliers. We had worked with MNOS devices for over a decade, starting in 1965, and this experience combined with the long-term endurance of these devices to cycling[12]

---

[6] M. H. White, D. R. Lampe, J. L. Fagan, "CCD & MNOS Devices for Programmable Analog Signal Processing and Digital Nonvolatile Memory," IEDM Technical Digest, (Dec. 1973) pg. 130-3.

[7] D. R. Lampe, M. H. White, J. H. Mims, and G. A. Gilmour, "CCD's for Discrete Analog Signal Processing (DASP)," INTERCON 74, (New York, March 1974).

[8] B. Widrow, "Adaptive Filters I: Fundamentals," Rept. SEL-66-126 (T. R. No. 6764-6) Stanford Electronics Labs., (Stanford, Calif., Dec. 1966).

[9] D. R. Lampe, H. C. Lin, I. A. Mack, M. H. White, "CMOS Analog Multipliers for CCD Analog Signal Processing" 1976 GOMAC Digest of Papers.

[10] M. H. White and J. R. Cricchi, "Characterization of Thin-Oxide MNOS Memory Transistors", IEEE Trans. Electron Devices, ED-19, 1280 (1972).

[11] M. M. Sondhi and A. J. Presti, "A Self-Adaptive Echo Canceller," B. S. T. J., 1851 (1966).

[12] M. H. White, J. W. Dzimianski, and M. C. Peckerar, "Endurance of Thin-Oxide Nonvolatile MNOS Memory Transistors," IEEE Trans. Electron Devices, ED-24, 577 (1977).

made the MNOS memory transistor a logical choice for the electrically reprogrammable analog conductance weight. In addition to the storage or integration requirement, the electrical programmability function could be implemented in a simple manner with the erase/write features of the MNOS device structure. Thus, this report discusses the combination of CCD discrete analog delay line technology with thin-oxide MNOS memory technology to form a basic linear combiner for adaptive filtering. The CCD/MNOS technologies have been used already in a monolithic charge-addressed memory cell[13] and, therefore, the results presented in this report are extendable to a complete monolithic adaptive filter integrated circuit. In the latter phases of the program, a bidirectional CCD control technique was developed to obtain analog weighting. This method offers an "all CCD" adaptive filter and is discussed in this report.

This report begins with an introduction to adaptive filtering followed by the LMS algorithm to optimize the selection of tap weights in the filter. The filter is comprised of a basic linear combiner, which consists of a CCD discrete analog delay line with electrically reprogrammable MNOS analog conductance tap weights to weight the nondestructively sensed signals in the delay line, and an algorithm to control the programming of the tap weights. In addition, signal condition and reconstruction circuitry together with antialiasing filters are employed to generate the appropriate analog waveforms. To demonstrate the feasibility of the approach, a 2-tap weight adaptive filter breadboard is described. Such a configuration represents the basic adaptive filter element in a multitap weight adaptive filter. Preliminary evaluation of this basic adaptive filter element indicates this approach should open-the-door to the realization of low-cost, compact, adaptive systems for such applications as filtering, prediction, system modeling, spectral analysis, noise

[13] M. H. White, D. R. Lampe, J. L. Fagen, F. J. Kub, and D. A. Barth, "A Nonvolatile Charge Addressed Memory (NOVCAM) Cell," IEEE J. of Solid-State Ckts, SC-10, 281 (1975).

suppressions, echo cancellation, etc. Specific systems which would benefit from such an adaptive filter are secure speech processing with adaptive linear prediction[14], sonar beam forming with adaptive sidelobe clutter cancellers,[15] and adaptive noise cancellers for sensor-oriented systems.[16]

[14] D. F. Barbe, "The Use of Charge-Coupled Devices in Voice Processing Systems," 1977 IEEE International Symposium on Circuits and Systems. Phoenix, Arizona, April 25, 1977.

[15] M. H. White, K. Petrosky, I. A. Mack, L. I. Lewis, "Adaptive CCD Signal Processing for Sonar Applications," 1977 International Symposium on Circuits and Systems, Phoenix, Arizona, April 25, 1977.

[16] B. Widrow, et. al., "Adaptive Noise Cancelling; Principles and Applications," Proc. IEEE, 63, 1692 (1975).

2. INTRODUCTION TO ADAPTIVE SIGNAL PROCESSING

The history of adaptive signal processing might well begin with the introduction of least squares estimation theory by Gauss[17] and Legendre[18]. Gauss introduced this technique to solve a large number of redundant equations to extract the "most probable values" of certain astronomical parameters. Modern adaptive filter theory began with the work of Kolmogorov[19] and Wiener[20] on the prediction and filtering of stationary time series. Wiener treated continuous signals while Kolmogorov examined sampled data systems, thus, anticipating the need for coherent signal processing. The Wiener/Kolmogorov work provided the basic design criteria for optimal linear filters to suppress noise, perform signal prediction, and smooth statistically stationary signals. The design of these filters for known statistics is well understood[21], but practical considerations often place limits on the implementation of such filters. Kalman and Bucy[22] extended the Kolmogorov/Wiener

---

[17] Gauss, K. G., Theory of Motion of the Heavenly Bodies, (Dover, New York, 1963).

[18] H. W. Sorenson, "Least-Squares Estimation: from Gauss to Kalman" IEEE Spectrum, pg. 63, (July 1970).

[19] A. Kolmogorov, "Interpolation und Extropolation von Stationären Zufalligen Folgen." Bull Acad. Sci, USSR, Ser. Math., 5, 3 (1941)

[20] N. Wiener, The Extrapolation, Interpolation and Smoothing of Stationary Time Series, Cambridge, Mass, MIT Press (1949)

[21] Y. W. Lee, Statistical Theory of Communication, New York: John Wiley & Sons, (1960).

[22] R. Kalman and R. Bucy, "New Results in Linear Filtering and Prediction Theory" Trans, ASME (Ser. D), J. Basic Eng., 83, 95 (1961).

techniques to consider the design of time-varying linear filters for nonstationary signals. In general, these types of filters have parameters whose values are determined by apriori information on the signal statistics. The so-called Kalman filter represents essentially a recursive solution of Gauss' original least-square problem in which the computations benefits of todays digital computers are used to advantage.[23]

Adaptive filters are a class of "learning machines" in which the filter design (weight or parameter adjustments) is self-learning and based upon estimated (measured) statistical characteristics of the input and output signals. Adaptive filtering based on a recursive algorithm, (correlation-cancellation loop (CCL),) was employed in the RF-antenna field in the 1950's.[24] Two groups working independently, developed techniques for adaptive interference or clutter cancelling. One group worked on radar IF sidelobe clutter cancellers[25] with optimization achieved by an algorithm that maximized a generalized signal-to-noise ratio (SNR).[26] The other group worked on a self-optimizing array for control systems based on sampled signals and a least mean square (LMS) error algorithm.[27] These two adaptive algorithms, although arrived at with different approaches and different objectives, are nevertheless very similar since they both derive their adaptive parameter

---

[23] A. G. Carlton and J. W. Follin, "Recent developments in Fixed and Adaptive Filtering," AGARDograph, No. 21 (1956).

[24] W. F. Gabriel, "Adaptive Arrays - An Introduction," Proc. IEEE, 64, 239 (1976).

[25] P. W. Howells, "Intermediate Frequency Side-Lobe Canceller," U.S. Patent, 3,202,990, Aug. 24, 1965 (filed May 4, 1959).

[26] S. P. Applebaum, "Adaptive Arrays," Syracuse University Res. Corp. Rep. SPL TR 66-1, Aug. 1966.

[27] B. Widrow, "Adaptive Filters I: Fundamentals," Stanford University Tech Rept. No. 6764-6, Dec. 1966.

adjustments by sensing the correlation between element signals. Thus, both algorithms use the covariance matrix of the set of system inputs and both converge toward the optimum Kolmogorov/Wiener solution. In this report, we use the LMS adaptive algorithm developed by Widrow and Hoff at Stanford University[28] in 1959. Widrow, in a recent survey and tutorial article on adaptive noise cancelling,[29] describes the work performed during the 1960's by he and his colleagues at Stanford University.

The adaptive filter operates without apriori knowledge of the signal statistics and the filter uses the available data to design an appropriate filter. The general form of an adaptive filter is limited by practical considerations since the inversion and storage of large matrices of data requires a sizeable volume of computer space and real-time signal processing is difficult to accomplish. The iterative LMS algorithm of Widrow and Hoff[28] requires very little computer time or memory, and the algorithm is suitable for real-time processing of large amounts of data. With this algorithm, the statistics of the signals are not measured explicitly to design the filter but, instead, through a recursive algorithm, the weight adjustments are made automatically with the arrival of each new data sample. In order to appreciate the degree of computation required in the direct computation form of the least-square estimation problem, consider the adaptive filter shown in figure 1. We treat the adaptive system as a discrete-time system with the instantaneous error

$$\epsilon_m = d_m - Y_m . \tag{1}$$

where d_m is the so-called desired or primary signal and Y_m is the filter output. Suppose we can represent the filter output as a weighted summation of delayed input signal samples,

---

[28] B. Widrow and M. Hoff, Jr., "Adaptive Switching Circuits," IRE WESCON Conv. Rec; Pt. 4, 96 (1960).

[29] B. Widrow, et. al., "Adaptive Noise Cancelling: Principles and Applications" Proc. IEEE, 63, 1692 (1975).

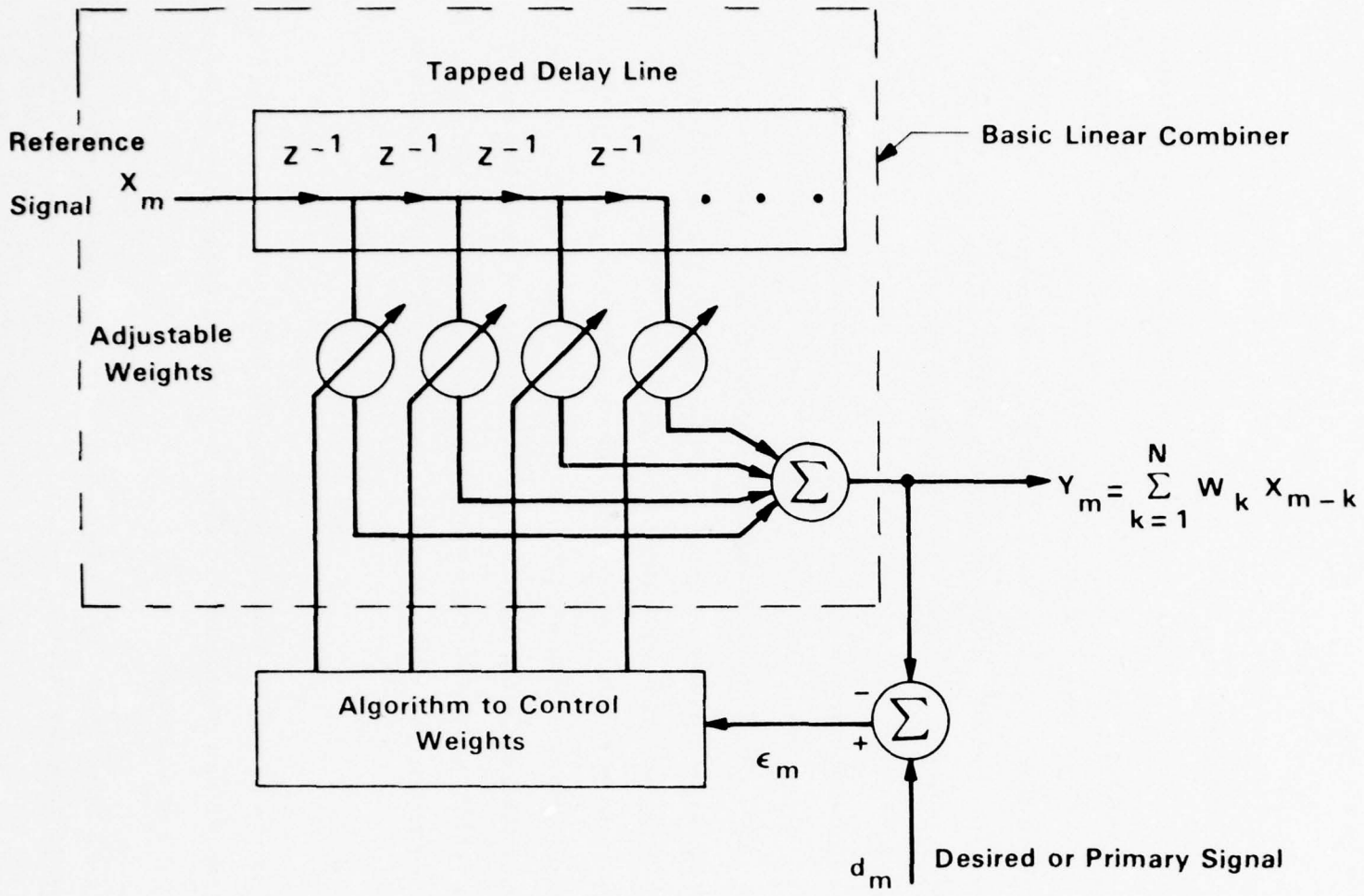

Figure 1. Adaptive Transversal Filter

$$Y_m = \sum_{k=1}^{N} W_k X_{m-k} = W^T X_m . \tag{2}$$

Where W_k are the adjustable weights. The major component of most adaptive systems is the basic linear combiner which weights and sums a set of input signals to form the output signal. The input signal vector is defined as,

$$X_m \triangleq \begin{pmatrix} X_1(m) \\ X_2(m) \\ \vdots \\ X_k(m) \\ \vdots \\ X_N(m) \end{pmatrix} = \begin{pmatrix} X_{m-1} \\ X_{m-2} \\ \vdots \\ X_{m-k} \\ \vdots \\ X_{m-N} \end{pmatrix} \tag{3}$$

Where the input signal components appear simultaneously on all tap positions along the tapped delay line and indexed by the time index m. The weight vector is given as,

$$W \triangleq \begin{pmatrix} W_1(m) \\ W_2(m) \\ \vdots \\ W_k(m) \\ \vdots \\ W_N(m) \end{pmatrix} \tag{4}$$

The error is,

$$\epsilon_m = d_m - X_m^T W = d_m - W^T X_m \tag{5}$$

The desired signal generally requires some imagination and the form of this signal determines the type of adaptive processor. For example, if d_m were

derived from the input to the adaptive filter, then we would have an adaptive linear predictor.[30] A second selection of d_m is to make this input the signal and noise while the input of the filter is selected as the noise, thereby realizing an adaptive noise canceller.[29]

The purpose of the adaptive algorithm is to adjust the weights of the adaptive linear combiner to minimize the mean-square error. We may ask the question "for which class of signals is this optimization procedure justified?". There are two broad classes of signals: deterministic and random signals. Within the deterministic class of signals we have signals which exist over an infinite time interval and thus, autocorrelation techniques can be applied. Similarly, stationary ergodic random signals may be handled with autocorrelation techniques which may be computed as a time average.[21] Finite duration deterministic signals may be analyzed with the covariance method and similarly, nonstationary signals that are locally stationary over a finite time duration[31] may be handled with the same method. We will assume signals that are statistically stationary with the knowledge nonstationary signals may also be handled with such adaptive filters. We begin with the formulation of the squared error,

$$\epsilon_m^2 = d_m^2 - 2d_m X_m^T W + W^T X_m X_m^T W \tag{6}$$

and taking the expected value of both sides.

$$E(\epsilon_m^2) = E(d_m^2) - 2P^T W + W^T R W \tag{7}$$

---

[30] G. S. Kang, "Application of Linear Prediction Encoding to a Narrowband Voice Digitizer," Naval Research Laboratories Report 7774, Oct. 31, 1974.

[31] John Makhoul, "Linear Prediction: A Tutorial Review," Proc. IEEE, 63, 561 (1975).

where

$P \triangleq$ steering vector representing a cross-correlation between desired response and input signal

$$= E \begin{pmatrix} d_m X_{m-1} \\ \vdots \\ d_m X_{m-k} \\ \vdots \\ d_m X_{m-N} \end{pmatrix} \tag{8}$$

$R \triangleq$ input correlation matrix for stationary signals or autocovariance matrix for quasi-stationary signals over finite time interval.

$$= E \begin{pmatrix} X_{m-1}X_{m-1} & X_{m-1}X_{m-2} & \cdots \\ X_{m-2}X_{m-1} & X_{m-2}X_{m-2} & \cdots \\ \vdots & \vdots & \\ & & X_{m-N}X_{m-N} \end{pmatrix} \tag{9}$$

The important feature of equation (7) is the mean square-error (MSE) is a quadratic function of the weights or may be considered as a concave hyperbuloidal surface. The process of weight adjustment to minimize the MSE involves descending along this surface to reach the so-called "bottom of the bowl". A popular method to descend along this surface is the gradient technique.

$$\nabla E\left(\epsilon_m^2\right) = -2P + 2RW \tag{10}$$

and the optimum weight rector, generally called the Wiener weight vector, is obtained by setting the gradient equal to zero.

$$W_{opt.} = R^{-1}P \tag{11}$$

which is the matrix form of the Kolmogorov/Wiener-Hopf equation. The minimum MSE is obtained by substitution of (11) into (7).

$$\min\left\{E\left(\epsilon_m^2\right)\right\} = E\left(d_m^2\right) - P^T W_{opt}$$

The conventional approach used to solve for the optimum weights involves a two-step process computing and updating the sample covariance matrix with a block of data and then solving equation (11). In order to accomplish this computation, various numerical algorithms have been investigated such as triangularization,[32] Levison-Robinson,[33] householder/transformation,[34] and Gaussian elimination.[35] These methods, even the most efficient one, require a considerable amount of hardware for real-time operation.[36, 37] The size and power dissipation, not to mention the cost, is a principle liability of the so-called direct approach for solving equation (11). An alternative approach to the elephant-computer method is to use a well-known recursive stochastic algorithm known as the LMS adaptive algorithm.[29]

---

[32] B. S. Atal and S. L. Hanauer, "Speech Analysis and Synthesis by Linear Prediction of the Speech Wave," J. Acoustical Soc. An., 50, 637 (1971).

[33] J. D. Markel, "Digital Inverse Filtering - A New Tool for Forment Trajectory Estimation," IEEE Trans. Audio and Electroacoustics, Au-20, 129 (1972).

[34] J. Rogers, "Digital Inverse Filtering of the Speech Waveform," Proc. British Acoust. Soc., 2, Spring Meeting April 1973.

[35] J. R. Welch and J. D. Oetting, "Forment Extraction Hardware Using Adaptive Linear Predictive Coding," Proc. Nat'l Telecom. Conf., November 1973.

[36] J. G. Dunn, "An Experimental Gigabit/Sec Voice Digitizer Employing Adaptive Prediction," IEEE Trans. or Comp. Tech, Com-19, 1021 (1972).

[37] Voice Processor LSI/Organization Optimization Study, S. E. Hutchins, et. al., TRW Systems, Final Report Contract No. DCA 100-75-C-0020, Sept. 1975.

3. THE LMS ALGORITHM

The least-mean square (LMS) algorithm has its roots in the method of steepest descents. The weight adjustment is in a direction proportional to the negative gradient of some functional F,

$$\frac{dW_j}{dt} = -\mu \nabla_{W_j} F \tag{12}$$

where the gradient is taken with respect to the weight vectors and μ is the so-called "convergence" factor. In this particular instance, the functional is defined in terms of the mean-square error.

$$F \triangleq E(\epsilon^2) = \overline{\epsilon^2} \tag{13}$$

Since we are concerned with discrete-time, sample-data, systems the difference equation formalism is appropriate,

$$W_j(m+1) = W_j(m) - \mu \nabla_{Wj} \overline{\epsilon^2}(m) \tag{14}$$

If we combine equation (14) with equation (11), then we may write

$$W(m+1) = (I-2\mu R)\, W(m) + 2\mu P \tag{15}$$

in matrix notation. Equation (15) is a first order difference equation which can be used to solve for the response of the mean weight vector,[38]

$$\overline{W}(m) = (I-2\mu R)^m W_o + R^{-1}\left[I-(I-2\mu R)^m\right] P \tag{16}$$

---

[38] B. Widrow, et. al., "Adaptive Antenna Systems," Proc. IEEE, 55, 2143 (1967).

where W_o is the initial value of the weight vector. The mean weight vector converges to the Wiener Solution $R^{-1}P$ when

$$0 < \mu < \frac{1}{\lambda_i \text{ (max)}} \tag{17}$$

Where i = 1, 2, ... N and λ_i (max) is the maximum eigenvalue of the covariance matrix. Note the discrete time nature of the problem leads to the stability criteria expressed by equation (17).

The continuous time equation for the weight vector may be written for comparison as,

$$\frac{dW}{dt} = 2\mu P - 2\mu RW \tag{18}$$

with solution for the mean weight vector given by,

$$\overline{W} = e^{-2\mu Rt}\left(W_o - R^{-1}P\right) + R^{-1}P \tag{19}$$

Thus, we notice the total response may be thought of as a linear transformation of the eigenfunctions $e^{-2\mu \lambda_i t}$ for continuous time or $(1-2\mu \lambda i)^m$ for discrete time. The "convergence" factor determines the rate of adaption or response time of the system and because the weight algorithm is stochastic, the variance of the weights will introduce a certain amount of degradation in the mean-square error. The fractional increase in the latter or "misadjustment"[39] is given by the expression,

$$M = \mu \sum_{j=1}^{N} \lambda_j \tag{20}$$

We should note that small values of μ will minimize the misadjustment; however, this will result in long response time constants which may influence

[39] B. Widrow, et. al., "Adaptive Noise Cancelling," Principles and Applications" Proc. IEEE 63, 1962 (1975).

the convergence rate for nonstationary type signals. In these instances, the weights may not adapt rapidly enough to follow the time-varying covariance matrix.

The LMS algorithm is a practical technique to solve equation (11) for the optimal weights in real-time. The important features of the algorithm are (1) no explicit measurements of correlation functions, (2) no large memory storage or matrix inversion, and (3) the accuracy is determined by the statistical sample site. We shall see these advantages permit us to realize an adaptive signal processing system on a monolithic integrated circuit. Before we introduce the specific form of the LMS algorithm, we can combine equations (2) and (14) to write,

$$W_j(m+1) = W_j(m) + 2\mu\,\overline{\epsilon(m)X(m-j)} \tag{21}$$

where the incremental weight update is a cross-correlation between the error sequence and the data sequence. The process of weight optimization is concluded when the error sequence is orthogonal to the data sequence at the particular tap location of interest. The particular form of the LMS algorithm introduced by Widrow and Hoff[40] makes the approximation,

$$\overline{\epsilon(m)^2} \cong \epsilon^2(m) \tag{22}$$

thereby eliminating the need to average over a large block of data. The consequence of this approximation is to alter equation (21) to the form,

$$W_j(m+1) = W_j(m) + 2\mu\,\epsilon(m)X(m-j) \tag{23}$$

[40] B. Widrow and M. Hoff, Jr., "Adaptive Switching Circuits," IRE WESCON Conv. Rec., pt. 4, 96 (1960).

with cross-correlation function

$$\rho_j \triangleq \sum_{m=1}^{M} \epsilon(m)\, X\,(m-j) \tag{24}$$

as defined for the j^{th} tap over M data samples. Equations (21) and (23) may be pictured as a correlation cancellation loop[41] which is a type 1 servomechanism that removes or cancels from the output signal any component of the desired (main) input signal that is correlated with the tapped data signal (auxiliary). The cancellation (as shown in figure 2) is obtained by a controlled subtraction of the auxiliary input from the main input after the former has been adjusted in amplitude to maximize its correlation with the main input. This subtraction process continues until no correlation is detected between the output error (residue) and the auxiliary input at which time the mean input to the integrator is zero. Thereafter, the integrator output, which controls the amplitude adjustment, remains constant unless the input changes.

The correlation cancellation loop (CCL) has two aspects: (1) a correlation between input signal samples from the auxiliary input of the form X(m-i) X(m-j) and (2) a correlation between the main input and the auxiliary input of the form d(m)X(m-j). In order to realize an adaptive filter, N such CCL stages are cascaded as shown in figure 3. Each CCL stage is designed to cancel a component of the main input that is correlated with the delayed version of the auxiliary input (i.e., the tapped signal at the CCL stage itself). We should note that this adaptive filter is an implementation of the orthogonality principle in[42] N-dimensions with a real-time technique and no intermediate calculations are required. The method shown in figure 3 was

---

[41] D. R. Morgan, "A Note on Real-Time Linear-Prediction of Speech Waveforms," IEEE Trans. Acoust. Speech, Signal Processing, Au-21, 306 (1975).

[42] A. Papoulis, Probability, Random Variables and Stochastic Processes, McGraw-Hill (1965).

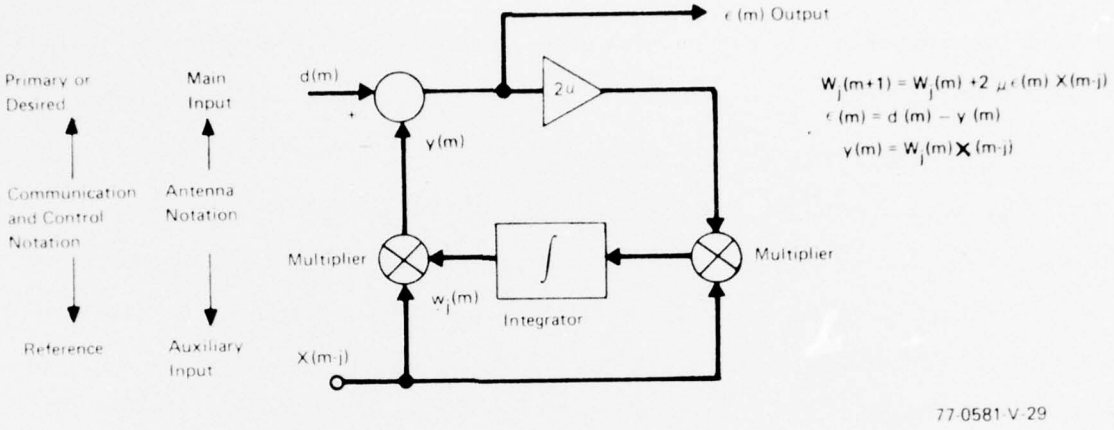

Figure 2. Correlation Cancellation Loop (CCL)

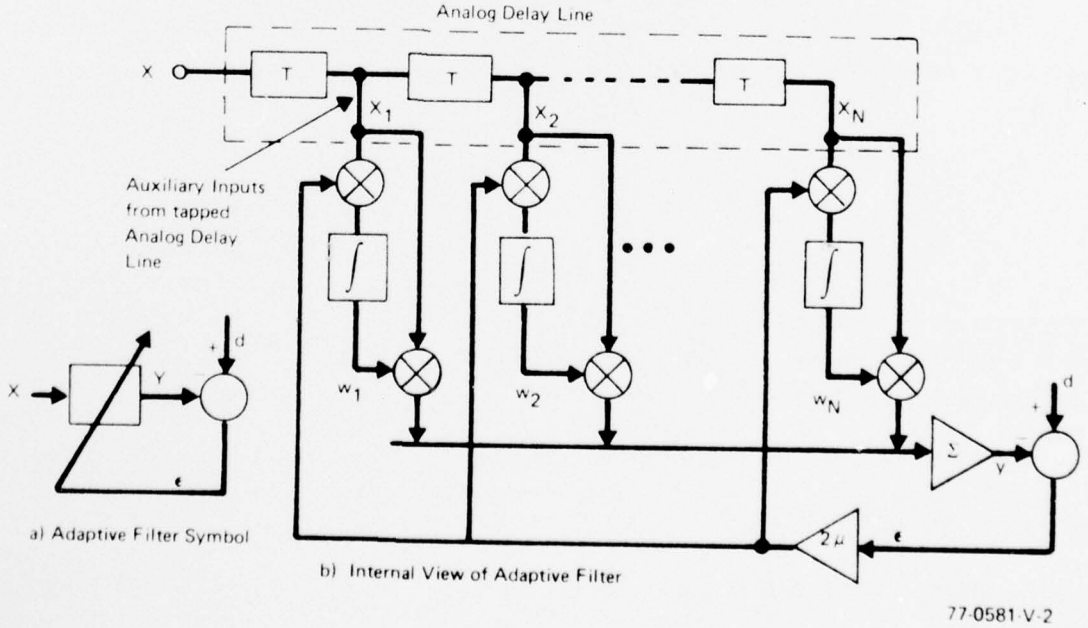

Figure 3. Internal View of Adaptive Filter

proposed by Lucky[43] for adaptive data compression and later by Widrow[44] as an extension of his original work. We should notice the linear LMS algorithm requires two 4-quadrant analog multipliers and an integrator or storage element for each CCL stage. In addition, we require an analog delay line with low loss and nondestructive taps to provide delayed signals to the tap positions (x_1, x_2, ... x_N).

3.1 THE CLIPPED DATA LMS ALGORITHM

The use of conventional 4-quadrant analog multipliers to implement the LMS algorithm is not only expensive, but from a power and size standpoint, quite impractical, not to mention the difficulties with accuracy, speed, and the eventual realization on an IC chip. Thus, in applications where a large number of multipliers is anticipated such as adaptive echo cancellation in long distance telephone communication,[45] analysis has been performed[46-48] to indicate the analog multipliers may be replaced by devices which can be implemented inexpensively and with characteristics quite different from the conventional multipliers. The convergence of the filter weights with nonideal multipliers is an important property of the adaptive filter and makes such a filter very attractive for system identification as, for instance, in the

---

[43] R. W. Lucky, "Adaptive Redundancy Removal in Data Transmission," B. S. T. J., , 549 (1968).

[44] B. Widrow, "Adaptive Filters", in Aspects of Network and System Theory Part IV, R. E. Kalman and N. DeClaris, Ed., New York: Holt, Rienhart and Winston, p. 563 (1971).

[45] M. M. Sondhi, "An Adaptive Echo Canceller," B. S. T. J., 46, 497 (1967).

[46] J. R. Rosenberger and E. J. Thomas, B. S. T. J., 50, 785 (1971).

estimation of speech parameter. The nonideal multiplier may be of the general form,[47]

$$(a \cdot b)(t) = a(t)\, f\left[b(t)\right] \tag{25}$$

where $(a \cdot b)(t)$ denotes the output of the nonideal multiplier at time t with inputs a(t) and b(t). $f\left[b(t)\right]$ is a monotonic function of b(t) and the multiplier output need only to be linear in one of the inputs. For example, the multiplier which generates the product $2\mu\epsilon(t)\,X(t)$ might be written as,

$$\begin{aligned}(\epsilon \cdot X)(t) &= \epsilon(t)\, f\left[X(t)\right] \\ &= \epsilon(t)\ \mathrm{sgn}\ X(t)\end{aligned} \tag{26}$$

where the auxiliary or delay input data is "clipped" to retain information about the polarity of the received data. Notice the error $\epsilon(t)$ is still computed with the amplitude and sign information of X(t) (i.e., in a linear manner), whereas the polarity is used to determine the direction of weight adjustment. Moschner[48] was the first author to treat this particular modification of the LMS algorithm and he referred to the algorithm

$$W_j(m+1) = W_j(m) + 2\mu\epsilon(m)\,\mathrm{sgn}\left[X(m-j)\right] \tag{27}$$

as the "clipped data" LMS algorithm, where

$$\begin{aligned}\mathrm{sgn}\left[X(m-j)\right] &= 1 \quad X(m-j) \geq 0 \\ &= -1 \quad X(m-j) < 0\end{aligned} \tag{28}$$

As Moschner noted,[48] "Once $W^T X$ has been computed, the LMS algorithm requires an additional N+1 additions or subtractions and N+1 multiplications.

---

[47] D. Mitra and M. M. Sondhi, "Adaptive Filtering with Non-Ideal Multipliers," Applications to Echo Cancellation," Int'l Conf. on Communications Vol. II (1975), pg. 30, June 1975, San Fancisco, Calif.

[48] J. L. Moschner, "Adaptive Filter with Clipped Input Data," Stanford Lab. Rept. No. 6796-1, June 1970.

For the clipped LMS algorithm, however, the components of X must be either +1 or -1, so multiplication by X is not required. The N multiplications can be replaced by N conditional-branch operations, which check the sign of X(m-j)and on this basis add or subtract the quantity $2\mu\epsilon(m)$. By eliminating N multiplications, the clipped algorithm offers a distinct advantage in speed of operation." Moschner went on to show this simplification slowed the speed of adaption by a factor of $\pi/2$ (when compared with the LMS algorithm) with no change in the converged level of performance since the estimation is still performed with the complete data signals. The simplicity of this algorithm, from the standpoint of IC implementation, is immediately apparent since N 4-quadrant analog multiplications are replaced by N simple polarity switches to steer $\pm 2\mu\epsilon(m)$ to the appropriate weight. Furthermore, the polarity of the data may be determined in a sequential operation with the analog data X(m-j) in an analog delay line (i.e., tapped CCD delay line) and its polarity sgn [X(m-j)] in a parallel digital delay line (i.e., tapped PMOS shift register), both delay lines synchronously clocked. Thus, because of the sequential nature of the data flow in the adaptive transversal filter, the N conditional-branch operations require only a single input comparator instead of a comparater for each CCL stage in the filter.

The adaptive filter of figure 3 may be modified as shown in figure 4. The exclusive OR gates perform a binary multiplication of the quantities sgn [ϵ(m)] and sgn [X(m-j)] {i.e., sgn [ϵ(m)] $\otimes$ sgn [X(m-j)]} to generate an output signal to control the polarity switches. The polarity switches serve as single pole-double-throw type to direct the scaled error $\pm 2\mu\epsilon(m)$ to the appropriate weight. As we will see later, the functions of integration (storage) and multiplication (weighting) can be performed by a single MNOS nonvolatile memory transistor operating in its triode region as a linear conductance multiplier to convert a tapped analog voltage to current. An alternative method is to use bidirectional charge-control to set the analog conductance of a MOS multiplier. These techniques are discussed in Section 5.

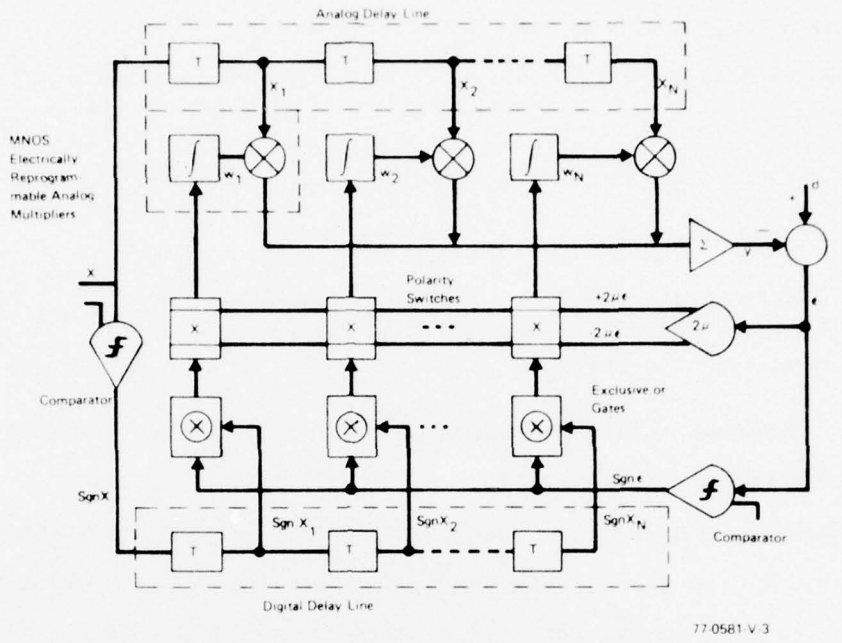

Figure 4. Adaptive Filter with Cascaded CCL's to Implement "Clipped Data" LMS Algorithm

3.2 OTHER FORMS OF THE LMS ALGORITHM

We have discussed two forms of the LMS algorithm which lead to cross-correlation functions:

$$\rho_j \left(\begin{matrix} \text{Linear} \\ \text{LMS} \end{matrix} \right) = \sum_{m=1}^{M} \epsilon(m)\, X(m-j) \tag{29}$$

$$\rho_j \left(\begin{matrix} \text{Clipped} \\ \text{Data} \\ \text{LMS} \end{matrix} \right) = \sum_{m=1}^{M} \epsilon(m)\, \text{sgn}\left[X(m-j) \right]$$

The LMS algorithm, as we have discussed, cross-correlates the output error with the tapped data (i.e., delayed data signal) at each tap to generate the

update or incremental adjustment for the tap weight. There are two other forms of the LMS algorithm which have been treated in the literature:[49]

$$\rho_j \text{ (Hybrid)} = \sum_{m=1}^{M} X(m-j)\ \text{sgn}\left[\epsilon(m)\right]$$

$$\rho_j \left(\begin{matrix} \text{Modified} \\ \text{Zero} \\ \text{Forcing} \end{matrix} \right) = \sum_{m=1}^{M} \text{sgn}\ \left[\epsilon(m)\right]\ \text{sgn}\ \left[X(m-j)\right] \tag{30}$$

The work of Hirsch and Wolf is interesting since they compared various types of algorithms for the application of adaptive equalization as well as introduce the field-effect transistor for voltage-controlled conductance tap weights.[49] In the 1960's, the use of adaptive filters was an important commercial outgrowth of research and development of algorithms by the Bell Telephone Laboratories.[50, 51] The adaptive equalizer is used in high-speed MODEM's for digital communication and connecting remote terminals to computers as well as computer to computer. The rate and accuracy of the data transmission is increased by equalizing the baseband distortion and reducing the intersymbol interference. The early adaptive equalizer development[52] used the so-called zero-forcing (ZF) algorithm which minimized the expression

$$\rho_j \text{ (ZF)} = \sum_{m=1}^{M} \text{sgn}\ \left[\epsilon(m)\right]\ \text{sgn}\ \left[Y(m-j)\right] \tag{31}$$

---

[49] D. Hirsch and W. Wolf, "A Simple Adaptive Equalizer for Efficient Data Transmission," IEEE Trans. Comm. Tech., Com-18, 5 (1970).

[50] R. Lucky, "Automatic Equalization for Digital Communications," B.S.T.J., 44, 547 (1965).

[51] R. Lucky, et.al., Principles of Data Communications, New York: McGraw-Hill (1968).

[52] R.W. Lucky, "Techniques for Adaptive Equalization of Digital Communication Systems," B.S.T.J., 44, 547 (1965).

where the output error is cross-correlated with delayed versions of the equalized output. For random data and unequalized inputs with so-called "open" binary-eye patterns, the ρ_j's are estimates of the equalized pulse response and the ZF algorithm adjusts the j^{th} tap weight to force ρ_j to zero (except the center tap of the equalizer which corresponds to the peak of the pulse). The convergence properties of the ZF algorithm were inferior to the mean square error (MS) algorithm because for "closed" binary-eye patterns the covergence was not guaranteed since the slicing operations (with comparators) yielded an unreliable estimated reference (main or desired input). Subsequently, the adaptive equalizer development emphasized the use of the MS algorithm. An interesting comparison of the ZF, MS, Hyb., and MSF algorithms was presented by Hirsch and Wolf[49] as illustrated in figure 5 for the equalized peak distortion defined by the expression

$$D_{peak} \equiv \sum_{\substack{\text{summed over all taps} \\ \text{except center tap}}} |\rho_j| \tag{32}$$

3.3 A 2-TAP WEIGHT ADAPTIVE FILTER UNDER THE CONTROL OF THE "CLIPPED DATA" LMS ALGORITHM

In this section, we will present a simple analysis of a 2-tap weight adaptive filter under the control of the "clipped data" LMS algorithm. Figure 6 illustrates a block diagram of the adaptive filter. We will analyze this adaptive filter for a sinusoidal signal in the presence of white noise. The desired signal may be written as,

$$d(t) = d_o \cos(\omega t + \phi) \tag{33}$$

where ϕ is a relative phase-shift with respect to the signal at tap 1. The tapped signals are,

$$\begin{aligned} X_1(t) &= X_o \cos \omega t + n_1(t) \\ X_2(t) &= X_o \cos \omega(t-T) + n_2(t) \end{aligned} \tag{34}$$

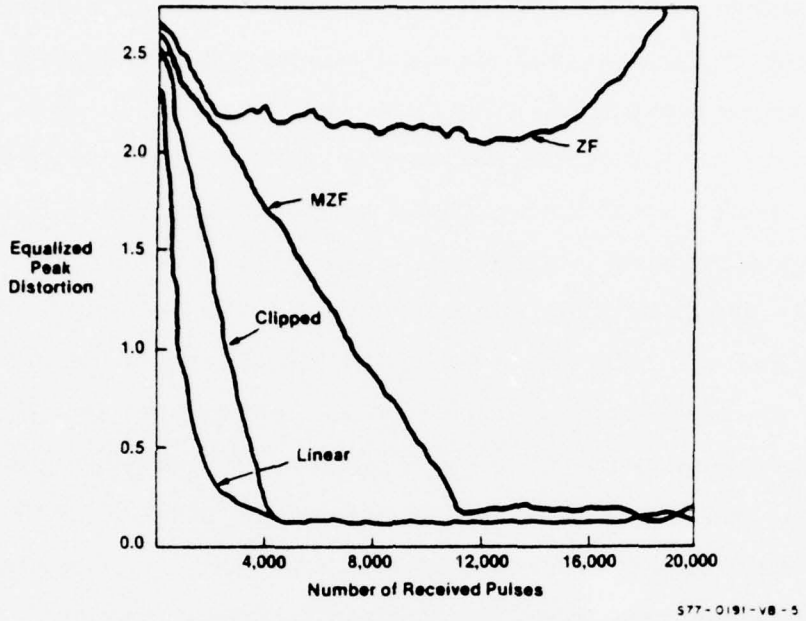

Figure 5. Comparison of Various Algorithms for an Adaptive Equalizer

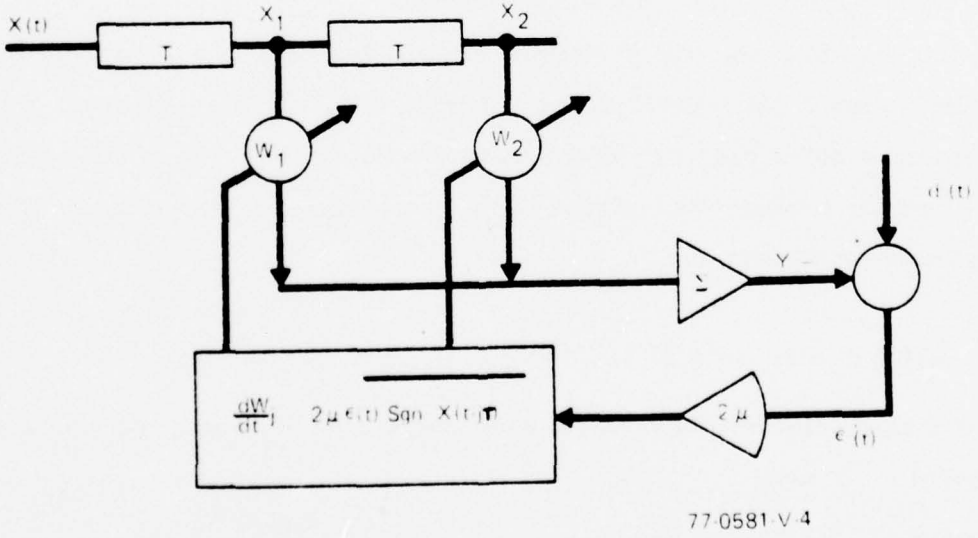

Figure 6. A 2-Tap Weight Adaptive Filter with "Clipped Data" LMS Algorithm

where T is the time delay between tap positions and $n_1(t)$, $n_2(t)$ are uncorelated noises at the tap positions. The matrix elements of the covariance matrix (see equation 9) become,

$$\overline{X_1(t)\ \mathrm{sgn}\left[X_1(t)\right]} = \overline{(s+n_1)\ \mathrm{sgn}\ (s+n_1)} = \overline{s\ \mathrm{sgn}\ s} + \overline{n_1\ \mathrm{sgn}\ n_1} \tag{35}$$

$$= \frac{2X_o}{\pi} + \sqrt{\frac{2}{\pi}}\ \sigma_n$$

where

$$\overline{n_1^2(t)} = \overline{n_2^2(t)} = \sigma_n^2$$
$$\overline{n_1(t)n_2(t)} = \overline{sn_1} = \overline{sn_2} = 0 \tag{36}$$

Calculation of the remaining matrix elements yields

$$\overline{X_1(t)\ \mathrm{sgn}\left[X_2(t)\right]} = \overline{X_2(t)\ \mathrm{sgn}\left[X_1(t)\right]} = \frac{2X_o}{\pi}\cos\omega T \tag{37}$$

$$\overline{d(t)\ \mathrm{sgn}\left[X_1(t)\right]} = \frac{2d_o}{\pi}\cos\phi$$

$$\overline{d(t)\ \mathrm{sgn}\left[X_2(t)\right]} = \frac{2d_o}{\pi}\cos(\omega T+\phi)$$

which yields the weight equation (see equation 18):

(38)

$$\frac{d}{dt}\begin{pmatrix} W_1 \\ \hline W_2 \end{pmatrix} = \frac{4\mu d_o}{\pi}\begin{pmatrix} \cos\phi \\ \hline \cos(\omega T+\phi) \end{pmatrix} - 2\mu\left(\begin{array}{c|c} \frac{2X_o}{\pi}+\sqrt{\frac{2}{\pi}}\,\sigma_n & \frac{2X_o}{\pi}\cos\omega T \\ \hline \frac{2X_o}{\pi}\cos\omega T & \frac{2X_o}{\pi}+\sqrt{\frac{2}{\pi}}\,\sigma_n \end{array}\right)\begin{pmatrix} W_1 \\ \hline W_2 \end{pmatrix}$$

The above equation for the weights illustrates the cross-coupling between the taps caused by the delay T and when $\omega T = (2k+1)\pi/2$, $k = 0, 1, 2\ldots$ the system is decoupled and in so-called normal form. We can transform the weights into a normal coordinate system with

$$W = \Phi\,\eta \tag{39}$$

where

$$\Phi = \left(\begin{array}{c|c} \frac{1}{\sqrt{2}} & \frac{1}{\sqrt{2}} \\ \hline -\frac{1}{\sqrt{2}} & \frac{1}{\sqrt{2}} \end{array}\right) \tag{40}$$

is the transformation matrix. Application of this transformation to equation (18) yields

$$\frac{d}{dt}\begin{pmatrix}\eta_1\\ \eta_2\end{pmatrix} = \frac{4\mu d_o}{\sqrt{2}\,\pi}\begin{pmatrix}\cos\phi - \cos(\omega T + \phi)\\ \cos\phi + \cos(\omega T + \phi)\end{pmatrix}$$

$$- 2\mu\left(\begin{array}{c|c} \frac{2X_o}{\pi}(1 - \cos\omega T) + \sqrt{\frac{2}{\pi}}\,\sigma_n & 0 \\ \hline 0 & \frac{2X_o}{\pi}(1 + \cos\omega T) + \sqrt{\frac{2}{\pi}}\,\sigma_n \end{array}\right)\begin{pmatrix}\eta_1\\ \eta_2\end{pmatrix}$$

with equations (39) and (41) we can write the transient weight response of the normal weights in terms of time constants.

$$\tau^- = \frac{1}{2\mu\left[\frac{2X_o}{\pi}(1 - \cos\omega T) + \sqrt{\frac{2}{\pi}}\,\sigma_n\right]}$$

$$\tau^+ = \frac{1}{2\mu\left[\frac{2X_o}{\pi}(1 + \cos\omega T) + \sqrt{\frac{2}{\pi}}\,\sigma_n\right]} \tag{42}$$

and a steady state solution for the weights becomes

$$W_1(s.s.) = \frac{d_o\left[\left(X_o + \sqrt{\frac{\pi}{2}}\,\sigma_n\right)\cos\phi - X_o\cos\omega T\cos(\omega T + \phi)\right]}{\left(X_o + \sqrt{\frac{\pi}{2}}\,\sigma_n\right)^2 + \cos^2\omega T} \tag{43}$$

$$W_2(s.s.) = \frac{d_o\left[\left(X_o + \sqrt{\frac{\pi}{2}}\,\sigma_n\right)\cos(\omega T + \phi) - X_o\cos\phi\cos\omega T\right]}{\left(X_o + \sqrt{\frac{\pi}{2}}\,\sigma_n\right)^2 + \cos^2\omega T}$$

which we observe is a function of frequency providing $\omega T \neq (2k + 1)\pi/2$, $k = 0, 1, 2, \ldots$. When this condition is approached, the optimal weights approach the values,

$$W_1 \text{ (opt.)} \rightarrow \frac{d_o \cos \phi}{X_o + \sqrt{\frac{\pi}{2}}\, \sigma_n}$$

$$W_2 \text{ (opt.)} \rightarrow \frac{-d_o \sin \phi}{X_o + \sqrt{\frac{\pi}{2}}\, \sigma_n} \qquad \omega T \simeq (2k + 1)\, \pi/2 \qquad (44)$$

and the weights are decoupled from one another as the coordinate system approaches normal form.

Glover[53] has analyzed the particular case when there is a 90 degree phase shift between the weights for adaptive noise cancelling in the form of a notch filter. He showed when a sum of sinusoids is applied to an adaptive filter, the filter converges to a dynamic solution in which the weights are time varying. This time-varying solution gives rise to a tunable notch filter with a notch located at each of the reference frequencies. In the example considered, the desired and reference inputs were operating at the same frequency (i.e., $f_d = f_r$). Glover showed[53] for $f_d \neq f_r$ the weights have a dynamic stealy-state response with an oscillation at the difference frequency $f_d - f_r$ and the instantaneous response at f_r. This time-varying solution should not be considered as noise in the adaptation process. In essence, the time-varying weights modulate the reference frequency f_r and hetrodyne it into the desired frequency f_d, thus, creating a notch effect.

---

[53] J. R. Glover, "Adaptive Noise Cancelling of Sinusoidal Interference," Naval Underseas Center, San Diego, Calif. Rep't # TN 1617, Dec. 1975. (Stanford University Ph. D. Thesis).

3.3.1 A 2-TAP ADAPTIVE NOTCH FILTER

In this section we will examine a simple single-frequency noise canceller with 2-adaptive weights under the operation of the "clipped data" LMS algorithm. Figure 7 illustrates the single frequency noise canceller in which the desired input may be any type of signal (i.e., stochastic, deterministic, periodic, transient, or combination thereof) while the input signal is a pure cosine wave $X_o \cos(\omega_o t - \phi)$. The desired and input signals are sampled synchronously at $f_c = 1/T$ with a 90 degree phase between X_1 and X_2 taps. The algorithm for updating the weights is,

$$W_1(m+1) = W_1(m) + 2\mu\epsilon(m)\,\mathrm{sgn}\,[X_1(m)]$$
$$W_2(m+1) = W_2(m) + 2\mu\epsilon(m)\,\mathrm{sgn}\,[X_2(m)] \tag{45}$$

where,

$$X_1(m) = X_o \cos(\omega_o mT - \phi)$$
$$X_2(m) = X_o \sin(\omega_o mT - \phi) \tag{46}$$

The first step in the analysis is to consider the adaptive noise canceller as a feedback network with the filter output $Y(m)$ disconnected. Under these conditions, a unit impulse at $m = k$ is applied at the desired input to create an error,

$$\epsilon(m) = \delta(m-k) \begin{cases} 1 & m=k \\ 0 & m\neq k \end{cases} \tag{47}$$

The transfer function of the incremental weight change may be written as,

$$z\{W_1(m+1) - W_1(m)\} = (Z-1)\,W_1(Z) \tag{48}$$

or

$$W_1(Z) = U(Z)\,z\{2\mu\epsilon(m)\,\mathrm{sgn}\,[X_1(m)]\} \tag{49}$$

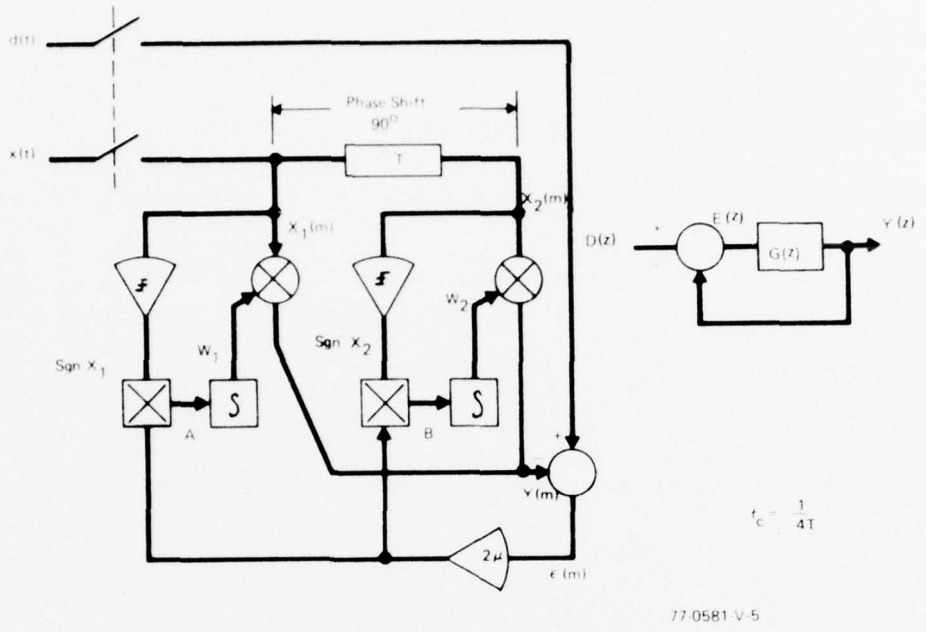

Figure 7. Single Frequency Adaptive Noise Canceller

Where $U(Z) = (Z-1)^{-1}$. The impulse response of U(Z) is the step response,

$$u(m-1) = \begin{cases} 1 & m \geq 1 \\ 0 & m < 1 \end{cases} \tag{50}$$

Convolution of $u(m-1)$ with $2\mu\,\epsilon(m)\,\mathrm{sgn}\,[X_1(m)]$ yields the weight,

$$W_1(m) = 2\mu\ \mathrm{sgn}\,[\cos(\omega_o\, kT - \phi)] \qquad m \geq k+1 \tag{51}$$

and the corresponding filter output is,

$$Y_1(m) = 2\mu\, X_o \cos(\omega_o\, mT - \phi)\ \mathrm{sgn}\,[\cos(\omega_o\, kT - \phi)] \qquad m \geq k+1 \tag{52}$$

Similarly,

$$Y_2(m) = 2\mu\, X_o \sin(\omega_o mT - \phi)\ \mathrm{sgn}\,[\sin(\omega_o\, kT - \phi)] \qquad m \geq k+1 \tag{52}$$

with the total output,

$$Y(m) = Y_1(m) + Y_2(m) = 2\mu X_o \left[\cos(\omega_o mT - \phi)\ \mathrm{sgn}\left[\cos(\omega_o kT - \phi)\right] + \sin(\omega_o mT - \phi)\ \mathrm{sgn}\left[\sin(\omega_o kT - \phi)\right]\right] \qquad m \geq k+1 \qquad (53)$$

Equations 47 and 53 may be Z-transformed to yield the pulse transfer function.

$$G(Z, k) = 2\mu\sqrt{2}\ X_o \frac{\left\{Z\cos\left[(k+1)\omega_o T - \phi - \pi/4\right] - \cos\left[k\omega_o T - \phi - \pi/4\right]\right\}}{Z^2 - 2Z\cos\omega_o T + 1} \qquad (54)$$

where $0° \leq k\omega_o T - \phi \leq \pi/2$, since the above transfer function repeats every 90 degrees. In the above form, G(Z, k) is nontime-invariant,and in order to remove the k-dependence,we will average over the period indicated to obtain

$$\overline{G(Z)} = \frac{8\mu X_o}{\pi} \frac{(Z\cos\omega_o T - 1)}{Z^2 - 2Z\cos\omega_o T + 1} \qquad (55)$$

Since the closed-loop transfer function is

$$H(Z) = \frac{E(Z)}{D(Z)} = \frac{1}{1 + \overline{G(Z)}} \qquad (56)$$

with closed-loop zeroes given as

$$Z = e^{\pm j\omega_o T} \qquad (57)$$

and poles from the solution of $1 + \overline{G(Z)} = 0$. If we make the narrowband approximation with $\mu X_o < 1$, then the poles are inside the unit circle with a radial distance.

$$\left(1 - 8\mu\frac{X_o}{\pi}\right)^{1/2} \simeq 1 - 4\mu\frac{X_o}{\pi} \qquad (58)$$

from the origin as shown in figure 38. The angles of the poles are almost identical to those of the zeroes with a notch filter bandwidth

$$\text{B.W.} = \frac{8\mu X_o}{\pi T} \qquad (59)$$

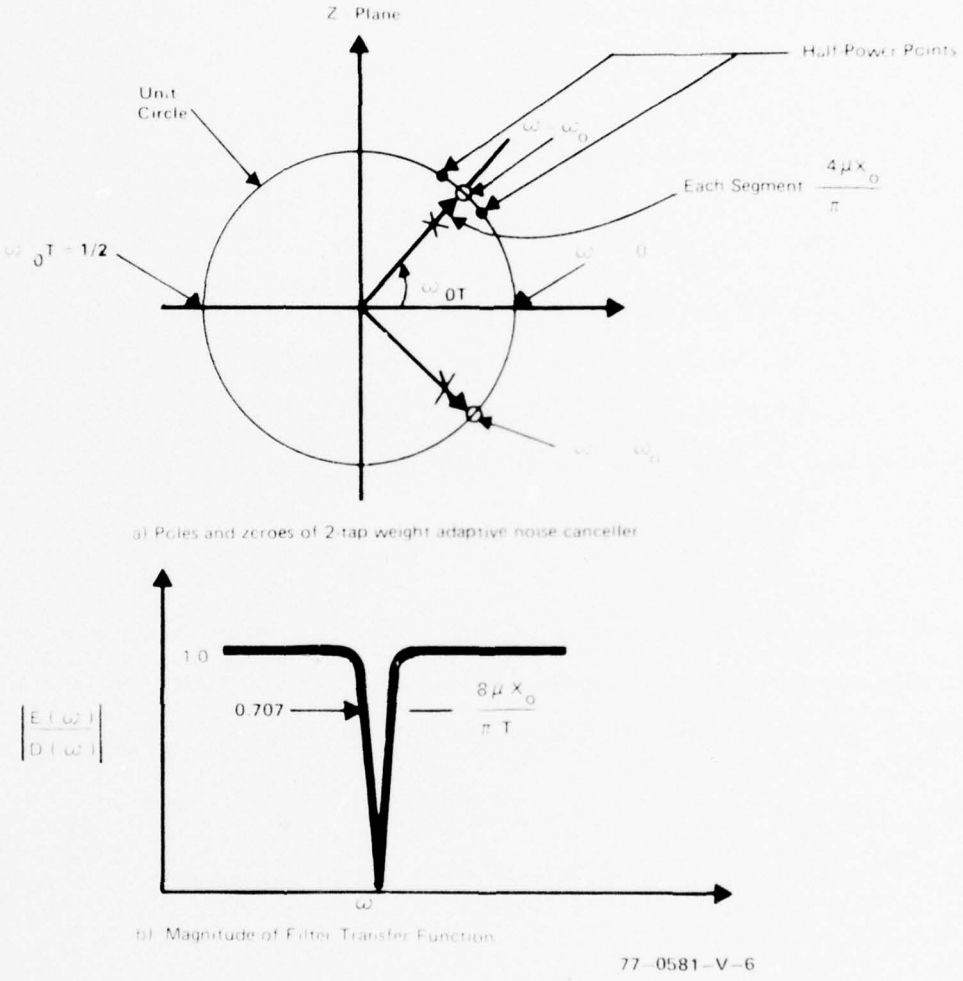

a) Poles and zeroes of 2-tap weight adaptive noise canceller

b) Magnitude of Filter Transfer Function

77-0581-V-6

Figure 8. Characteristics of a 2-Tap Weight Adaptive Noise Canceller Under the Control of a Clipped-Data LMS Algorithm

with a Q,

$$Q = \frac{\omega_o}{B.W.} = \frac{\pi}{8} \frac{\omega_o T}{\mu X_o} \tag{60}$$

A special case of the notch filter is to $\omega_o = 0$ in equations 55 and 56 to yield

$$H(Z, \omega_o = 0) = \frac{Z - 1}{Z - (1 - 8 \frac{\mu X_o}{\pi})} \tag{61}$$

which places the notch at zero frequency to cancel low frequency drift. Since there is no need to match the phase of the signal, only one weight is needed. The bandwidth is given by equation 59 and the transfer function, expressed by equation 61, indicates a pole-zero separation of,

$$\frac{8 \mu X_o}{\pi}$$

on the real axis. The use of a bias weight can remove slowly varying drift components in the input signal and may be used simultaneously with operation to cancel periodic or stochastic interference.

4. CHARGE-COUPLED DEVICES (CCD'S) WITH ANALOG CONDUCTANCE WEIGHTS

In figure 1 we observed that a basic requirement of the linear combiner is the analog delay line. The charge-coupled device (CCD)[54] analog shift register processes discrete analog samples of input data through the translation of charge packets in synchronization with an external clock. CCD basic building blocks provide a flexible approach to discrete analog signal processing in systems.[55] One-dimensional basic building blocks[56] (linear arrays) may be classified according to the characteristic information flow patterns:

a. Serial in/serial out (SI/SO)

b. Parallel in/serial out (PI/SO)

c. Serial in/parallel out (SI/PO)

A simplification of the CCD analog shift register (SI/SO) is shown in figure 9 and the clock timing in figure 10. The timing is arranged so the switch toggling frequency is one-half of the 4-phase clock frequency. Thus, the input sampling switch, S_1, alternately samples data and zero reference.[57]

---

[54] W. S. Boyle and G. E. Smith, "Charge-Coupled Semiconductor Devices," B. S. T. J., 49, 587 (1970).

[55] M. H. White and D. R. Lampe, "Charge-Coupled Device (CCD) Analog Signal Processing," IEEE Press Selected Reprint Series, Charge-Coupled Devices: Technology and Applications, R. Melen and D. Buss, eds., IEEE, N. Y. - (1977).

[56] D. R. Lampe, M. H. White, W. R. Webb, J. H. Mims and G. A. Gilmour, "CCD's for Discrete Analog Signal Processing (DASP)," INTERCON 74, March 1974, New York.

[57] J. Mattern and D. R. Lampe, "A Reprogrammable Filter Tank Using CCD Discrete Analog Signal Processing," 1975 ISSCC, pg. 148, Technical Digest, Feb. 12-14, 1925, Phil. Pa.

At the output, switch S_2 clamps during zero reference, samples during data, and holds when it is not actually sampling. The output capacitor, therefore, contains only the "time-stretched" data samples. In a shift register with N pairs of stages, there will be N signal samples and N zero reference samples, each of duration T/2. There are several advantages associated with this technique of data flow:

- Increased isolation between data samples (i.e., reduction in cross-talk between samples) with minimal signal loss
- The reference sample and signal sample pass through the same path and first-order offsets can be corrected in PI/SO and SI/PO structures
- Increased spatial extension between taps on a SI/PO structure to aid in layout of peripheral processing circuitry.

Figure 10 illustrates a complementary 4-phase clock sequence for operating a SI/SO CCD. The waveforms ϕ_1 through ϕ_4 are the 4-phase clocks whose function is to propagate charge down the line without dispersion. Waveform S_1 demonstrates the input switch functions: data is sampled in the up position, and zero reference is sampled in the down position. V_o demonstrates the appearance of the delay line output voltage with the alternate data and zero reference outputs confined to 3/8T. S_2 demonstrates the output processing functions: the data is sampled in the up position, the zero is clamped in the down position, and the data is held when it is not sampled (center). The interval from data sample to data sample is T and the total transport time is NT where N is the number of CCD analog delay line data stages. Thus, the signal delay for a SI/SO CCD analog shift register is,

$$\tau = NT = N/f_c \tag{62}$$

which illustrates the electrically alterable delay feature of the CCD delay line. Since the sampling therein requires the analog signal to be sampled at least twice during the period of the highest component of interest, we may write

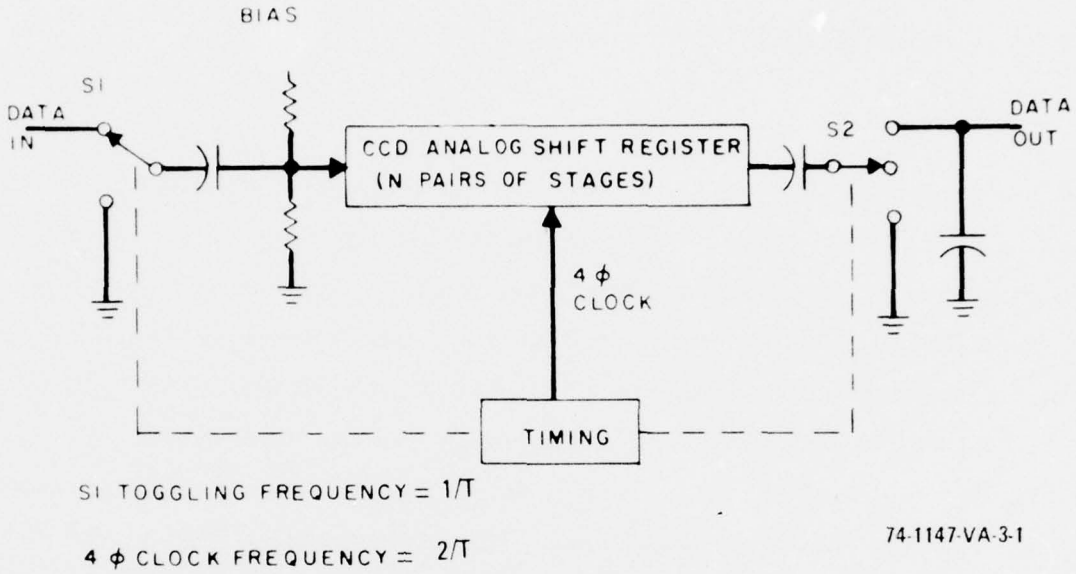

Figure 9. CCD Analog Shift (SI/SO)

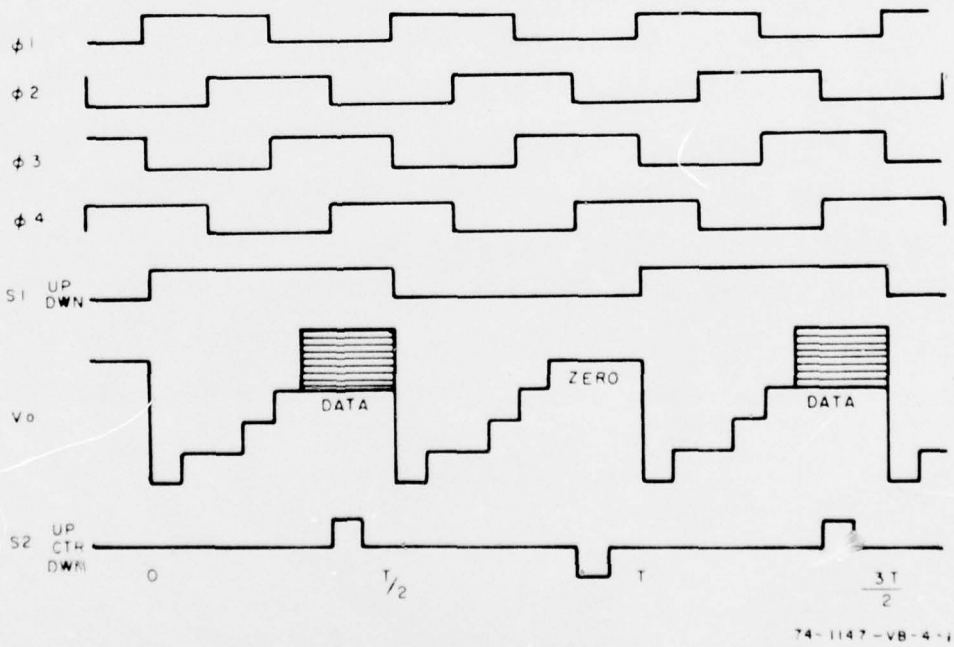

Figure 10. Basic CCD 4-Phase Clock Timing for SI/SO CCD

$$f_s \leq \frac{1}{2} T = f_s \text{ (max)} \tag{63}$$

and the time-delay bandwidth product becomes,

$$f_s \leq N/2 \tag{64}$$

The low frequency limit is set by the thermal leakage current which accumulates in each stage, and the upper frequency limit is determined by input charge injection, transfer efficiency, and output charge detection and reconstruction circuitry. Figure 11 illustrates a cross-section of a 4-phase electrode CCD with transfer and storage electrode dimensions. The CCD is fabricated with PMOS silicon-gate technology and the insulator is a dual-dielectric comprised of silicon nitride (Si_3N_4) over thermal silicon dioxide (SiO_2). The electrodes are fabricated with polycrystalline silicon and aluminum, to give coplanar but overlapping electrodes. The overlapping electrode feature provides a "sealed" CCD surface and stable operation under temperature-bias excursions. Structures may be fabricated with both electrodes made of polycrystalline silicon. Although, the dimensions used in the CCD's discussed in this report are 8μm Al and 12μm PolySi., we have fabricated CCD's with 4μm length Poly Si electrodes.

The CCD delay line[58] provides a unidirectional transfer of charge $q_s(x, t)$ from one storage cell to another adjacent cell. The signal charge is designated in cell X at time t, where X and t assume integer values; i.e., the unit of distance is the cell-to-cell separation X_o, and the unit of time is the clock period T. The frequency response of the CCD delay line due to transfer inefficiency ϵ per stage delay may be calculated from a discrete formulation:

$$q_s(x, t) = \epsilon\, q_s(x, t-1) + (1-\epsilon)\, q_s(x-1, t-1) \tag{65}$$

---

[58] W. B. Joyce and W. J. Bertram, "Linearized Dispersion Related and Green's Function for Discrete Charge Transfer Devices with Incomplete Transfer," B.S.T.J., 50, 1741 (1971).

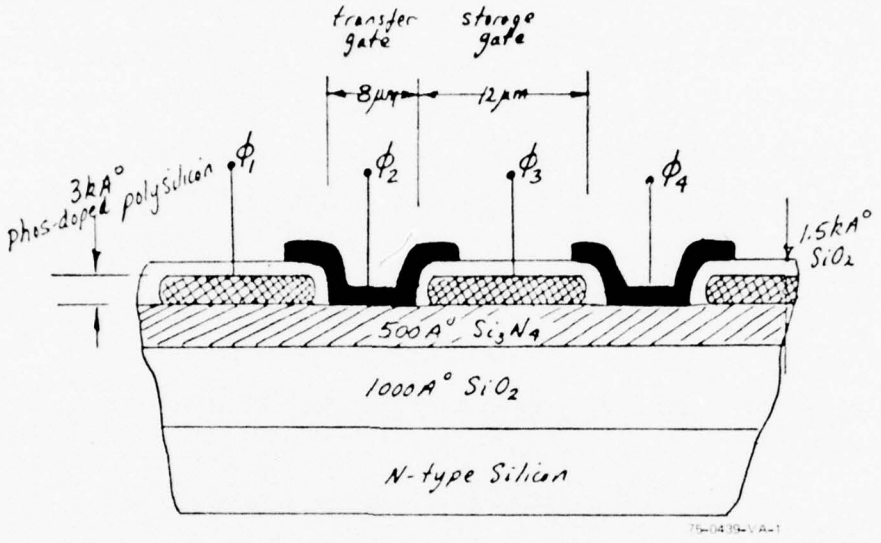

Figure 11. Cross Section of 4-Phase CCD Stage Delay

where $\epsilon \leq 1 \times 10^{-4}$ for $f_s < 1$ MHz. We may transform equation (65) to the Z domain.

$$Q_s(x, Z) = \frac{Z^{-1}(1-\epsilon)}{1 - Z^{-1}\epsilon} \quad Q_s(x-1, Z) \tag{66}$$

and the transfer function for a N-stage CCD delay becomes[59]

$$H(Z) = \frac{V_{OUT}(Z)}{V_{in}(Z)} = \frac{g_m R_F C_{in}}{C_{OUT}} \left[\frac{1 - \epsilon}{1 - \epsilon Z^{-1}}\right]^N Z^{-N} \tag{67}$$

---

[59] D. D. Buss and W. H. Bailey, "Applications of Charge Transfer Devices to Communication" 1973 CCD Application Conference, Sept. 1973, p. 83 Technical Papers Digest, San Diego, Calif.

where C_{in}/C_{OUT} is the ratio of input to output capacitances and g_m is the transconductance of the on-chip amplifier while R_F is the off-chip feedback resistor in an operational summing amplifier. In order to minimize amplitude and frequency dispersion in a CCD analog delay line, we should restrict $N\epsilon < 0.1$ and preferrably considerably less. For example, if $N\epsilon = 0.1$, then the insertion loss is -1.8 dB at two Nyquist limit ($f_s = 0.5\, f_c$) and the maximum phase deviation from linearity is ±3° at $f_s = 0.25\, f_c$.

The SI/SO block is a simple CCD analog shift register to provide the basic function of delay for the linear combiner of the LMS adaptive filler. Typical dynamic range has been measured on SI/SO structures as,

$$\text{D.R.}_{S/N}\left(\frac{\text{Pk. to Pk. Signal}}{\text{r.m.s. noise}}\right) \geq 100 \text{ dB} \quad \text{narrowband} \quad f_s = 15 \text{ kHz} \quad \text{with } \pm 0.5\text{V input signal}$$

$$\text{D.R.}_{\text{Lin.}}\left(\frac{\text{fundamental of output at } f_s}{\text{2nd harmonic of output at } 2f_s}\right) \geq 55 \text{ dB} \quad f_s = 1 \text{ kHz} \quad f_c = 200 \text{ kHz} \quad \text{with } \pm 0.5\text{V input signal}$$

in which the linear dynamic range illustrates the accuracy of the analog delay line (i.e. equivalent to 9 digital bits). This accuracy improves as the input signal is reduced since the distortion associated with the input injection and output detection circuitry is reduced. The clock requirements may vary from TTL level on buried channel CCD's to CMOS/MOS levels on surface channel CCD's. In general, CMOS levels (i.e. 10 to 18V) are needed to obtain the dynamic range and frequency response. Since the CCD is a sampled data system pre- and post-filtering of the signal is required (ideally a filter with a sharp cutoff at $0.5\, f_c$) to limit aliasing effects.[60]

---

[60] C.H. Sequin and M.F. Tompseff, Charge Transfer Devices (Supplement 8 to Advances in Electronics and Electron Physics), New York: Academic Press (1975).

4.1 SERIAL IN/PARALLEL OUT (SI/PO) TRANSVERSAL FILTERING WITH CHARGE-COUPLED DEVICES (CCD's)

CCD transversal filters with fixed analog tap weights have been implemented with the split-electrode weighting technique.[61] In this method, a CCD delay line becomes a transversal filter by splitting one of the electrodes in each delay line and placing a differential current integrator in the clock line instead of the conventional output amplifier. In the adaptive filter approach, we require adaptive or electronically reprogrammable filters. In this section, a SI/PO CCD is discussed which features independent, nondestructive, low-impedance voltage readouts of delayed analog signals at specified locations or taps along the CCD delay line. In general, the signal voltage at each tap may be multiplicatively weighted by a conductance to give a current proportional to the product of the signal voltage and the weighting conductance. Figure 12 illustrates a photomicrograph of a SI/PO block (N = 20 outputs) which uses a floating clock electrode sensor at alternate stage delays along the CCD delay line.[62] This permits the use of a "reference-only" and "signal and reference" to compensate for nonuniformities in the SI/PO structure. Numerous taps with multiplicative analog weighting can be accommodated without signal amplitude degradation due to stray parasitic capacitance, by paralleling SI/PO blocks of feasible size due to the summation of product currents. Furthermore, the independent nondestructive voltage taps of the SI/PO block can provide the analog voltage signals needed by multipliers to give CCD real-time analog correlation. Use of programmable conductances such as the nonvolatile MNOS type or conventional MOS type permit such device applications as adaptive transversal line equalizer or programmable matched filter (or correlation detector) for secure voice/data communications systems.

---

61 D. D. Buss, D. R. Collins, W. H. Bailey, and C. R. Reeves, "Transversal Filtering Using Charge Transfer Devices," IEEE J. Solid-State Circuits, SC-8, 134 (1973)

62 M. H. White, I. A. Mack, F. J. Kub, D. R. Lampe, and J. L. Fagan, "An Analog CCD Transversal Filter with Floating Clock Electrode Sensor and Variable Tap Gain," ISSCC 76, Technical Digest pg. 194, Phildelphia, Pa.

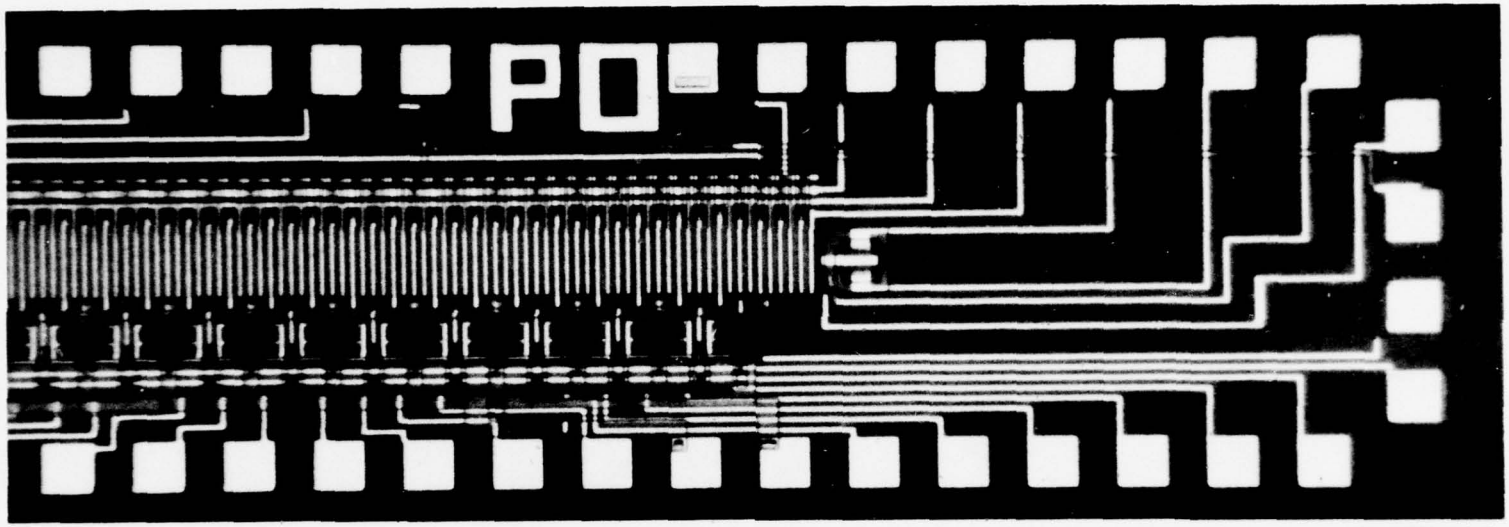

Figure 12. Photomicrograph of SI/PO CCD Basic Building Block for Tapped Analog Delay Line of Linear Combiner

The ability to easily change or modify the transfer function of a system or subsystem requires central components whose characteristics are determined by a few variable parameters. In applications involving filtering of sampled data, the transversal filter is the primary component. Figure 13 illustrates a transversal filter which consists of an N-stage tapped delay line and associated weights at each tap point.[63]

The output of the transversal filter at the m^{th} clock time can be represented as

$$e_o(mT) = \sum_{k=1}^{N} W_k \, e_i(mT - kT) \tag{68}$$

where T is the time delay between successive tap locations in the delay line. If the input to the filter is written in the form

$$e_i(mT - kT) = e^{j2\pi f_s (mT - kT)} \tag{69}$$

where f_s is the frequency of the input signal, the magnitude of the output becomes

$$\left| e_o(U) \right| = \left| \sum_{k=1}^{N} W_k \, e^{-j \frac{2\pi Uk}{N}} \right| \tag{70}$$

where $U = Nf_s T$ is the normalized frequency. $e_o(U)$ is the discrete Fourier transform of the weights W_k. The type of filter, bandpass, low-pass, high-pass, etc, is determined by the weighting coefficients W_k while the characteristics of the filter are determined by the number of taps, N, and the interstage delay time, T.

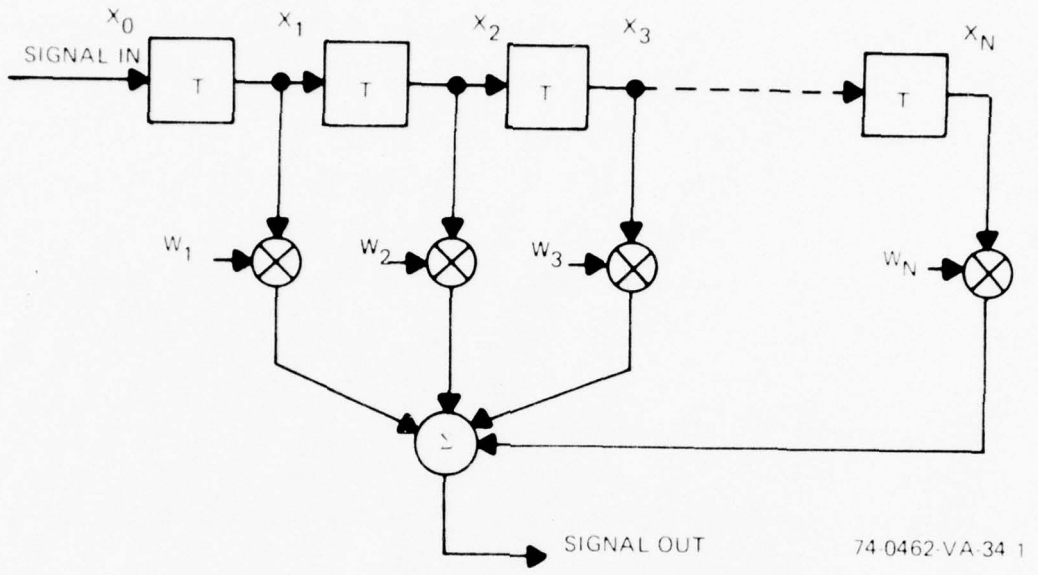

Figure 13. Transversal Filter

The analog delay line nature of the CCD provides a means for implementing an analog transversal filter[64-66] providing:

1) the signal in the delay line can be sensed nondestructively

2) the signal at each tap location is appropriately weighted, and

3) the outputs are simultaneously summed.

---

[64] D. D. Buss, D. R. Collins, W. H. Bailey, and C. R. Reeves, "Transversal Filtering Using Charge Coupled Devices," IEEE Journal of Solid-State Circuits, SC-8, pp. 138 - 146.

[65] A. Ibrahim and L. Sellars, "CCD's for Transversal Filter Applications," IEEE International Electron Devices Meeting, Technical Digest, December 1974, pp. 240-243.

[66] J. J. Tiemann, W. E. Engler, R. D. Baertsch, and D. M. Brown, "Intracell Charge - Transfer Structures for Signal Processing, "IEEE Transversal on Electron Devices, ED-21, May 1974, pp. 300.

One technique for implementing a CCD transversal filter is to sense displacement current with a floating gate electrode sensor and weight the charge at each tap with split electrodes.[64] The filter(s)[67], implemented on a particular chip, is formed during chip fabrication via the configuration of the split electrodes. A second technique employs a floating clock electrode sensor with tap weights which are independent of the intrinsic CCD structure.[68]

4.2 FLOATING CLOCK ELECTRODE SENSOR

Figure 14 illustrates the "floating clock electrode sensor" (FCES) monolithic bipolar/MOS circuit which is employed at each tap location of the CCD. Operation of the FCES circuit may be explained with the use of figure 14 and the timing diagram shown in figure 15.

As $\phi 2R$ goes negative and $\phi 2$ goes positive, charge under the $\phi 2$ electrode, the "sensing" electrode for the FCES circuit, is transferred under the $\phi 3$ electrode which is low and hence "accepting" charge. (Negative clock levels are repulsive to charge packets.) After $\phi 2$ goes low, the $\phi 2$ electrode is made attractive and hence ready to receive charge when $\phi 1$ goes attractive. The turnoff of ϕ_{2R} disconnects the ϕ_2 clock line from the ϕ_2 electrode, which now "floats". Next, the ϕ_1 barrier is lowered and charge is transferred in a progressive push-clock manner under the ϕ_2 electrode, and the displacement current is sensed by Q_2. The voltage change on the gate of Q_2 is transferred to the bipolar emitter-follower via the inverter or source-follower operation of the Q_2/Q_3 pair. The purpose of the bipolar device

---

[67] A. A. Ibrahim, G. J. Hupe, L. P. Sellars, "Multiple Filter Characteristics Using a Single CCD Structure," in 1975 Proceedings of CCD Applications Conference, October, 1975, pp. 245-249.

[68] M. H. White, I. A. Mack, F. J. Kub, D. R. Lampe, and J. F. Fagan, "An Analog CCD Transversal Filter with Floating Clock Electrode Sensor and Variable Tap Gain," ISSCC Technical Digest, February 1976, pp. 194-195.

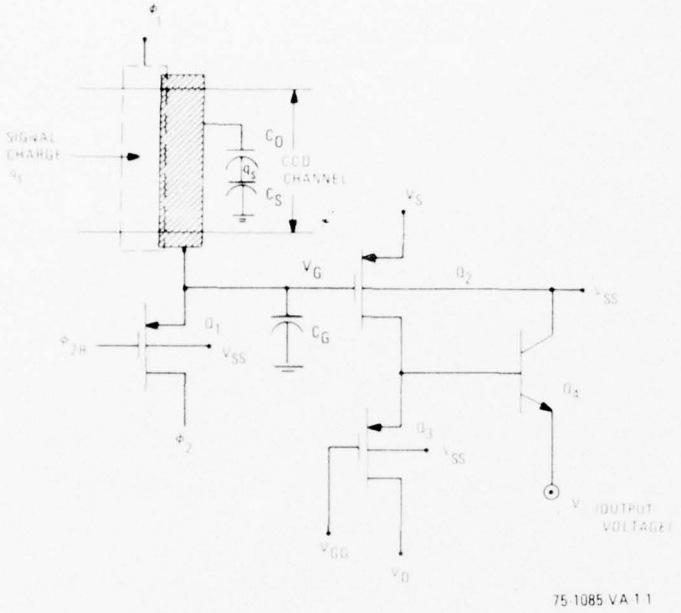

Figure 14. Floating Clock Electrode Sensor Circuit

is to provide a buffer for the MOSFET pair and serve as a voltage source for the tap weight connected to the emitter.

To achieve interchannel isolation[69], eliminate nonuniformities caused by the input circuit, and increase the spacing between tap points, a "reference or a-c zero" is interlaced between successive signal samples. In an off-chip analog reconstruction circuit, consisting of a summing amplifier and a clamp/sample circuit, the voltage corresponding to the reference is clamped and the sample operation is performed on the "reference + signal" voltage. As the clamp/sample sequence performs a differencing operation,

---

[69] T. F. Cheek Jr., J. B. Barton, S. P. Emmons, J. E. Schroeder, and A. F. Tasch Jr. "Design and Performance of Charge-Coupled Device Time - Division Analog Multiplexers," 1973 Proceedings of CCD Applications Conference, September 1973, pp. 127-139.

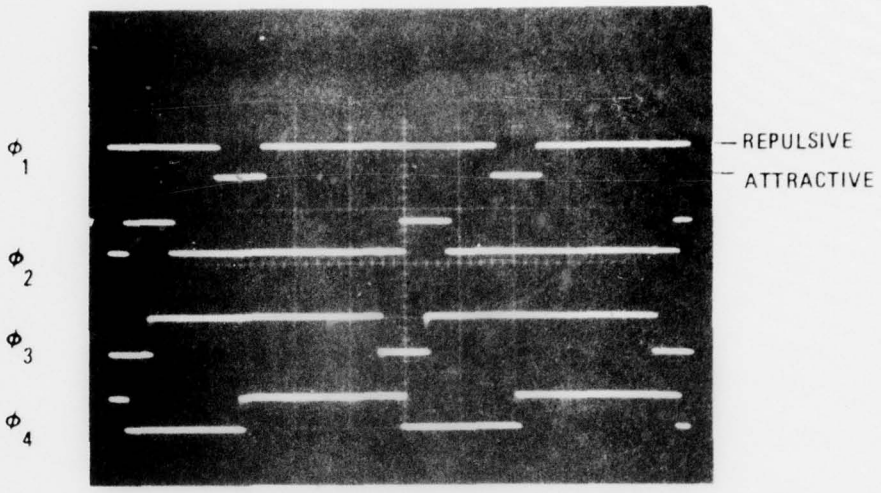

CLOCK WAVEFORMS FOR SI/PO OPERATION
20V/div. VERT, 20 μsec/div, HOR.

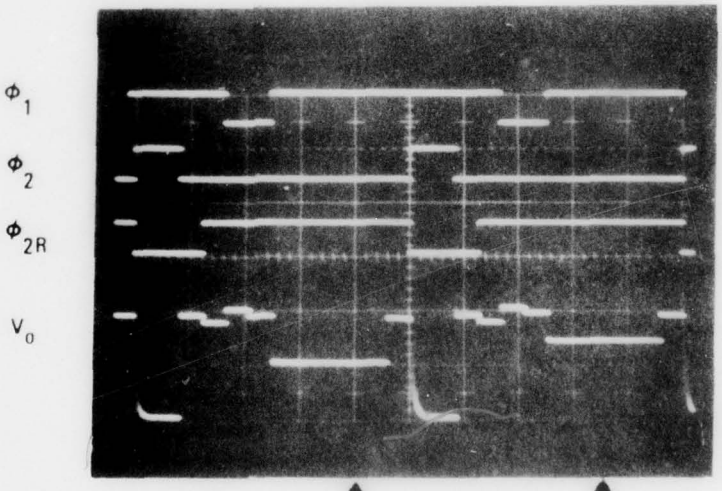

FLOATING CLOCK ELECTRODE SENSOR
(INVERTER MODE OPERATION) CLOCKS: 20V/div. V_0 2V/div.-Vert.
20μsec/div. HOR.

75-1085-PA-2

Figure 15. Clock Waveforms for FCES Circuit and Serial In/Parallel Out Operation

the output of the reconstruction circuit does not reflect offsets caused by the input circuit or crosstalk between successive signal samples. In the lower trace of figure 15 is the emitter waveform showing the output of the FCES circuit corresponding to the "reference" and "reference + signal." Figure 16 is a photomicrograph of a SI/PO CCD chip using the FCES output circuit at each tap location.

4.3 TRANSVERSAL FILTER UTILIZING THE FCES OUTPUT CIRCUIT

The harmonic content for a single tap was measured under the following conditions

$f_{clock} = 50$ kHz

$f_{sample} = f_{clock}/2$
$= 25$ kHz

$f_{signal} = 1$ kHz

Tap weight = 5 kΩ fixed resistor

$V_{input} = 1$V peak-peak

Less than 0.3 percent (-50 dB) total harmonic distortion was measured for a 1.2 volt variation of the dc bias on the G2 electrode[70] used in the stabilized charge injection input method[71, 72].

---

[70] C. H. Sequin and A. M. Mohsen, "Linearity of Electrical Charge Injection into Charge-Coupled Devices," IEEE J. Solid-State Circuits, SC-10, April 1975, pp. 81-92

[71] S. P. Emmons and D. D. Buss, "Techniques for Introducing a Low-Noise at Zero in CCD's," Device Research Conference, June 1973, Boulder, Colorado

[72] M. H. White, D. R. Lampe, J. L. Fagan, "CCD and MNOS Devices for Programmable Analog Signal Processing and Digital Nonvolatile Memory," IEDM Technical Digest, December 1973, pp. 130-131.

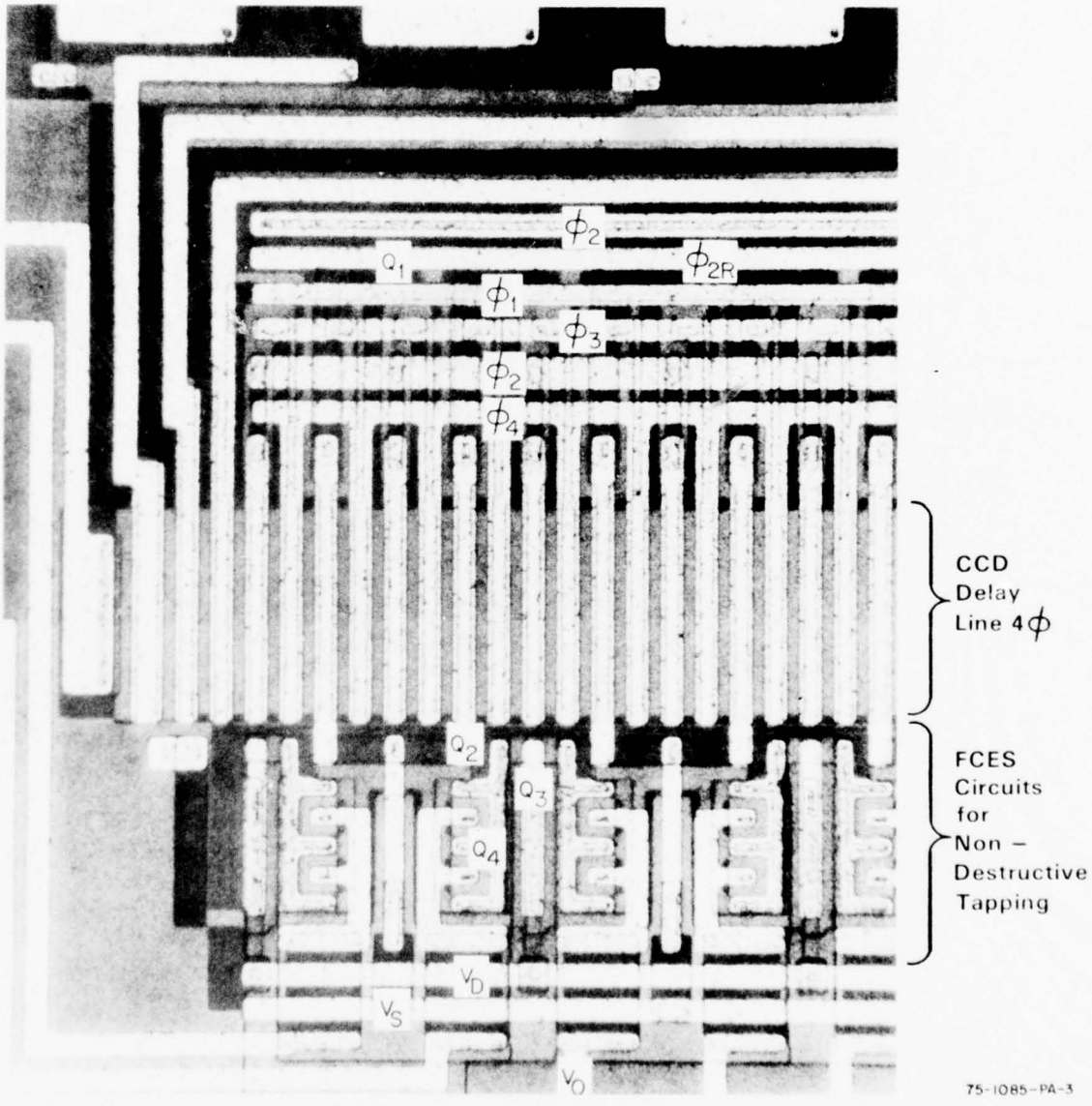

Figure 16. Photomicrograph of SI/PO CCD Chip

Figure 17 shows the impulse response of a 20 tap SI/PO CCD with the taps weighted according to a Hamming function. Each resistor value is determined by

$$R_k = \frac{R_o}{W_k} \tag{71}$$

where R_k is the resistance value of the n^{th} tap location, W_k is the Hamming weighting coefficient given by

$$W_k = 0.54 - 0.46 \cos \frac{2\pi(k-1)}{N-1} \quad 1 \leq k \leq N \tag{72}$$

and R_o is the resistance value of the center tap(s). The individual resistors are selected to within ±1 percent and the gain variations are within ±3 percent without trimming. Figure 17 also shows the frequency response of the filter with tap weights untrimmed.

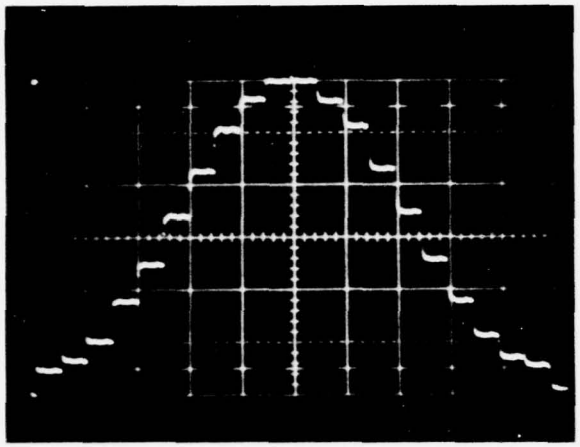

Impulse Response
(Hamming Untrimmed Weights)
1V / Div Vertical,
60 μsec/Tapweight Horizontal

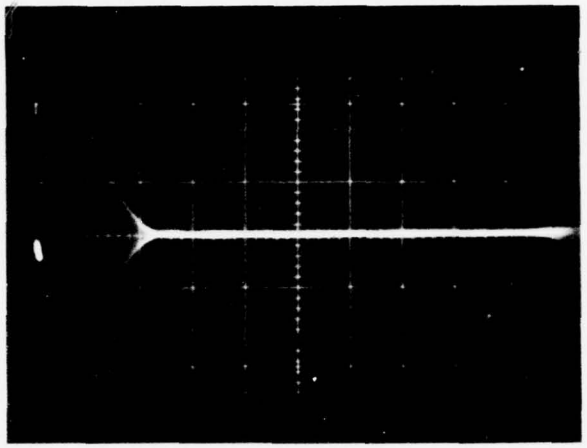

0 $f_{Sample/2}$

Spectral Response
(Hamming Untrimmed Weights)
f_{sample} = 16.67 kHz, N=20 Taps
Sidelobe Suppression=-41.5 dB

75-0990-VA-4

Figure 17. SI/PO Hamming Weight Transversal Filter

5. MOS TRANSISTORS AS ELECTRICALLY REPROGRAMMABLE ANALOG CONDUCTANCE ADAPTIVE FILTER WEIGHTS

Historically, there has been many attempts to realize variable analog weights for the adaptive filter. One of the earliest was the motor-driven potentiometer[73] of servo-mechanisms. A photo-optic device[74] was used where the transmittance decreased on exposure to yellow light and reading was performed with red light. Other devices[75, 76] which were essentially electrochemical, were employed with limited success. The memistor[76] was an interesting concept in which the passage of an electric current through a chemical solution resulted in the plating or deplating of a conductive electrode weight. In order to be compatible with electrical delay lines, the programmable weight should be electrically controlled. This was discussed in connection with ferrielectric structures[77] and later with respect to MIS transistors with a Ferroelectric gate material. Ferroelectric materials are difficult to prepare and the control of their properties in an integrated

---

[73] F. . Hey, "The Mark I Perceptor, Design and Performance" IRE Nat'l. Co v. Rec., Pt. 2, New York (1960)

[74] S I. Campur, "Self-Organizing Networks", Armour Research Foundation Illinois, Institute of Technology, Armour Rep't E154, Chicago, Ill. (1962)

[75] exas Research & Electronics Corp. "An Introduction to Solions" Dallas, Texas, June 1961.

[76] "An Adaptive Adaline Neuron Using Chemical Memistors," Stanford Electronic Labs. Tech Rep't 1553-1, Stanford University, Oct. 1960.

[77] C. F. Pulvari, "Ferroelectrics and their Applications in Solid-State Devices and in Adaptive Control," Proc. 1963 Bionics Symp.

circuit structure is extremely difficult. In 1966, Szedon[78] discussed the charge instability under electrical stress in a silicon nitride (SigNa)/silicon dioxide (SiO_2) dual dielectric structure and Wegener described the potential of a MNOS nonvolatile memory transistor[79]. Since these early papers, a number of papers have appeared in the literature with regards to the MNOS memory transistor[79a]. The MNOS memory transistor may be used as a digital nonvolatile store in memory arrays or as an electrically reprogrammable analog conductance. In order to use this latter property, the MNOS must be operated in its triode region similar to a MOS-FET voltage-controlled conductance.

5.1 MOS TRANSISTORS WITH BIDIRECTIONAL CCD CONTROL OF WEIGHTS

The MOS transistor, when operated in its triode region, displays an analog conductance between drain and source g_{ds} which is electrically alterable. The drain-to-source conductance for small drain-to-source offset voltages is given as:

$$g_{ds} = \bar{\mu}_p \left(\frac{W}{L}\right) C_o \ (V_{GS} - V_T) \tag{73}$$
$$= \beta \ (V_{GS} - V_T)$$

where β is a geometry and material parameter, V_{GS} the applied gate-to-source voltage, and V_T the intrinsic threshold voltage of the device. There are two methods by which the conductance can be altered:

(1) variable V_{GS} with V_T fixed

(2) fixed V_{GS} with V_T variable

---

[78] J. R. Szedon, "Charge Instability in Metal/Silicon-Nitride/Silicon-Dioxide/Silicon Structures," IEEE Solid-State Dev. Res. Cond. Evanston, Ill. June, 1966.

[79] H. A. R. Wegener, et. al., "The Variable Threshold Transistor, a New Electrically Alterable Nondestructive Read Only Storage Device," 1976 IEDM, Washington, D. C.

[79a] See the review paper, J. Chang, "Nonvolatile Semiconductor Memory Devices" Proc. IEEE, G4, 1033 (1976).

We will discuss the first method in this section and leave the variable threshold voltage approach to the MNOS memory transistor which is treated in Section 5.2.

The MOS transistor is to be used as the basic analog conductance multiplier, whether it is method 1 or 2 above, and figure 18 illustrates the attachment of this device to the CCD delay line. The delayed analog signal $\alpha_k X(t - kT)$, where $t = mT$ at the m^{th} clock time, is applied across the drain to source regions of a MOS transistor. The control voltage, which sets the conductance for analog weighting, is applied between the gate and source regions. The output voltage V_{out} is proportional to the delayed input signal and given as:

$$V_{out} = R_F g_{ds} \alpha_k X (m-k)T \tag{74}$$

where α_k is the gain associated with the k^{th} tap on-chip FCDS circuit. Since the MOS analog conductance has a limited V_{ds} which can be applied prior to

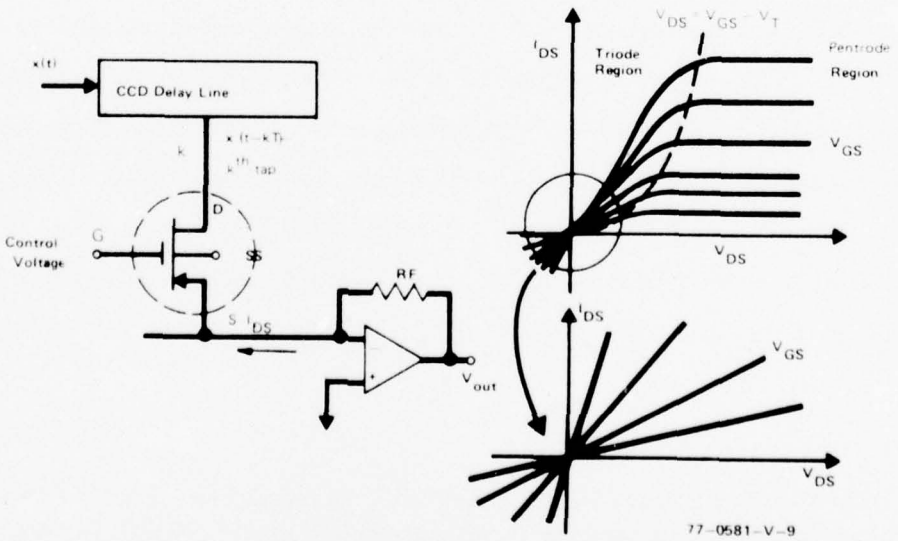

Figure 18. MOS Voltage-Controllable Analog Conductance for Adaptive Tap Weight Element

2nd order distortion effects, it is instructive to consider a comparison between a fixed resistor weight and a MOS transistor voltage-controlled conductance weight. Figure 19 illustrates the output observed on a spectrum analyzer. We can achieve less than 1 percent nonlinearity if the peak-to-peak tap signal does not exceed 0.2V and the operating point has less than ± 0.1V offset from $V_{ds} = 0$. Thus, it is important to maintain the proper bias point operation for all the MOS transistors in an array.

In order to achieve a variable V_{GS} we may convert the error to digital form with an A/D converter, achieve storage and accuracy with accumulators and finally, the multiplication with a multiplying digital-to-analog converter (MDAC). There is certainly not too much appealing with this approach as the complexity of the adaptive filter is increased enormously together with size and power dissipation which is reflected in cost. An 8-tap weight system has been built with this approach[80] to perform adaptive linear prediction with the LMS algorithm; however, the delay lines were lumped L-C type with different dispersive characteristics. A different approach, which deserves considerable merit and is compatible with CCD technology, is the use of bidirectional stabilized charge injection to increment or decrement analog signal charge onto the node of a MOS transistor. This concept is illustrated in figure 20 with voltage adjustment accomplished by means of CCD bidirectional charge-control. The analog, scaled, error signal $2\mu|\epsilon|$ is applied to a CCD storage or holding well whereas, the control signal to increment or decrement charge determines the function of the G_1 and G_2 electrodes. The charge increments are converted to voltage increments as follows:

---

[80] D. R. Morgan and S. E. Craig, "Real-Time Adaptive Linear Prediction Using the Least Mean Square Gradient Algorithm," IEEE Trans. on Acoustics, Speech and Sig. Proc., ASSP-24, 494 (1976).

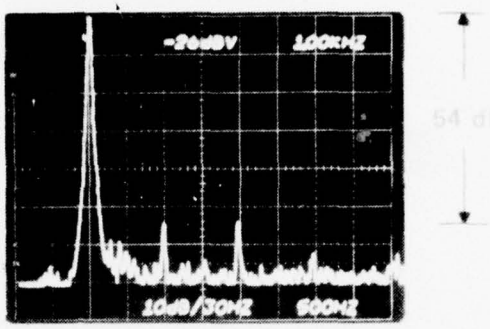

Spectral Components of SI/PO Single Tap Output

W_k = 5 KΩ Fixed Resistor

V_{in} = 1V p-p at 1 kHz

f_{sample} = 20 kHz

76-0512-VA-6

a. Fixed Resistor R = 5kΩ

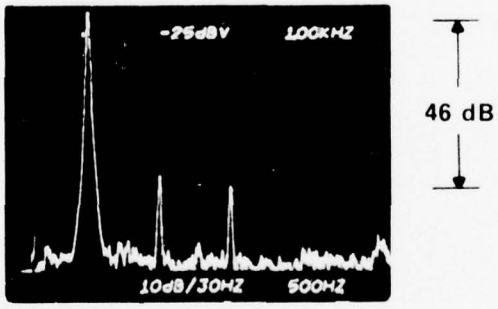

Spectral Components of SI/PO Single Tap Output

W_k = N-Channel MOSFET Biased for 5 KΩ Resistance

V_{in} = 1V p-p at 1 kHz

f_{sample} = 20 kHz

76-0512-VA-7

b. MOS-FET Analog Conductance R = 5kΩ

Figure 19. MOS-Transistor Analog Conductance Comparison with Fixed Resistor Performance

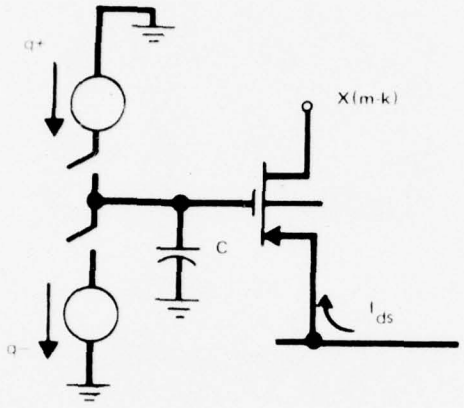

a. Simplified Concept

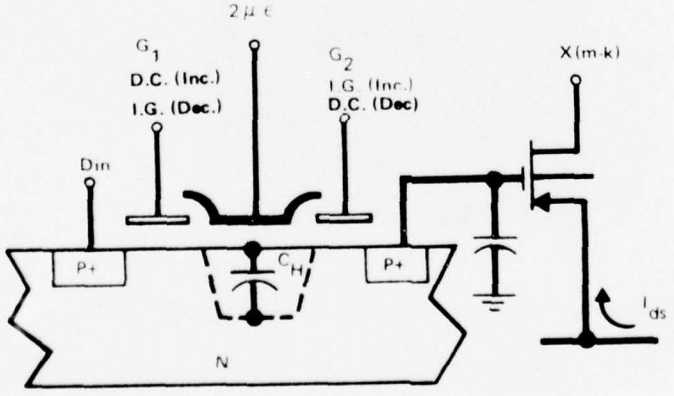

77-0581-V-10

b. CCD Implementation

Figure 20. Bidirectional Charge Control for Adjustment of Gate Voltage to Achieve a Variable Analog MOS Conductance

$$V^{+} = \frac{q^{+}}{C} = \frac{C_H}{C} \left(V_{G1} - 2\mu|\epsilon|\right)$$

$$V^{-} = \frac{q^{-}}{C} = \frac{C_H}{C} \left(V_{G2} - 2\mu|\epsilon|\right) \qquad (75)$$

This technique can provide gain through the selection of the holding-well capacitance (C_H) area.

5.2 METAL-NITRIDE-OXIDE-SILICON (MNOS) ELECTRICALLY REPROGRAMMABLE ANALOG CONDUCTANCE WEIGHTS

The metal-nitride-oxide-silicon (MNOS) nonvolatile memory transistor is the electrostatic analog of the magnetic core storage element. Memory is achieved in the MNOS transistor by electrically reversible tunneling of charge from the silicon semiconductor to deep traps near the SiO_2/Si_3N_4 interface in a thin SiO_2 (i.e. typically 20A°) structure. Figure 21 illustrates a photomicrograph of a drain-source protected (DSP) MNOS memory transistor, and figure 22 shows a cross-section of the DSP geometry.[81] The thicker oxides over the drain and source regions protect these regions from electrical and mechanical stress in addition to limiting the mode of operation to the "enhancement mode". One of the important advantages of this geometry is the extended endurance of MNOS memory transistors[82] under prolonged cycling with operation beyond 10^{12} erase/write cycles.

---

[81] J. R. Cricchi, et. al., "The Drain-Source Protected MNOS Memory Transistor", 1973 IEDM, pg. 126, Washington, D. C.

[82] M. H. White, J. W. Dzimianski, M. C. Peckerar, "Endurance of Thin-Oxide Nonvolatile MNOS Memory Transistors", IEEE Trans. Electron Dev., ED-24 577 (1977).

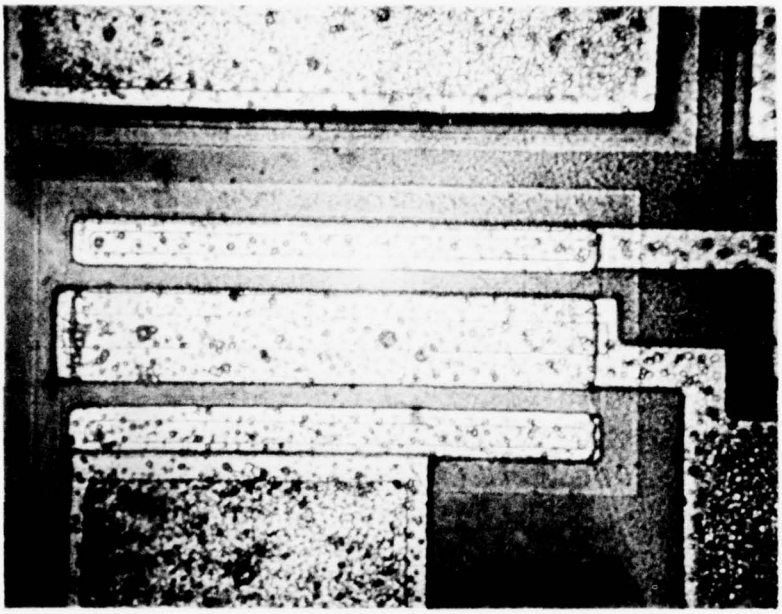

S76-1085-PA-7

Figure 21. Photomicrograph of Drain-Source Protected MNOS Nonvolatile Memory Transistor W/L = 7/1

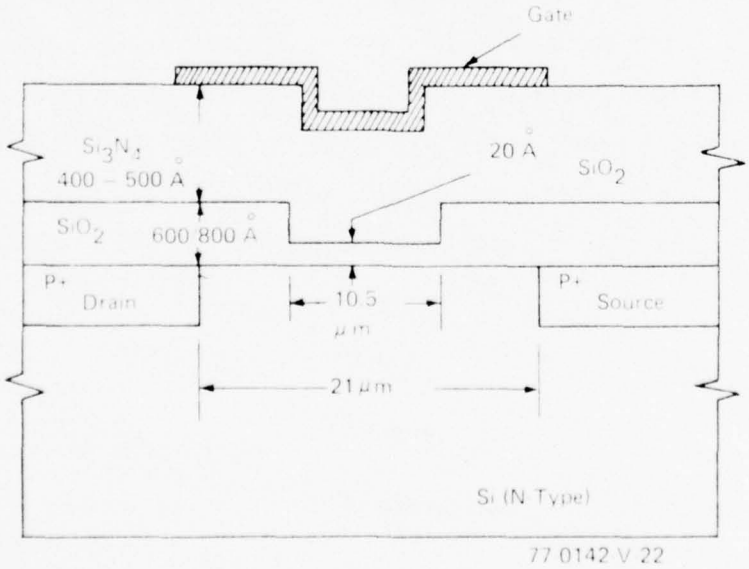

Figure 22. Cross-Section of DSP-MNOS Memory Transistor

The programming voltages $\pm V_P$ result in a - and + stored charge Q_I located near the SiO_2/Si_3N_4 interface with a change in device threshold voltage given by the expression,

$$\Delta V_{th} = \frac{-X_N \Delta Q_I}{K_N \epsilon_o} \tag{76}$$

where X_N is the Si_3N_4 thickness, K_N the Si_3N_4 relative dielectric constant, and ΔQ_I the shift in interface charge under a programming pulse. The change in threshold voltage may be written in terms of device parameters.[83]

$$\Delta V_{th} \doteq V_T \left(1 + \frac{C_o}{C_N}\right) \ln \left(1 + \frac{t_p}{\tau}\right) \tag{77}$$

where V_T is a characteristic tunneling threshold voltage, C_o and C_N are the oxide and nitride capacitances, t_p the programming pulsewidth, and

$$\tau = V_T \frac{(C_o + C_N)}{J_T} e^{-V_o/V_T} \tag{78}$$

where J_T is a pre-exponential oxide tunnel current term and V_o the initial voltage drop across the thin oxide region.

The charge in conductance of the MNOS memory transistor, operating in its triode region, is given as,

$$\Delta g_{ds} = \bar{\mu}_p \left(\frac{W}{L}\right) \left(\frac{C_o C_N}{C_o + C_N}\right) \Delta V_{th} = \beta \Delta V_{th} \tag{79}$$

where $\bar{\mu}_p$ is the effective carrier mobility, $\frac{W}{L}$ the width-to-length ratio and ΔV_{th} given by equation (77). In order to relate the applied gate-to-source

---

[83] M. H. White and J. R. Cricchi, "Characterization of Thin-Oxide MNOS Memory Transistors," IEEE Trans. Elec. Dev., ED-19, 1280 (1972)

programming voltage, V_P, to the oxide voltage drop, we use capacitance division to obtain,

$$V_o = \frac{C_N}{C_o + C_N} (V_P - V_{th}) \tag{80}$$

and the conductance

$$g_{ds} = \beta (V_R - V_{th}) \tag{81}$$

where V_R is the read voltage which is selected such that negligible programming of the MNOS structure occurs.

5.3 CALCULATION OF $2\mu_{eff}$ FOR THE CLIPPED DATA LMS ALGORITHM

Figure 23 illustrates a block diagram of a single MNOS weight connected to a CCD delay line at the k^{th} tap position. The object of this analysis is to calculate the effective convergence factor $2\mu_{eff}$ which appears in the LMS

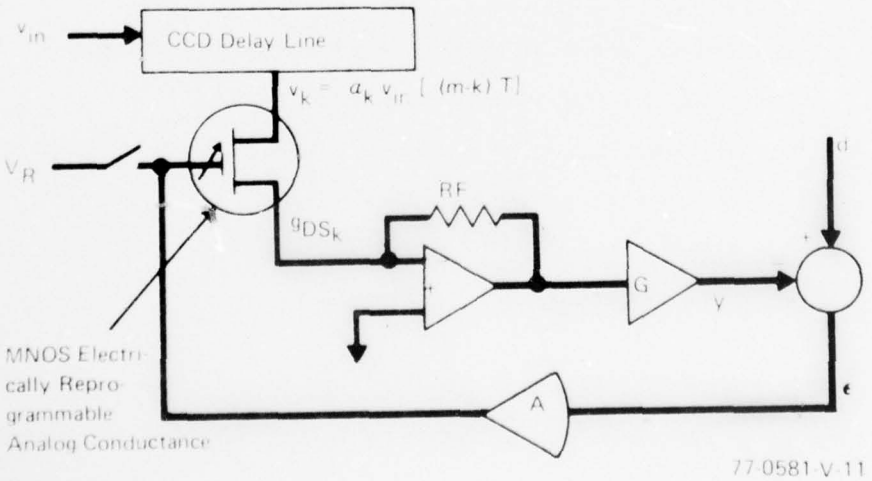

Figure 23. Simplified Block Diagram of MNOS Analog Conductance Programming Operation

algorithm. In order to do this we will use the preceding equations in section 5. Thus, from equation (81) we may write

$$g_{ds_k}(m+1) = g_{ds_k}(m) - \beta\, \Delta V_{th}(T) \tag{82}$$

where

$$\Delta V_{th}(T) = V_{th}(mT) - V_{th}\left[(m-1)T\right] \tag{83}$$

Since $W_k(m+1) = g_{ds_k}(m)\, R_F G$ is the effective weight we may write,

$$\begin{aligned} W_k(m+1) &= W_k(m) + R_F G\, \Delta g_{ds_k}(m) \\ &= W_k(m) + 2\mu_{eff}\, \epsilon\, \mathrm{sqn}\left[V_k(m)\right] \end{aligned} \tag{84}$$

Thus, we have

$$\begin{aligned} 2\mu_{eff} &= R_F G\, \partial\, \frac{\left(\Delta g_{ds_k}(m)\right)}{\partial \epsilon} \\ &= \beta\, R_F G\, \partial\, \frac{\left(\Delta V_{th}(T)\right)}{\partial \epsilon} \end{aligned} \tag{85}$$

Combining equations (77), (78), and (80) with $V_P = A\epsilon$ yields

$$2\mu_{eff} = \beta\, A\, R_F G\, \frac{(t_p/\tau)}{1+t_p/\tau} \tag{86}$$

which illustrates the variation of $2\mu_{eff}$ with t_p/τ. This variation is actually a dependence on the error ϵ which determines τ through equations (78) and (80). Thus, below a minimum error determined by $t_p/\tau = 1$, the $2\mu_{eff}$ is exponentially dependent upon the error whereas, when the error is above this minimum $2\mu_{eff}$ is independent of the error - analogous to a forward-biased P-N junction diode. This type of limiting action, in which the μ_{eff} becomes

vanishingly small below a minimum error, may nullify the so-called misadjustment error[84] described in connection with equation (20) at the expense of system response. The range of $2\mu_{eff}$ may be extended to smaller errors by increasing the gain A; however, there is a practical limit to due maximum gain based on input signal amplitude. Thus, AGC of the input signal or error would appear to be the best approach to extend the dynamic range.

5.4 SPEED OF RESPONSE AND PROGRAMMING VOLTAGE RANGE FOR MNOS ELECTRICALLY REPROGRAMMABLE ANALOG CONDUCTANCE WEIGHTS

The speed of response is a function of the amplitude of the programming voltage (i.e., the magnitude of the error), the pulsewidth t_p, and the initial state of $\pm 2\mu|\epsilon|$ stored charge in the MNOS device. Equation (77) incorporates all of these effects into a single expression from which we may draw the following conclusions:

(1) $\Delta W \sim \Delta V_{th} = \text{constant} \times \log_{10} t_p$

where the constant is typically 2 volts/decade for $t_p > \tau$

(2) $\Delta W \sim \Delta V_{th} = 2\mu\Delta\epsilon$

with the change of threshold proportional to a change in the error for $t_p > \tau$.

Figure 24 illustrates a set of response curves for a p-channel MNOS memory transistor. The electric field strength across the thin-oxide is determined by the nitride thickness, and it is important to control this parameter in the processing. Figure 25a illustrates a set of 4 MNOS devices with controlled, uniform, nitride thickness while figure 25b shows a set of 4 MNOS devices with nonuniform nitride thicknesses. These measurements

---

[84] C. Williams, Private Communications, Stanford University, June 1977

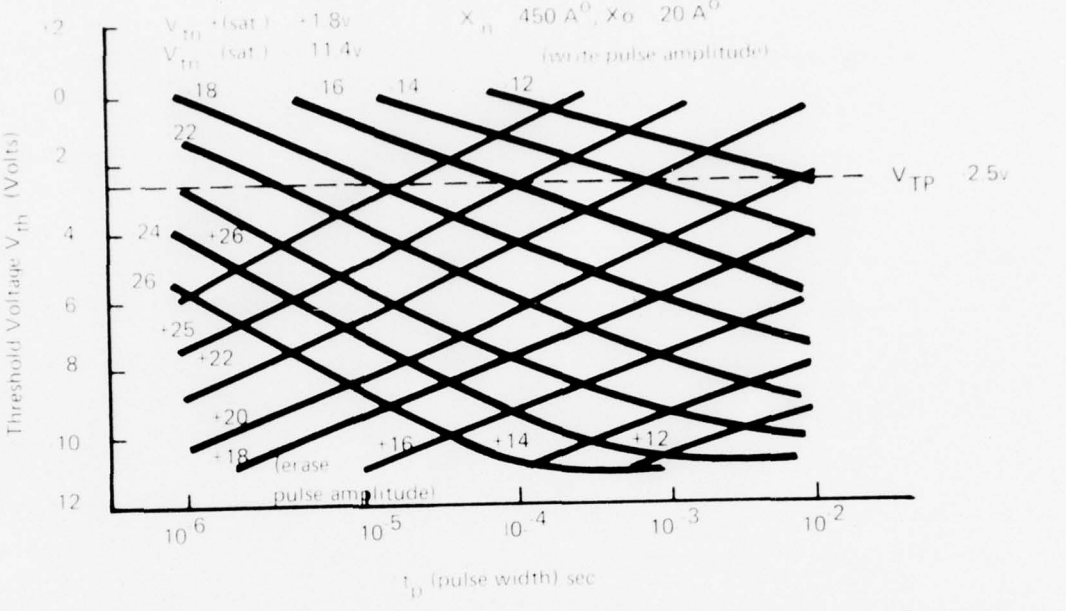

Figure 24. P-Channel MNOS Memory Transistor Erase/Write Characteristics (Single Pulse Response from a Saturated State)

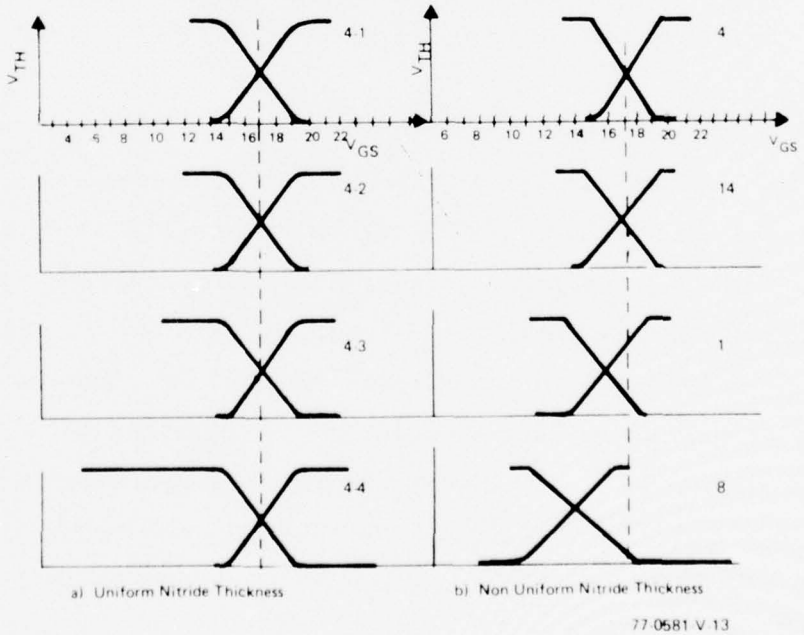

Figure 25. Uniform and Nonuniform Characteristics of MNOS Memory Transistors (t_p = 300μsec) X_N = 450°A°, X_o = 20A°

are taken on a Macrodata MD154 computer-controlled tester which uses 2μsec read voltages in a binary search routine to determine the transistor gate voltage when $I_{DS} = 10\mu A$. The thick-oxide threshold voltage $V_{TP} = -2.5V$ sets the limit for high conductance while the threshold may be changed to a maximum of -11.4V for this particular device. In operation, the read voltage is typically $V_R = -8B$ to give a reasonable conductance dynamic range. For p-channel MNOS transistors, a negative programming voltage (i.e., $-2\mu\epsilon$) will cause a positive increment in charge to be stored in the device ($\Delta Q_I > 0$) and a negative shift will occur in the threshold voltage [see equation (76)], thereby, decreasing the drain-source conductance g_{ds} for a fixed read voltage applied between gate and source [see equation (81)]. A positive programming voltage (i.e., $+2\mu\epsilon$) will remove the stored positive charge and tend to accumulate negative charge, thereby, decreasing the threshold voltage and shifting it in a positive direction. For a fixed read voltage, the conductance will increase under a positive (erase) programming voltage. The speed of response and voltage programming range are determined by the nitride thickness as figure 26 illustrates a thinner nitride of $X_N = 335A°$.

5.5 MNOS CHARACTERIZATION FOR ADAPTIVE WEIGHT CONTROL

Figure 27 illustrates the basic circuit used to characterize an MNOS device for the adaptive filter. The circuit incrementally writes and clears the MNOS device by applying a voltage staircase to the gate. For a p-channel MNOS FET, the staircase is positive going for the clear mode and negative going for the write mode. The offset of the staircases can be regulated between ground and ±20Vdc. To measure the ac conductance of the MNOS device, a read voltage is applied after each program step when a sinusoid is applied to the drain. After eight "write clear" sequences, the device is saturate "cleared" by applying a +20V pulse to the gate.

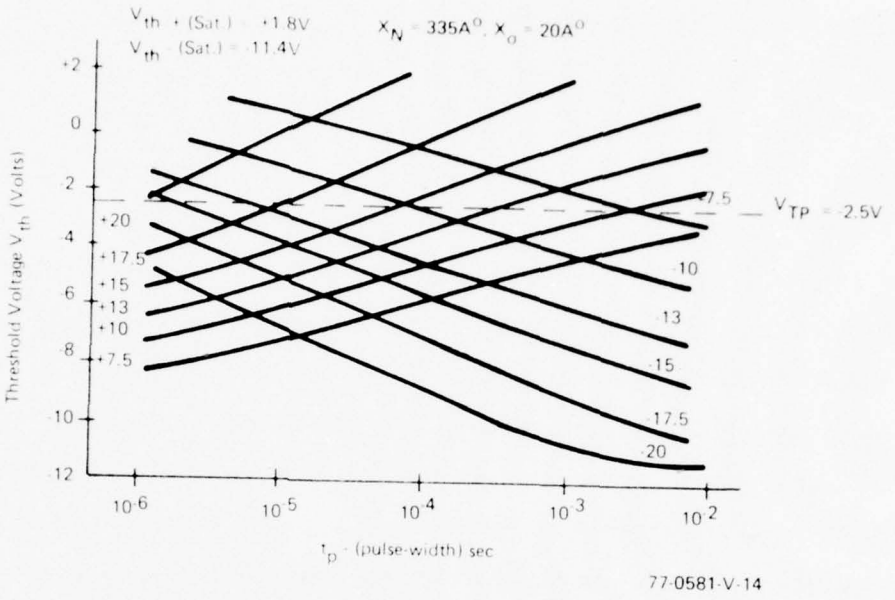

Figure 26. P-Channel MNOS Memory Transistor Erase/Write Characteristics (Single Pulse Response from a Saturated State)

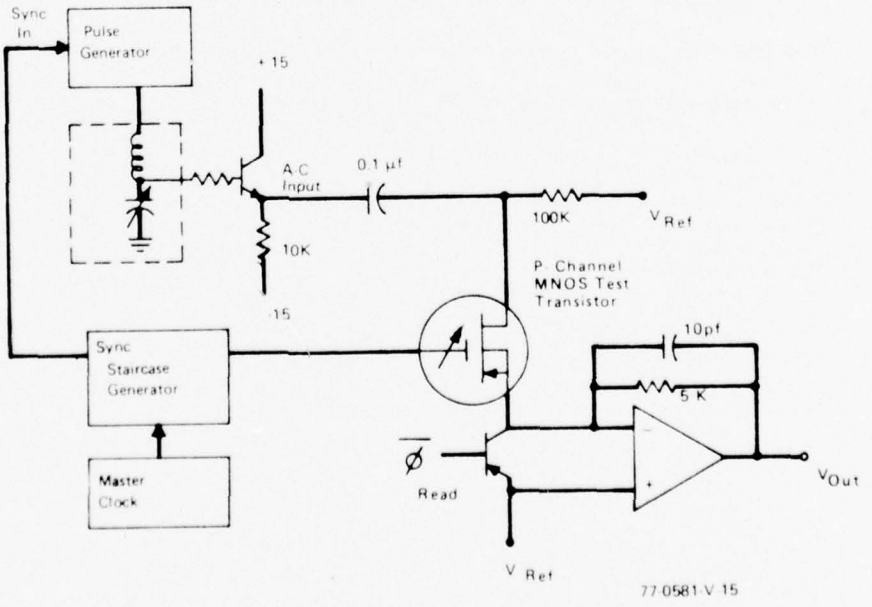

Figure 27. MNOS Characterization Circuit

The ac signal is generated by applying a 50 percent duty cycle square wave from a pulse generator into an LC resonant circuit. By strobing the pulse generator with a "sync" probe from the master clock pulse generator, we are able to synchronize the sinusoid with the systems timing. With a small ac signal applied to the MNOS drain, the amplitude will vary during each "read" cycle due to incremental threshold voltage shifts (i.e., channel conductance increase and decrease) for a given read voltage and series of write/clear ramps. We can therefore determine voltage levels necessary to operate the MNOS as an adjustable weight in an adaptive processor.

The upper trace of figure 28 shows the operational amplifier output voltage when the signal shown in the lower trace is applied to the gate and an 0.5V pp signal is applied to the drain. The saturate clear sets the conductance of the device to its highest state. The conductance then decreases when a write ramp is applied. After 16 incremental write steps, the MNOS is incrementally cleared with a positive going ramp. The rate of change of the conductance is a function of the dc levels of the ramps, the read voltage, and initial threshold levels as a ramp begins. The read voltage and pulse-width must be minimized to avoid the read-disturb effects since the read voltage is in the direction to write the device.

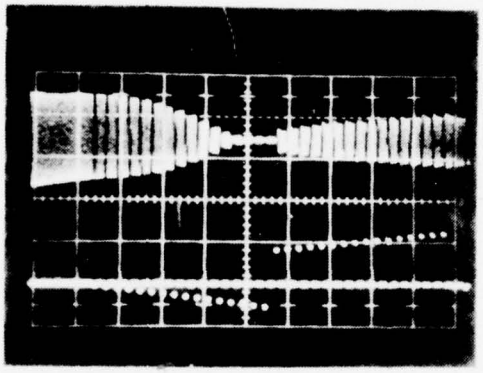

Figure 28. MNOS Characterization Circuit Output Pulsewidth t_p = 200μsec for Write and Clear Saturate = +20V ∅ Read = -9Volts

6. ADAPTIVE FILTER BREADBOARD AND EXPERIMENTAL CHARACTERISTICS

The purpose of the adaptive filter breadboard is to demonstrate the feasibility of implementing the LMS algorithm in an integrated circuit. In order to accomplish this task, the components of the breadboard must be compatible in the integrated circuit sense. The breadboard described in this section uses the "clipped data" LMS algorithm and the basic linear combiner is constructed with a CCD analog delay line and electrically reprogrammable MNOS analog conductance weights. Other techniques could have been employed such as the bidirectional charge-control method to provide a variable gate voltage on a MOS analog conductance; however, the availability of MNOS memory transistors and the potential for long-term analog storage with this device structure made this a convenient approach. Figure 29 illustrates a block diagram of the CCD adaptive filter and figure 30 is a more detailed description. The voltage output at each tap, denoted by X_1 and X_2, is multiplied by the MNOS conductances at each tap location. The resulting currents are converted to voltages by amplifiers 1 and 2. The voltage output of amplifier 1, donated by Y_1, is given by:

$$\begin{aligned} Y_1 &= - R_f (W_A X_1 + W_C X_2) \\ W_A &= g_{ds} \text{ / MNOS A} \\ W_C &= g_{ds} \text{ / MNOS C} \end{aligned} \tag{87}$$

Likewise, the voltage output of amplifier 2, denoted by Y_2, is given by:

$$Y_2 = -R_f (W_B X_1 + W_D X_2) \tag{88}$$

Therefore, depending on which weights are used, Y_1 and Y_2 can be used to determine the characteristics of the MNOS weights and to correlate theoretical predictions with experimented results after adaptation is completed.

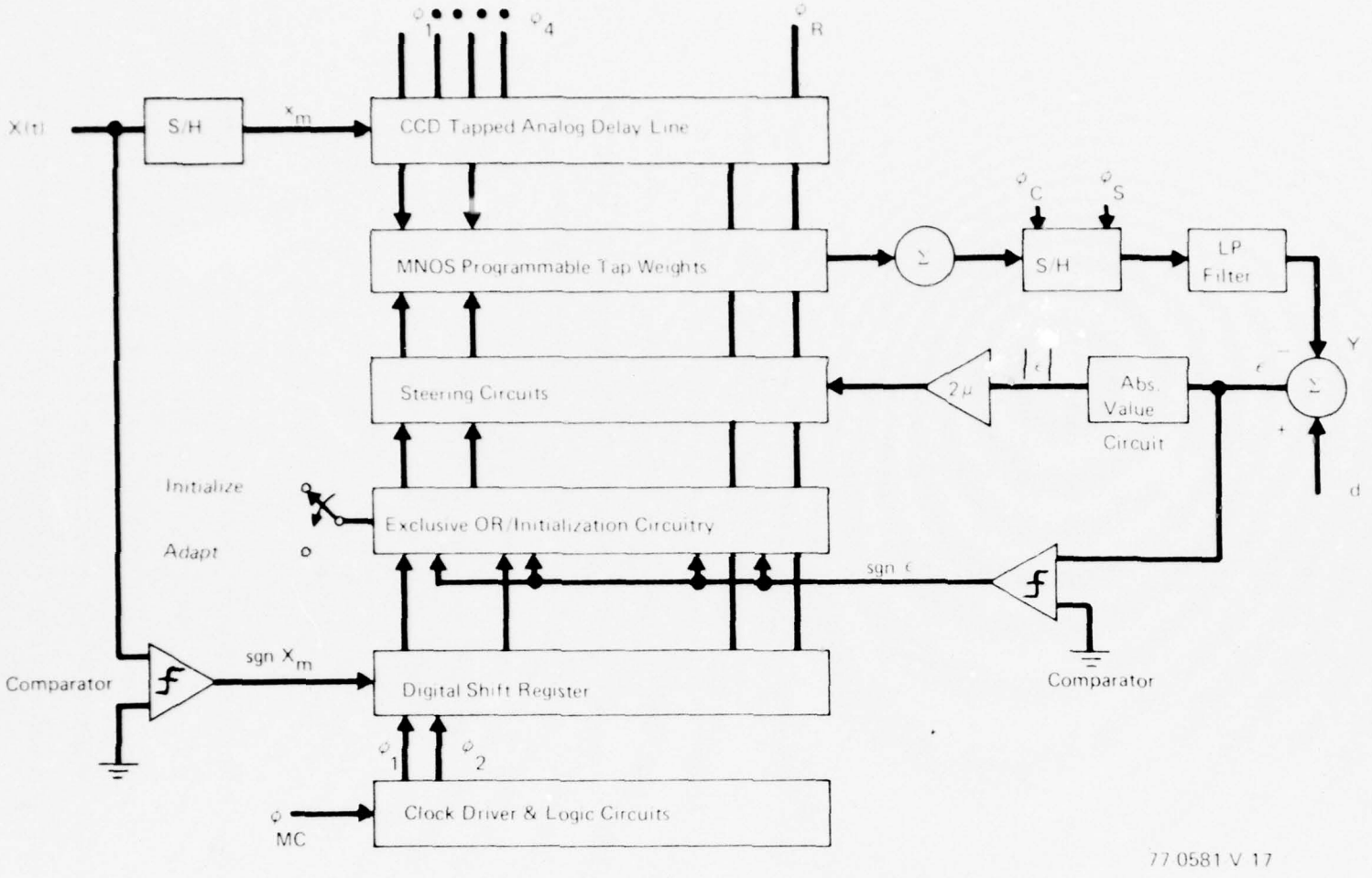

Figure 29. Block Diagram of CCD Adaptive Filter/Predictor Constructed with LMS Algorithm

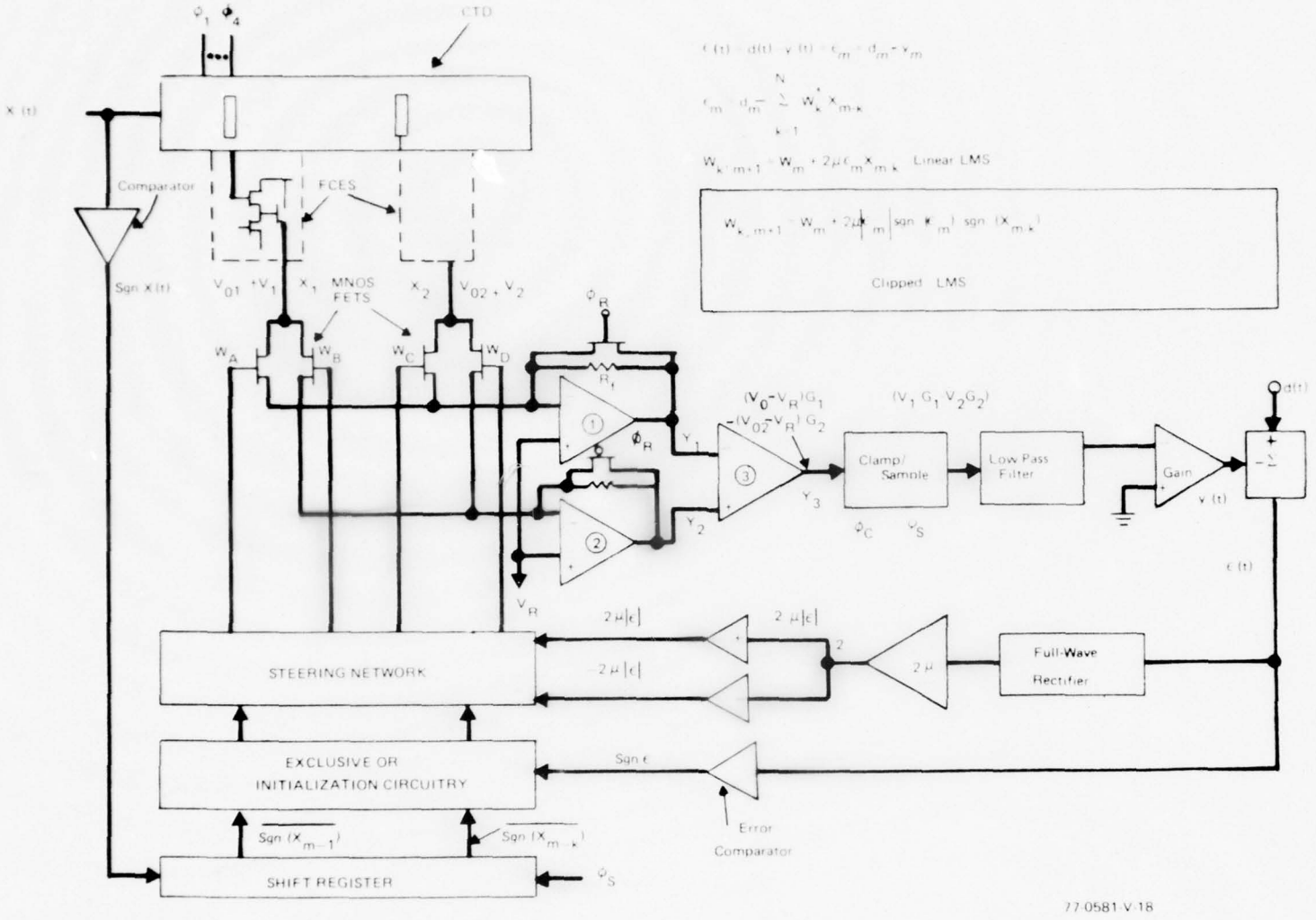

Figure 30. Adaptive Filter Block Diagram

The output of amplifier 3, deonted by Y_3 is given by:

$$Y_3 = Y_2 - Y_1$$
$$= -KR_f \left[(W_B - W_A) X_1 + (W_D - W_C) X_2 \right] \quad (89)$$

where K is the gain associated with amplifier 3(=2). From equation(89)it can be seen that both positive and negative effective weighting can be realized by the relative magnitude of (W_B and W_A) and (W_D and W_C). The voltage Y_3 is applied to a clamp/sample circuit to difference the a-c zero and (signal + a-c zero) formatted signal to retrieve the signal without causing a d-c level "bounce" in the system during the adaption process. The clamp/sample output voltage is filtered by a low-pass filter with a notch at the sample frequency. The filter output is a continuous time waveform which may be further amplified without amplifying the noise associated with aliasing and switching spikes inherent in a sampled-data signal.

The linear predictor output, y(t), is subtracted from the desired signal, d(t), which is also a continuous time signal. The difference or error, given by,

$$\epsilon(t) = d(t) - y(t) \quad (90)$$

is applied to a full wave rectifier to form the absolute value of the error. $|\epsilon|$ is amplified and d-c level shifted to form $+2\mu|\epsilon|$ and $-2\mu|\epsilon|$ which are unidirectional a-c signals superimposed upon a "no program" level. The voltages $\pm 2\mu|\epsilon|$ are directed to the MNOS gates by the steering network, which is controlled by the "exclusive OR" circuits. The "exclusive OR" output is determined by sgn $[\epsilon(m)]$ and sgn $[X(m-k)]$ as processed by the initialization circuit. It will be noted that since the error is in continuous time, the weight for the next clock period (m+1) is determined by sgn $[\epsilon(m)]$ and $|\epsilon(m)|$ just before the update mode terminates. However, it is assumed the error change is slow compared to the update time. The signals into the initialization circuit and exclusive "OR" circuit update the weights according to the format shown in table 1.

TABLE 1.

STEERING NETWORK UPDATE ALGORITHM

sgn X_{m-k}	sgn (t)	W_A	W_B	W_C	W_D
0	0	-	+	-	+
0	1	+	-	+	-
1	0	+	-	+	-
1	1	-	+	-	+

+ = incremental clear (conductance increase)
- = incremental write (conductance increase)

The "clipped data" LMS algorithm employed in the adaptive filter is given by the expression:

$$W_k(m+1) = W_k(m) + 2\mu\,\epsilon(m)\ \ \text{sgn}\,\epsilon(m)\ \ \text{sgn}\,X(m-k) \tag{91}$$

The weights associated with the taps are given as,

$$W_1 = W_B - W_A \tag{92}$$
$$W_2 = W_D - W_C$$

Figure 31 illustrates a timing diagram for the adaptive filter and figure 32 is a photograph of the analog processor board. The clock waveforms for the SI/PO CCD operation were discussed in section 4.2. The additional timing pulses are required to perform clamp and sample in the analog processor y(t) reconstruction circuit, strobe of sgn X and sgn ϵ, operation of the digital shift register, and the read/update mode selection as indicated in figure 31.

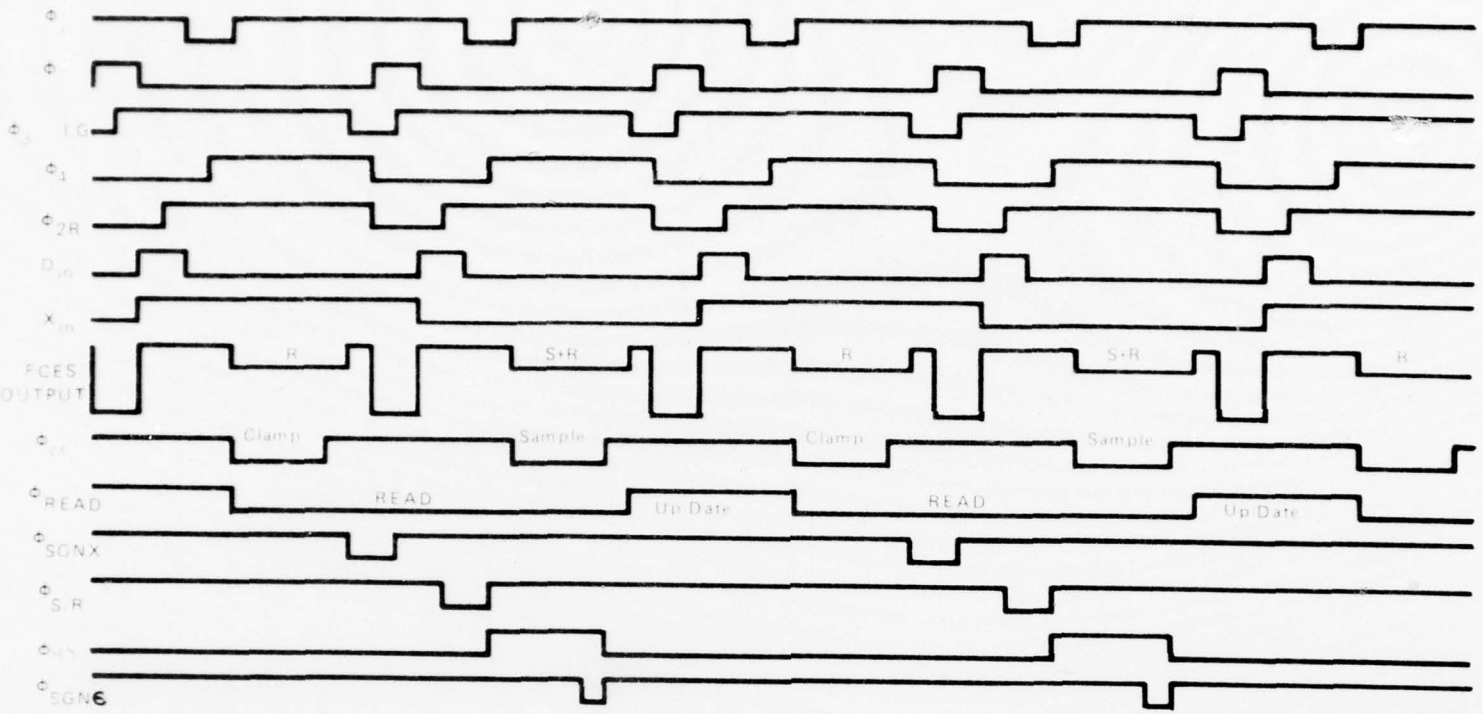

Figure 31. Timing Diagram for SI/PO CCD Adaptive Filter

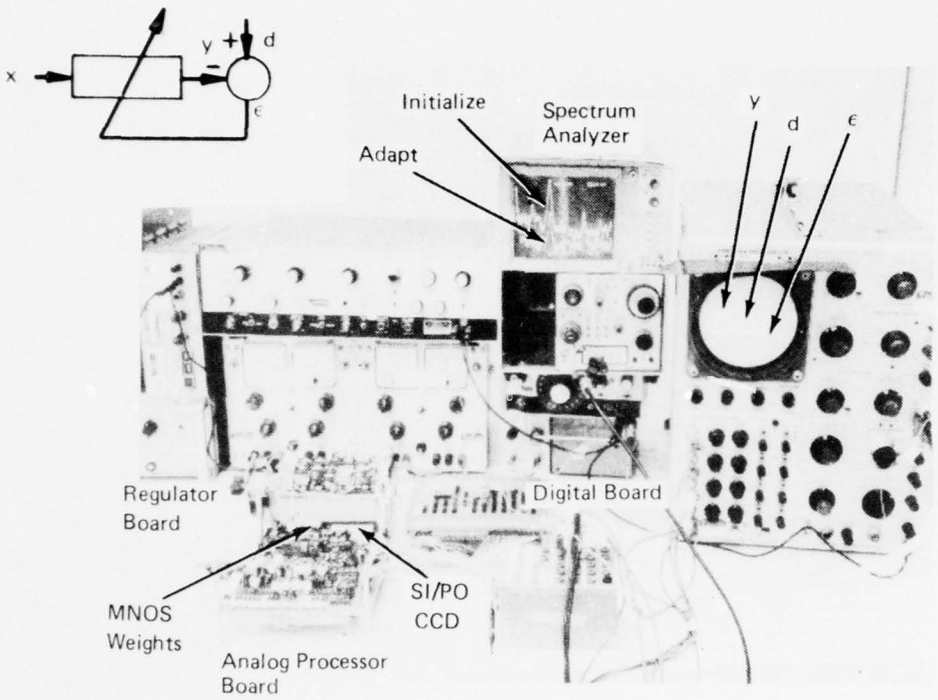

Figure 32. Analog Processor Adaptive Filter Breadboard

6.1 COMPUTER SIMULATION - TWO TAP LINEAR ADAPTIVE FILTER

Figure 33 illustrates the configuration used to simulate a 2-tap adaptive linear filter where the weights are updated according to equation (91) shown in figure 30. Table 2 shows the results of computer simulation in which the weights are updated in accordance with various combination of control signals from the steering network. It will be noted that if the weights are updated according to configuration 4, which is the configuration used on the breadboard and corresponds to table 1, a linear predictor can be implemented by using 1, 2, 3, or 4 weights with the constraints indicated in table 3. Therefore, by constraining the phase between y and d, restricting the weights used so that y_1 and y_2 each reflect only one weight, (not an effective weight), the values of individual weights after adaptive can be determined and compared to theoretical prediction.

6.2 EXPERIMENTAL RESULTS FOR 2-TAP LINEAR ADAPTIVE NOTCH FILTER

Figure 34 shows the y and d channels during initialization for the case where 2 weights ($W_1 = W_B - W_A$) are used at tap 1 and 2 weights ($W_2 = W_D - W_C$) are used at tap 2. Figure 34 shows the y and d channels after adaptation. After adaptation, the component of d in that error is reduced by 25 dB. Figure 35 shows the voltage at y_1 and y_2, respectively, during initialization, where W_A and W_C are saturate written ($g_{ds} = 0$) and W_B and W_D saturate cleared. Figure 35 shows the corresponding y_1 and y_2 waveforms after adaptation, where W_1 and W_2 have changed to produce voltage outputs which, when subtracted by amplifier 3 and further processed by the clamp/sample circuit, etc., forms a y which attempt to minimize the difference between y and d in the mean square sense.

Figure 36 illustrates the experimental results obtained on the adaptive filter with 2 weights/tap. The adaptivity is defined as[85]

$$\text{adaptivity} = 20 \log 10 \left(\frac{\epsilon}{d}\right) \tag{93}$$

---

[85] R. Riegler and R. Compton, Jr., "An Adaptive Array for Interference Rejection", Proc. IEEE, 61, 748 (1973).

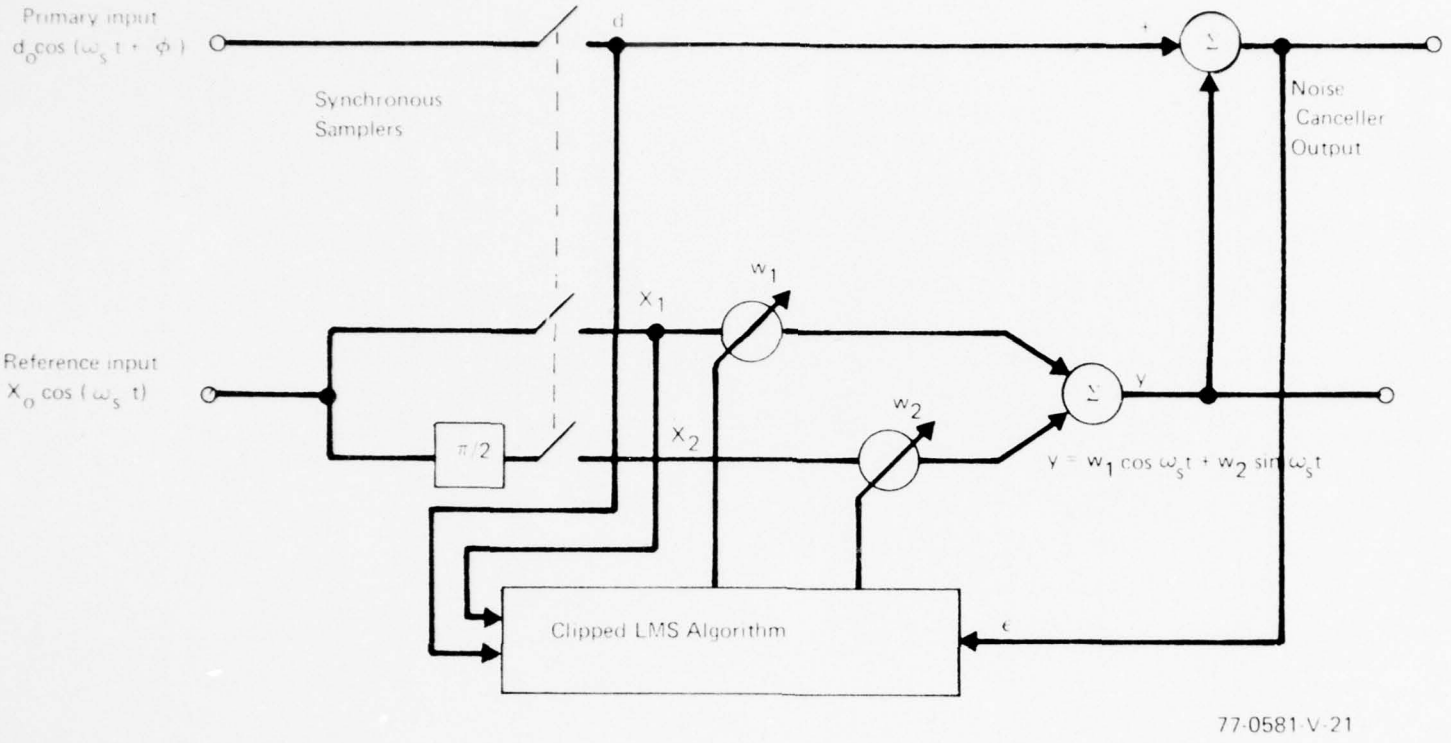

Figure 33. Two Tap Adaptive Linear Predictors

TABLE 2.

COMPONENTS SIMULATION RESULTS

Weight Update Algorithm

Weight	Configuration							
	1	2	3		4			
# of weights	4	4	4	2	4	3	2	1
W_A	+	+	–	0	–	0	0	0
W_B	–	–	+	+	+	+	+	+
W_C	–	+	+	+	–	–	–	0
W_D	+	–	–	0	+	+	0	0
	$\Phi = \pi/4$						$\Phi = 0$	

$$W_{j+1} = W_j + 2\mu \cdot |\epsilon| \cdot (\text{Sgn } X \text{ Sgn } \epsilon)$$

+ => Sgn x Sgn ϵ = 0 or 1
– => Sgn x Sgn ϵ = -1
0 => weight not used

Number of Clocks for Weights to Reach 0.1% of Final Value

2μ	Configuration							
	1	2	3		4			
# of weights	4	4	4	2	4	3	2	1
0.005	X		X	X	7200	7200		
0.02								
0.05	X		X	X	116	7200		
0.1		X					113	145
0.2		X						
0.5	4*		X	X	X	71		

X = no convergence
* diverges after 30 clocks

77-0581-VA-23

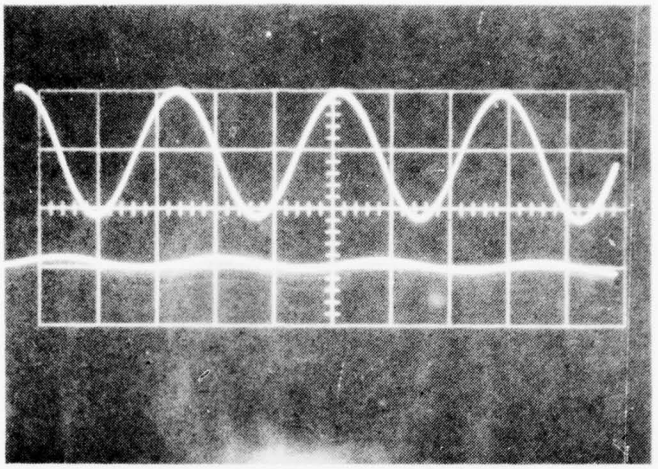

Initialized
(a) Vertical: 10V/Div
Horizontal: 2ms/Div

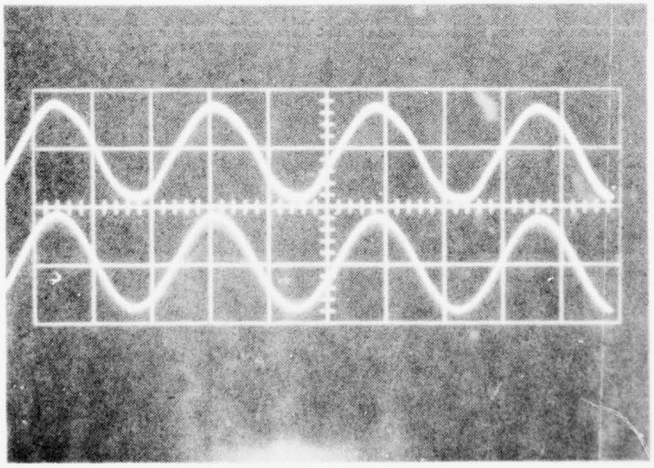

Adaptation
(b) Vertical: 1V/Div
Horizontal: 2ms/Div

$$y = W_1 X_1 + W_2 X_2$$

$f_{signal} = 180$ Hz

$f_{sample} = 2.88$ KHz

Figure 34. Two Tap Adaptive Linear Filter Output
(2 Weight/Tap)

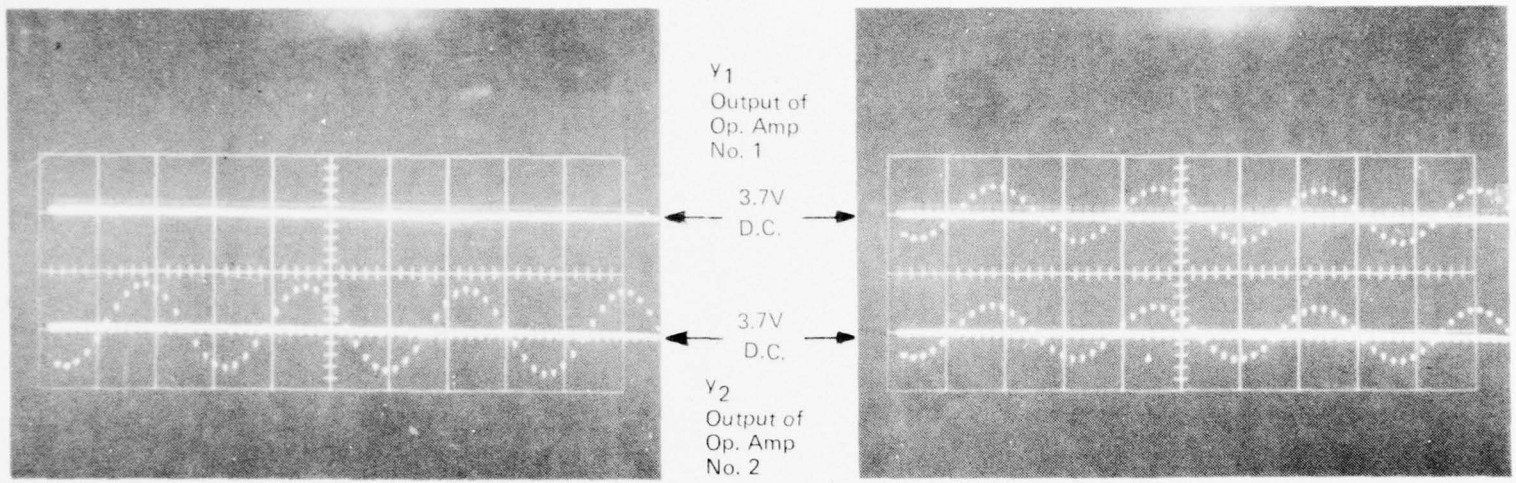

$$y_1 = -(W_A X_1 - W_G X_2)\, R_F$$

$$y_2 = -(W_B X_2' - W_D X_2')\, R_F$$

$$y = y_2 - y_1$$

Figure 35. Two Tap Adaptive Linear Filter Components Waveforms
(2 Weight/Tap)

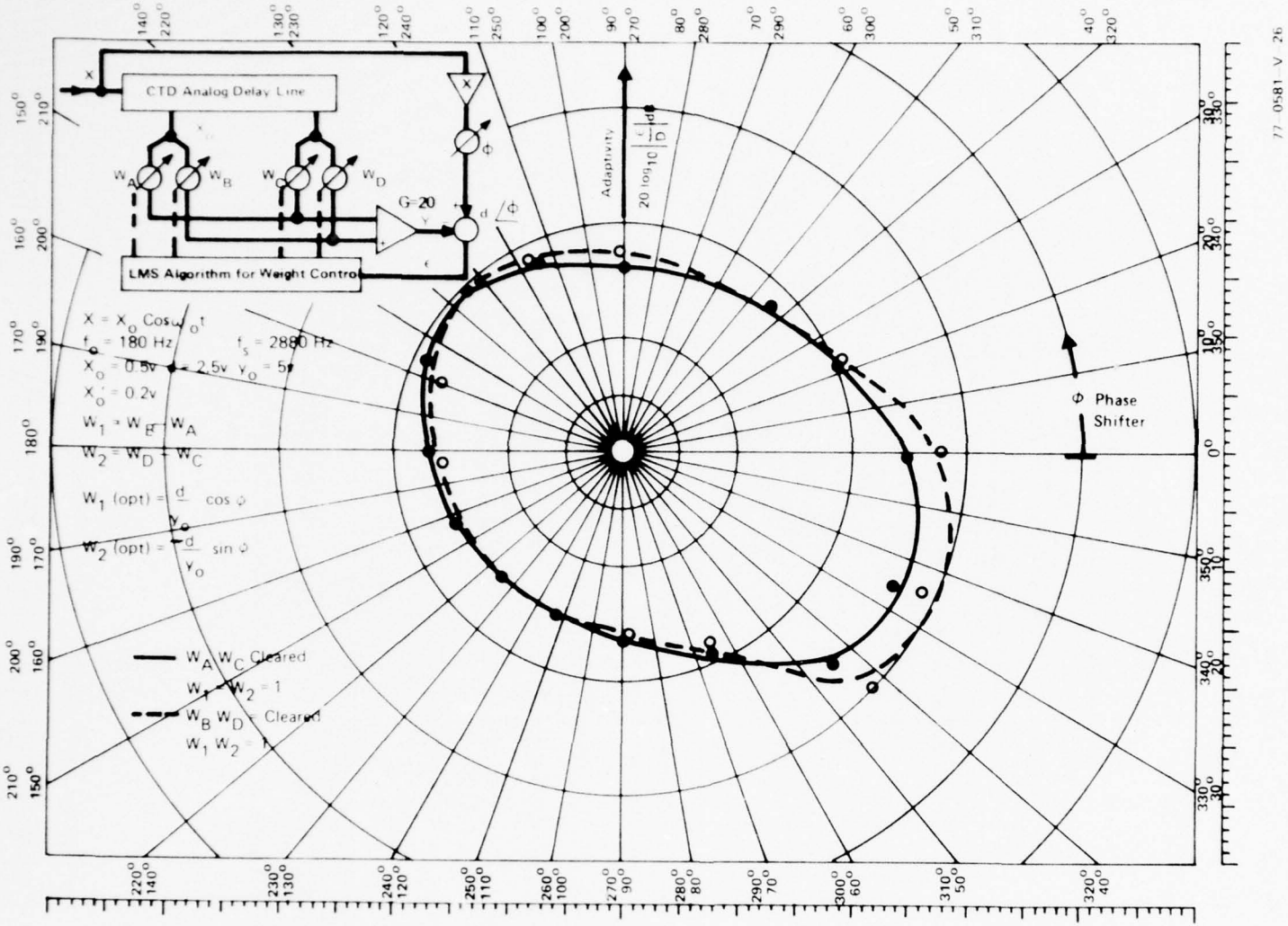

Figure 36. Experimental Results on "clipped data" LMS Algorithm for 2-Tap Weight Adaptive Notch Filter

TABLE 3.

PHASE TRACK CAPABILITY FOR
VARIOUS WEIGHT CONFIGURATIONS

Number of Weights	Tap 1	Tap 2	Amplitude Range	Range
	1	0	X	0
	2	0	X	$0, \pi$
	1	1	X	$0 \rightarrow \pi/2$
	2	1	X	$0 \rightarrow \pi/2\ \pi - {}^{3\pi}/2$
	2	2	X	$0 \rightarrow 2\pi$

Note: $\Phi = 0$ corresponds to y for:

$$W_A = 0$$
$$W_B = 1$$
$$W_C = 0$$
$$W_D = 0$$

X = don't care
1 = weight normalized to saturate cleared state
0 = saturate written state

and we notice the rejection improves in the II and IV quadrant as discussed in connection with figure 9. The measurements were performed for the two cases:

$$W_1 = W_2 = -1$$
$$W_1 = W_2 = 1 \qquad (94)$$

as initial states prior to adaptation. Essentially, the results are unchanged with respect to the choice of initial tap weight setting. The final value for the tap weights is given by equation 44 in the absence of noise

$$W_1 \text{ (opt.)} = \frac{d}{y_0} \cos \Phi$$
$$W_2 \text{ (opt.)} = \frac{-d}{y_0} \sin \Phi \qquad (95)$$

The experimental and theoretical valves agreed to within 1 to 3 percent, the measurement accuracy, and varied in accordance with amplitude and phase

as predicted by the Wiener solution. A value of $\mu = 0.15$ was used in these measurements. The transient response of the error as a function of μ is illustrated in figure 37. As noted in section 3.0, the transient response is experimentally dependent upon μ and this has been verified in experiments as shown in figure 37.

Figure 38 illustrates two experimental setups to examine the CCD adaptive filter as a notch filter for noise or interference cancellation. In this configuration, a 50 Hz desired signal was corrupted by a 250 Hz interference signal, where the latter is 15 dB larger than the former prior to adaptation. The error is monitored and the adaptation illustrates a 32 dB rejection in the interference which brings the desired signal 16 dB above the interference. Figure 39 illustrates the output waveforms before and after adaptation in the time domain.

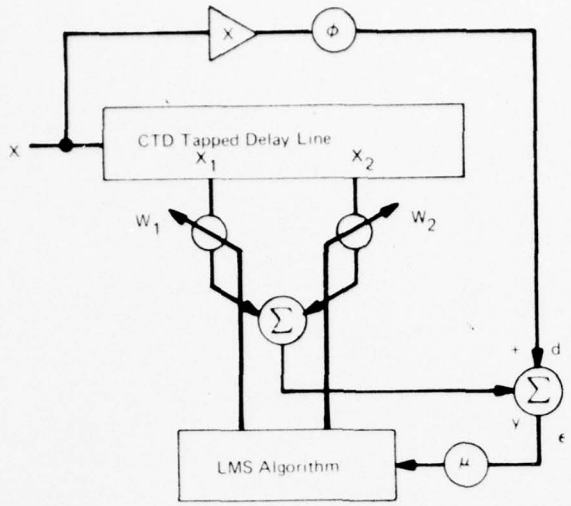

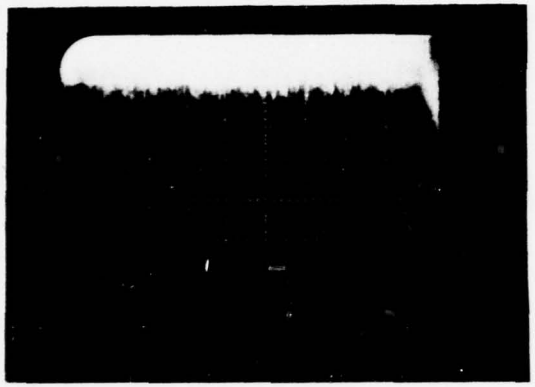

μ = .0075

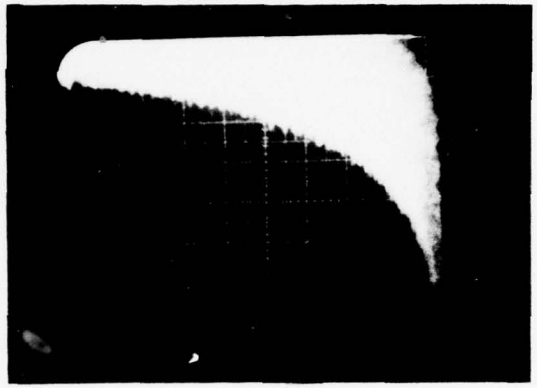

μ = 0.15

77-0581-P-27

Figure 37. Transient Response of LMS Algorithm

CCD ADAPTIVE NOISE CANCELLER

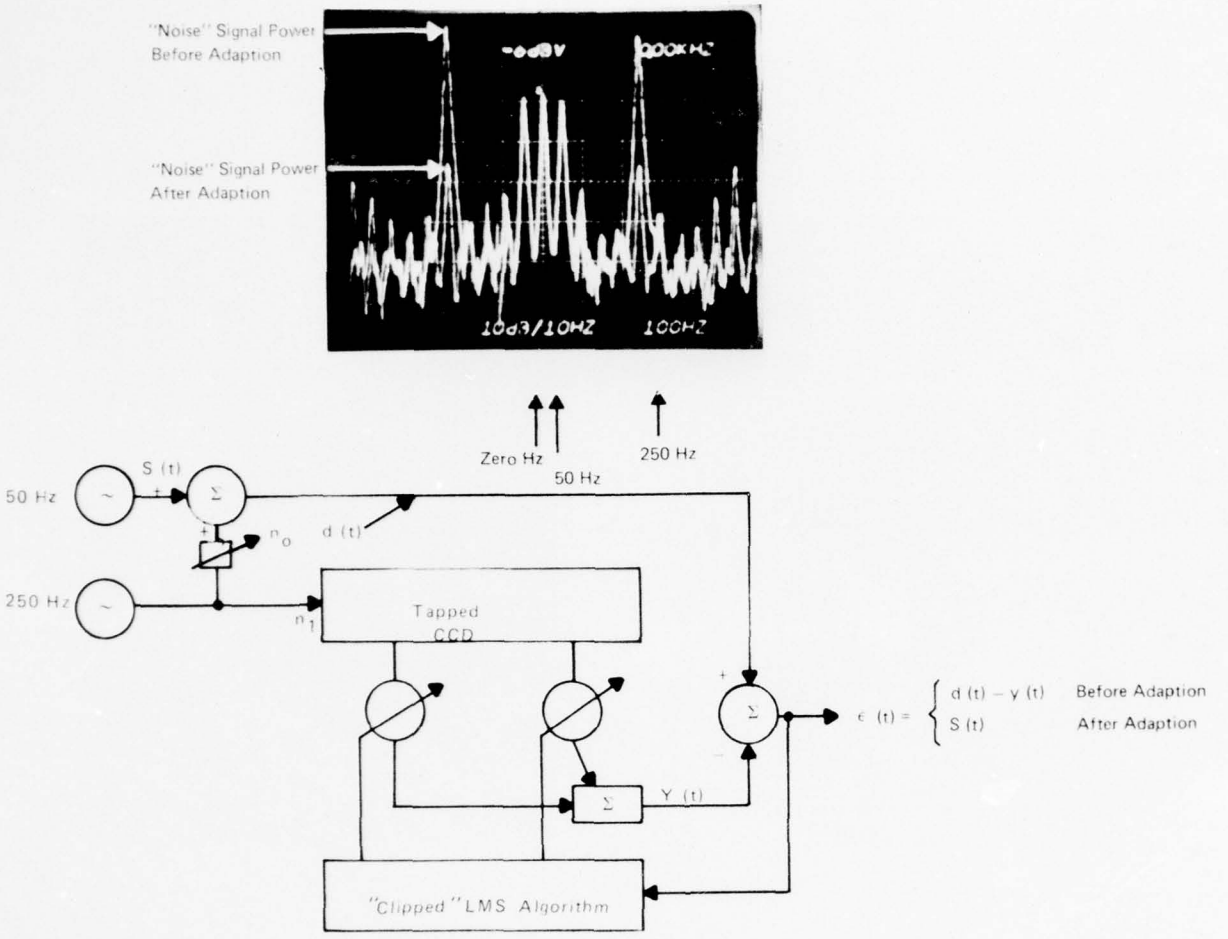

Figure 38. CCD Adaptive Noise Canceller

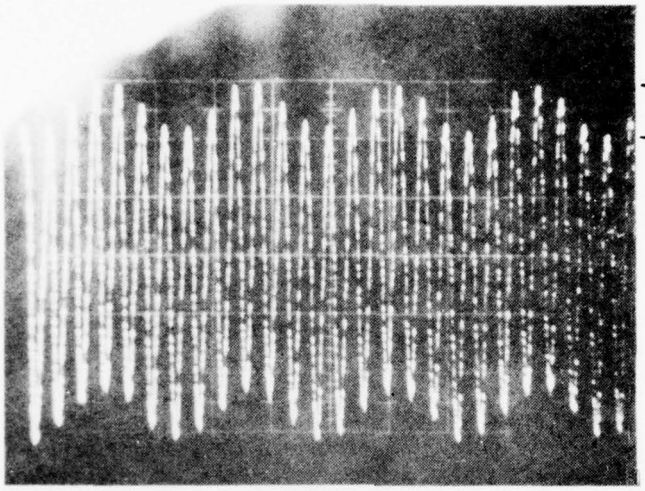

Before Adaptation
(a)

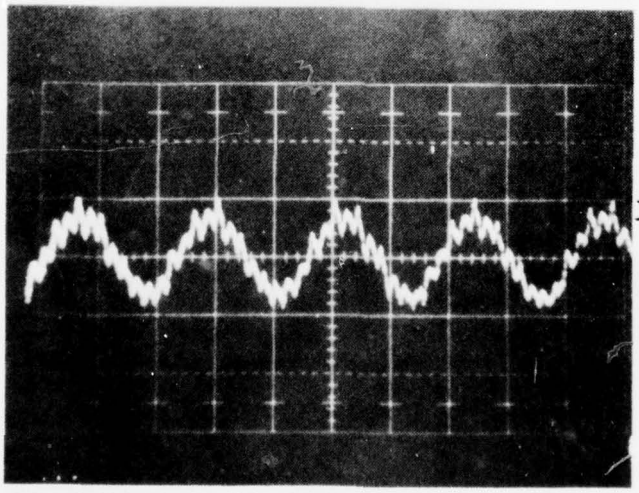

After Adaptation
(b)

f_{signal} = 50 Hz
$f_{interference}$ = 250 Hz

Figure 39. Output Waveforms of Adaptive Noise Canceller

7. APPLICATIONS

There are a number of applications for adaptive filters with special need for real-time signal processing. Several applications are:

- Estimation/Prediction
- Filtering
- Spectral Analysis
- Data Compression
- Interpolation
- Multiple Linear Regression
- Echo Cancellation
- Speech Analysis
- Noise Cancellation
- Coherent Signal Processing
- Frequency Measurement
- System Modeling

7.1 ADAPTIVE NOISE CANCELLATION

A very important application area is adaptive noise cancelling such as the removal of interference in electrocardiography, noise in speech signals, clutter cancellation in antenna (or similar type systems with hydrophones, seismic/acoustic transducers, electro-optical sensors, etc.) sidelobe interference, and coherent signal processing when periodic signals must be separated from broadband interference such as spectrum systems. Figure 40 illustrates the application of adaptive noise cancelling to electrocardiography. Cancellation of 60 Hz interference in conventional ECG, the donor ECG in heart transplants, and the maternal ECG in fetal electrocardiography Figure 38 in section 6.0 demonstrated the use of a 2-tap adaptive noise canceller to reject the interference of a single frequency. The advantage of this technique is the cancellation of the interference even when the latter drifts, since the reference input to the filter will also drift.

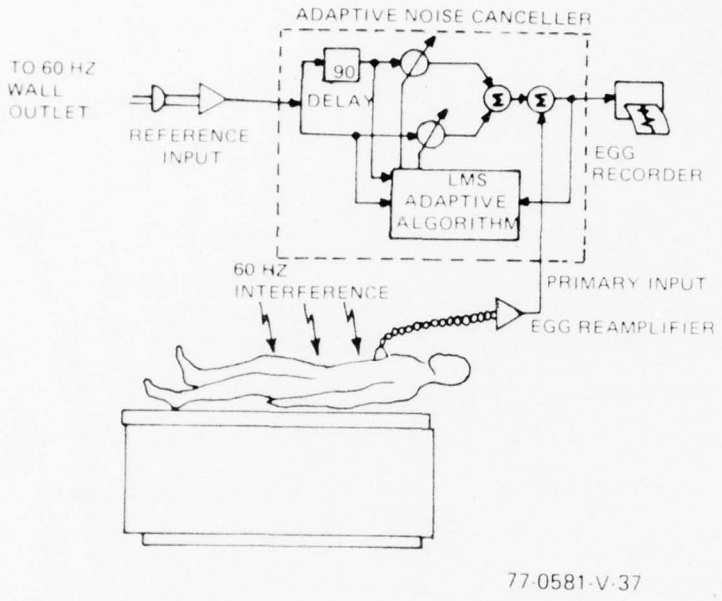

Figure 40. 60 Hz Interference Cancellation with a 2-Tap Adaptive Filter in Electrocardiography[86]

A second area is the cancellation of noise in speech signals such as the situation which arises in pilot communications with a high level of background engine noise. This interference contains strong periodic components in the speech frequency band and the intelligibility of the radio transmission is affected. A conventional filter would not be sufficient since the frequency and intensity of these interference signals vary with engine speed and load, in addition to the location of the pilots head. Figure 41 illustrates the cancellation of noise in this particular example. A reference input is obtained by placing a second microphone at a suitable location in the pilot's cabin. Experiments have been performed[86] to illustrate the concept of noise cancellation with strong acoustial interference in speech transmission. The interference consisted of an audio frequency triangular wave that contained

[86] B. Widrow, et. al., "Adaptive Noise Cancelling: Principles and Applications," Proc. IEEE 63, 1692 (1975).

AD-A043 608 WESTINGHOUSE DEFENSE AND ELECTRONIC SYSTEMS CENTER B--ETC F/G 9/5
CCD ADAPTIVE DISCRETE ANALOG SIGNAL PROCESSING.(U)
JUL 77 M H WHITE, I A MACK, L L LEWIS N00173-76-C-0147

UNCLASSIFIED NL

2 OF 2
AD A043608

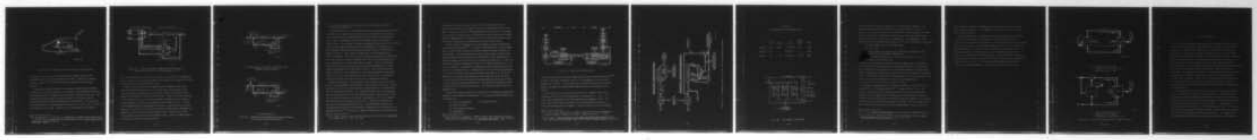

END
DATE FILMED
9 -77
DDC

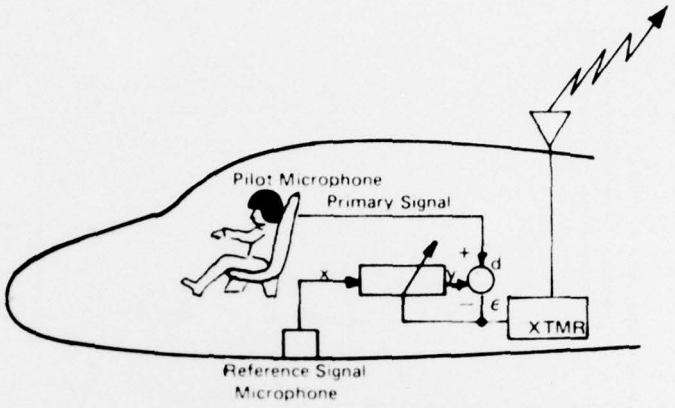

77-0581-V-38

Figure 41. Cancellation of Noise in Speech Communication

many harmonics which varied in amplitude and phase because of the multipath scattering effects throughout the room. Typically, 16 analog weights "rendored the interference barely perceptible to the remote listener."[86]

A third area of noise cancelling is in adaptive cancellation of sidelobe interference in receiving arrays. For example, a sensor beamformer may be constrained with the adaptive noise canceller as shown in figure 42. The multiple reference inputs to the noise canceller are obtained from the deloged beam former element outputs prior to summation. The operation of the beamformer is constrained by the selection of the weighting coefficients of the adaptive filter taps. The gains of the control taps in the adaptive

[87] B. Widrow and J. M. McCool, "A Comparison of Adaptive Algorithms based on the Methods of Steepest Descent and Random Search" IEEE Trans. Anten. and Prop., AP-24, 615 (1976).

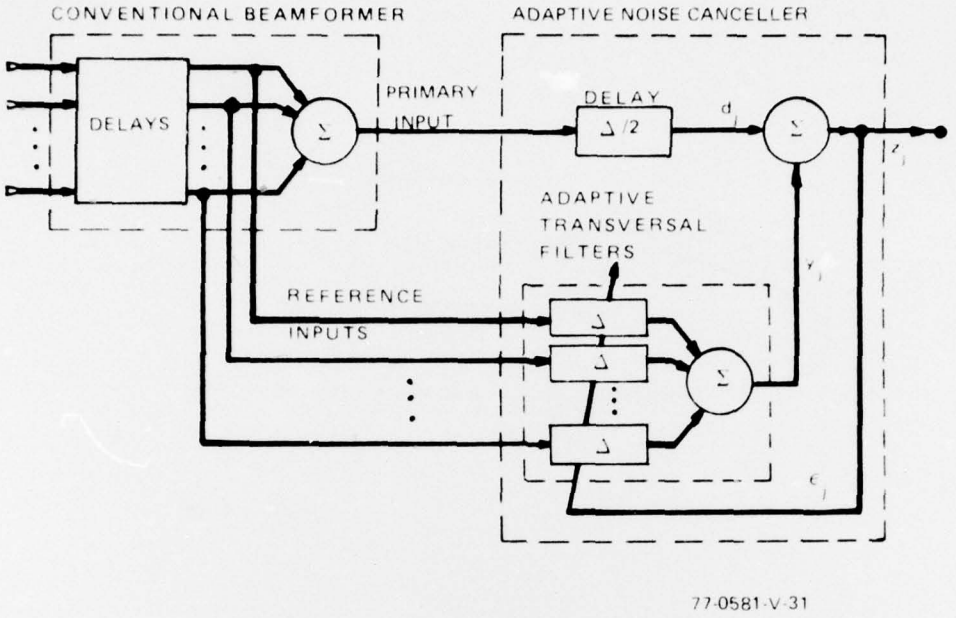

Figure 42. A Null-Constrained Adaptive Beamformer Array Tolerant Array Element Gain and Phase Errors[87]

filter are constrained to zero in some manner so as to provide compensation for variations in element gain and phase and to permit the reception of broadband signals over a desired angular sector.

A fourth area of interest is the separation of broadband and periodic signals as illustrated in figure 43. The insertion of a fixed delay in two reference path, as shown in figure 43a, decorrelates the broadband components will remain correlated with each other. This is an excellent method in the case when no external reference input is available such as speech or music playback in the presence of tape hum or turntable rumble. Another area of application is in spread-spectrum comm nication with narrow-band jamming. Figure 43b illustrates the recovery of the periodic components and application such as automatic signal seeking and the enhancement of low level sinusoidal signals buried in broadband noise. Thus, the adaptive filter functions as a coherent signal processor.

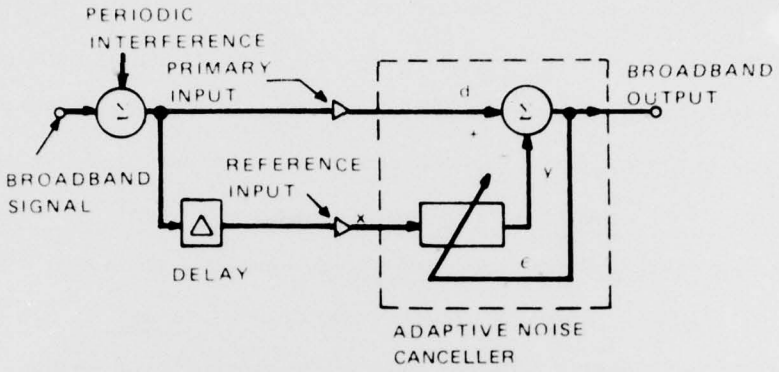

a) Cancellation of Periodic Interference with *Adaptive Noise Canceller*

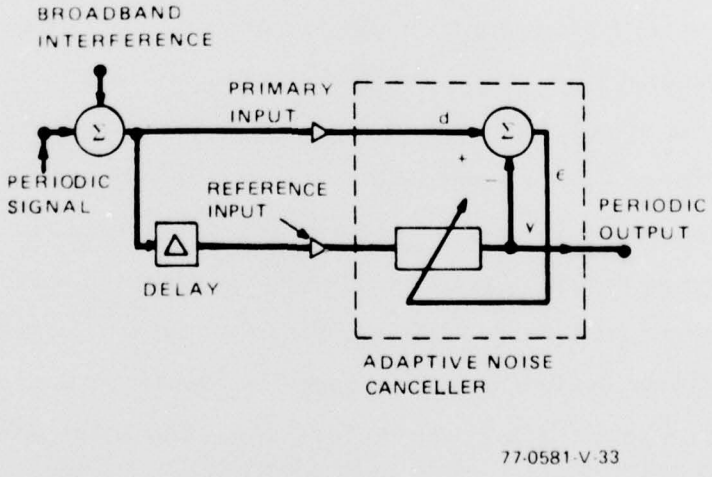

b) Self-Tuned Filter

Figure 43. Separation of Broadband and Periodic Signals as in Spread Spectrum Systems[86]

7.2 ADAPTIVE LINEAR PREDICTION FOR NARROWBAND SPEECH/ VOICE PROCESSING

A promising area for CCD adaptive filtering is in speech processing where redundancy in the spoken word has long been recognized by researchers. Electrical processing of speech which takes into account this redundancy can be used to substantially reduce the bandwidth required for speech transmission. For example, if speech is sampled and quantized at 56 k bits/sec (7 bits or 128 possible amplitude levels per sample at 8 k samples/sec) for acceptable fidelity and the channel bandwidth restricts transmission to below 4 k bits/sec, then a speech compression ratio of approximately 15:1 is attempted. This low data rate would permit speech to be transmitted over high frequency radio or telephone links which have bandwidths barely wide enough for the original analog speech sounds. Such a narrow-band voice digitizer may be used in frequency division multiplexing for simultaneous transmission over wide-band channels. Narrow-band digitized speech lends itself to encryption for secure communications and provides a better S/N then a wide-band digitizer particularly in RF transmission communication sattelite links with limited or fixed available power.

"Speech compression, which maintains intelligibility, nas always been difficult because speech consists of more than words and messages. Speech has the vocal timbre and conversational idiosyncrosies of the speaker and the emotion behind his words. It is normally constructed in an impromptu manner and delivered in a free and informal fashion. Speech flows in time as a continuation that a voice digitizer must process in real time, leaving no chance for later evaluation or correction. Although the information content of the message itself may be low, (possibly below 100 bits/sec), transmission of the subtle vocal inflections requires a date rate of several thousand bits/sec."[88] Historically, speech compression and reconstruction

[88] G. S. Kang, "Linear Productive Narrowband Voice Digitizer" EASCON 74, 51, Washington, D. C. Oct. 7-9, 1974

began with the Dudley channel vocoder in 1936 in which the Fourier Spectrum characteristics of speech determined the parameters of a filter bank. This vocal tract filter bank approximated the vocal tract resonance characteristics of speech and it was excited by a pulse generator (variable period) to approximate the vowels or larynx vibration and a random noise generator to represent the consonants or fricative nasal sounds.

Another technique has proven quite successful in speech compression: linear predictive analysis.[89] The Fourier analysis method treats the past signal, and the linear predictive analysis method attempts to predict the future signal. Linear prediction uses time domain characteristics of the speech signal and the voice signal is analyzed as a linear combination of present and past values to form a set of prediction coefficients. If 10 to 12 consecutive samples of speech are taken (i.e. a speech segment of 1.25 to 1.5 milliseconds), then prediction coefficients can be generated as the tap weights in an adaptive filter. Although only 10 to 12 prediction coefficients are needed, one must accumulate many speech samples (e.g. 100 to 200 samples) to determine these coefficients with some degree of accuracy. The accuracy of these measurements was discussed by Gauss (see section 2.0) with regards to highly redundant or over-determined equations and he formulated the method of least-squares. This method is used in the CCD adaptive filter.

Figure 44 illustrates a functional diagram of a conventional digital linear productive narrowband voice processor. The major functional elements of this system are

- vocal tract analyzer
- pitch extractor
- voice/unvoice analyzer
- synthesizer
- encoder/decoder

[89] B. S. Atal and S. L. Hanauer. "Speech Analysis and Synthesis by Linear Prediction of the Speech Wave", J. of Acoust. Soc. Amer., 50, 637 (1971).

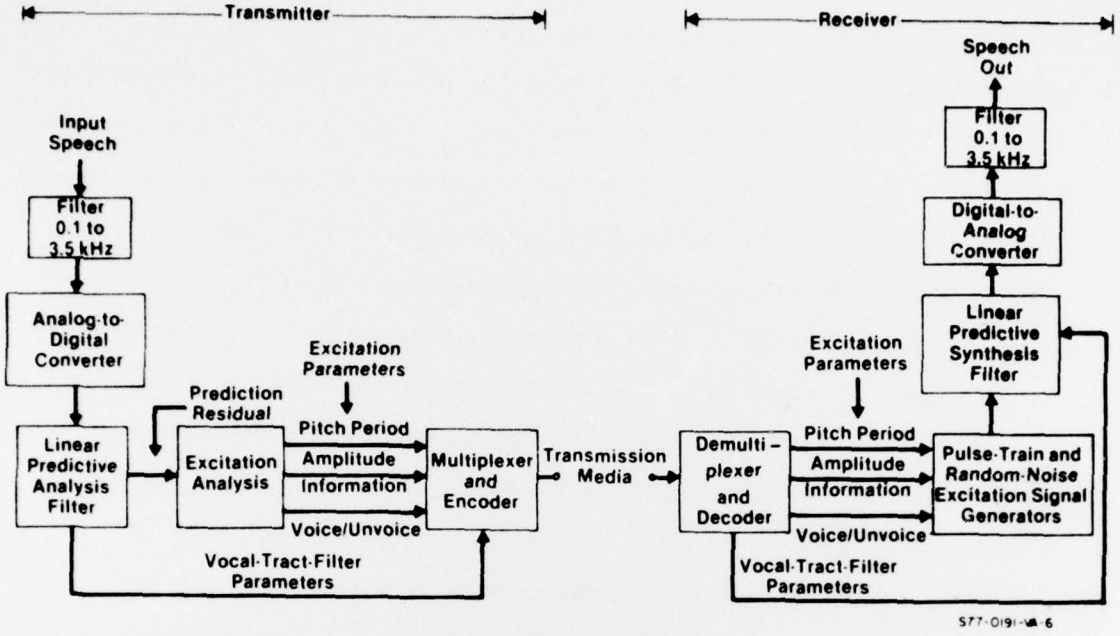

Figure 44. Narrowband Voice System

Digital systems which use linear prediction have been analyzed and built,[90-91] however, the major limitations to an all digital approach are size, power dissipation, and cost. Table 4 illustrates a comparison between the digital, hybrid, and discrete analog sampled approaches for a narrowband voice system.

Figure 45 and 46 illustrates the use of the CCD Adaptive filter as an Analysis filter to generate the prediction coefficients $W_1 \cdots W_N$. The voice input is band-pass filtered and inputted to the adaptive filter. The filter input is also used as the primary or desired signal to generate an error called the prediction residual. This error may be further messaged

---

[90] J. E. Dunn, J. R. Lowan and A. J. Russo, "Progress in The Development of a Digital Vocoder Employing on Itakura Adaptive Predictor" (1973)

[91] Final Report, Voice Processor LSI/Organization Optimitation Study, Contract No. DCA 100-75-C-0020, Sept. 1975 TRW Systems Group, Redundo Beach, Cal.

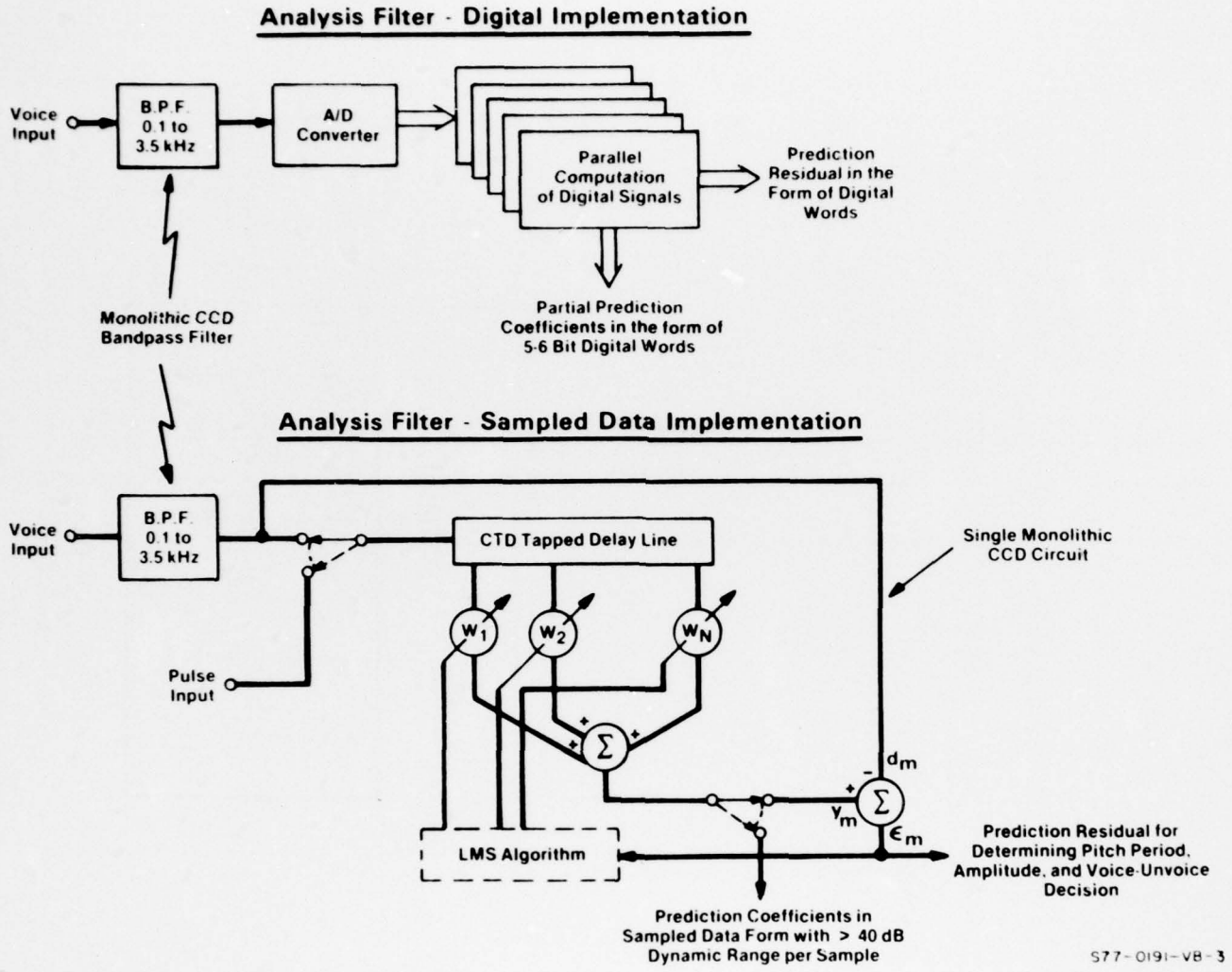

Figure 45. CCD Adaptive Filter for Linear Prediction Analysis of Speech

TABLE 4.

NARROWBAND VOICE DIGITIZER

	# of I. C.'s	Power	Size	Prod. Cost	Risk
Digital	125	50w	3"x5"x12"	10k	Low
Hybrid	40	-	3"x5"x6"	-	Med
DASP	12	7w	1"x5"x5"	0.5-1k	High

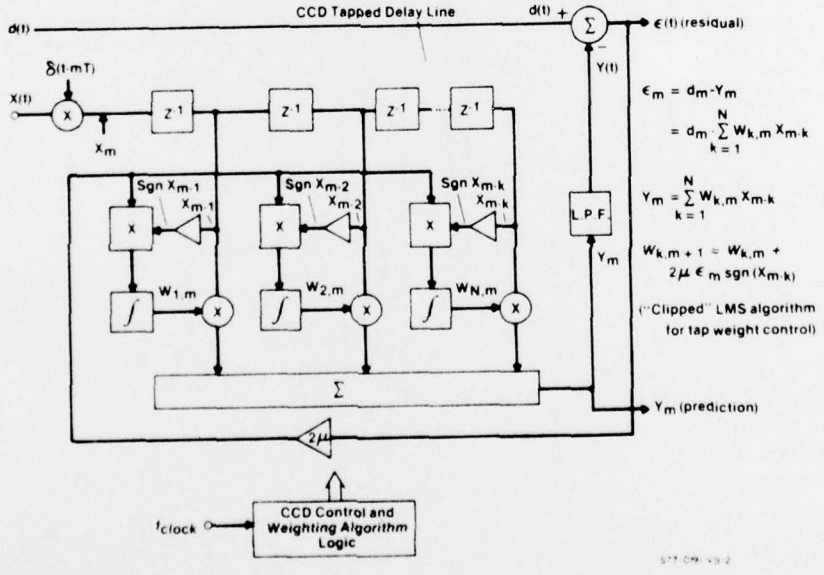

Figure 46. CCD Adaptive Prediction

to extract the pitch period, amplitude, and voice/unvoice decision. The speech sample may be nominally 20 msec in length and the error must converge to its minimum value in this time frame. Near the end of the time frame, a unit pulse in inserted into the filter and the filter output becomes the converged weights or prediction coefficients. The clipped data LMS algorithm has been computer/simulated at NRL[92] with the following constraints,

- preemphasis filter on the input signal
- $W_k \leq 0.98$
- an increase of the unit circle (Z-domain) by 10 percent with scaling of the prediction coefficients
- 10 prediction coefficients of bit levels: 8, 8, 8, 8, 7, 7, 7, 6, 5, 5
- data rate of 3600 bits/sec.

The prediction coefficients generated with the clipped date LMS algorithm and the above constraints were used to synthesize speech. Test sentences were employed and the playback of the reconstructed speech indicated good speech reproduction and quality, although the latter is a subjective parameter. Thus, a CCD adaptive filter with 10 weights operating at a 8 kHz sample rate would be an excellent candidate for this particular application.

7.3 ADAPTIVE ECHO CANCELLATION FILTERS

An important application of CCD adaptive transversal filters is in echo cancellation in the telephone network.[93] Weinstein says, "It is, to be honest, remarkable that a technique (echo cancellation) which has been studied, favorably appraised, and implemented in experimental hardware for more than 10 years has still not been commercially applied. The obvious reason is that echo cancellers which performs better than echo suppressors have tended to cost much more than echo suppressors, it is intrinsically

---

[92] G. S. Kang, Private Communication, Naval Research Laboratories (1977)

[93] S. B. Weinstein, "Echo Cancellation in the Telephone Network", IEEE Communications Society Magazine, pg. 9, Jan. 1977.

more difficult to discover and separate an echo from a mixture of signals than to block everything." CCD adaptive filters offer a means to realize such an echo canceller.

The study of echos in the telephone network has shown that it is difficult to conduct a conversation when a person's voice returns with a delay greater than a few tens of milliseconds. The long-delayed echos are irritating and returns attenuated -40 dB below the speakers voice level will cause the speaker problems. Echos occur due to impedance mismatches in the communication system as illustrated in figure 47a, which describes signal leakage and reflection at the hybrid coupler. Figure 47b illustrates how an echo canceller is used to model the echo channel and generate an output echo replica to cancel the echo. This is particularly important in satellite-routed circuits which experience signal delays in excess of 500 msec.

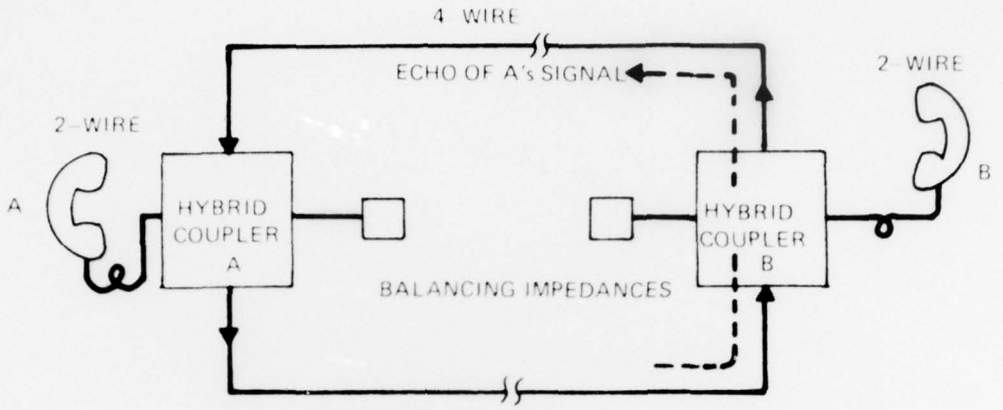

a) Model of Long-Distance Telephone Circuit Which May Include a Satellite Link

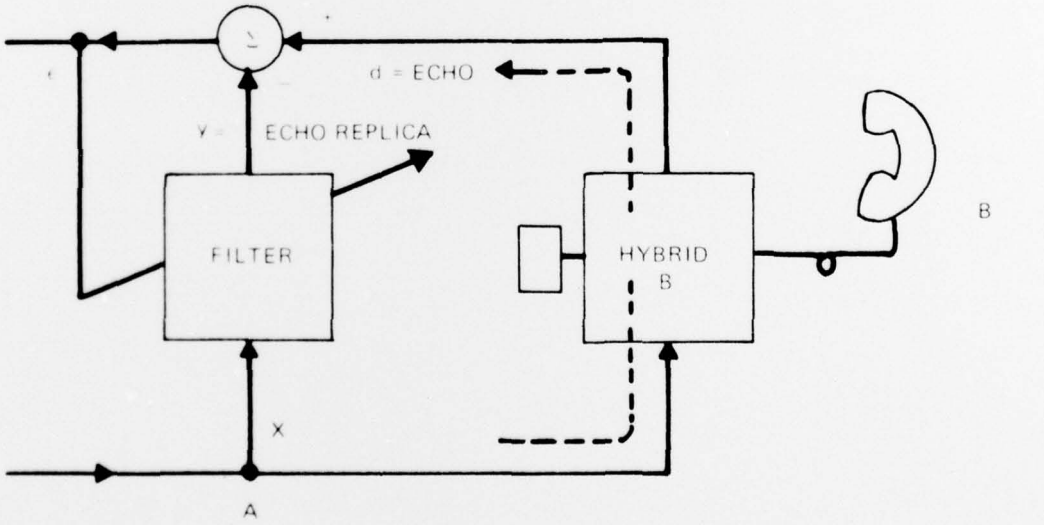

b) Echo Cancellation with CCD Adaptive Filter to Model Echo Channel from Points A to B

Figure 47. Echo Cancellation with CCD Adaptive Filters

8. CONCLUSIONS

We have demonstrated the feasibility of CCD Adaptive Discrete Analog Signal Processing with the implementation of a breadboard, 2-tap weight, adaptive filter based on the "clipped-data" LMS recursive algorithm of Professor B. Widrow and associates at Stanford University. The breadboard consists of components which may be integrated on a single monolithic silicon integrated circuit. For example, the basic linear combiner is a monolithic CCD-SI/PO transversal filter with MOS/bipolar circuitry at each tap position, and the adjustable weights are electrically reprogrammable MNOS analog conductances whose technology is compatible with CCD technology. The recursive algorithm is constructed with steering networks, exclusive ORs, and digital shift register which can be implemented in standard MOS technology. Thus, the basic linear combiner and recursive LMS algorithm may be integrated on a single silicon chip to represent the first step in the direction of integrated circuit discrete analog adaptive signal processing.

The performance of the CCD adaptive filter demonstrated the operation of the LMS algorithm in adaptive signal processing. An adaptive noise canceller was evaluated which provided excellent rejection (-35 dB) of an interfering signal with tolerance for phase-shift difference between desired and reference inputs to the filter (±3 dB for ±180°). Adjustments are required for the clear/write (10 - 20V operation) and read (5 - 10V operation) voltages to optimize the programmability (update mode) and measurement (read mode) operations for the adaptive filter. The "clipped-data" LMS algorithm offers distinct advantages over the linear LMS algorithm

since the former has a convergence time-constant inversely proportional to reference input amplitude and notch-filter bandwidth proportional to reference input amplitude, while the latter is a function of reference input power level. In addition, the hardware requirements are greatly simplified due to the elimination of a 4-quadrant analog multiplier. We have varied the reference input signal amplitude by 20 dB relative to the desired (primary) signal amplitude and maintained better than -20 dB rejection.

The advantages of CCD discrete analog adaptive signal processing lie in the ability of IC technology to provide a compact, low-power, low-cost, signal processor capable of performing real-time adaptive filtering. The terminology "filter" is quite broad, and the actual applications of this technology extend into prediction or estimation, spectral analysis based on maximum entropy considerations, system modeling, etc. The adaptive signal processor IC is analogous to the microprocessor IC in terms of evolutionary development with the added advantage of being a "learning machine" which measures the statistical characteristics of the signal inputs and applies these measurements to internally adjust parameters for optimization of specified system parameters. Once the CCD adaptive signal processor (with 10 - 32 taps) is constructed on an integrated circuit, there will be many areas of application such as speech processing, noise cancellation in medical and communication/control systems, spectral analysis, echo-cancellation, etc.

Although adaptive filtering has been the subject of many papers, conferences, and lectures over the past two decades, the basic limitation to the use of this exciting subject has been the cost in hardware construction, the site of the actual hardware, and the power consumption requirements. As a result of these limitations, adaptive filtering and signal processing has been restricted in usage. With the advent of an IC adaptive signal processor chip, a variety of applicable areas can be opened to the potential user.